The Dissertation Committee for Martha Iveth Garcia Certifies that this is the approved version of the following dissertation:

Control of Cardiac Hypertrophic Signaling by Inositol 1,4,5-Trisphosphate Receptors

Committee:

Darren F. Boehning, PhD, Mentor

MugéKuyumcu-Martinez, PhD, Chair

Gracie Vargas, PhD

David W Niesel, PhD

KartikVenkatachalam, PhD

_____

Dean, Graduate School

Control of Cardiac Hypertrophic Signaling by Inositol 1,4,5-Trisphosphate Receptors

by

Martha Iveth Garcia, BS

Dissertation

Presented to the Faculty of the Graduate School of

The University of Texas Medical Branch

in Partial Fulfillment

of the Requirements

for the Degree of

DOCTOR OF PHILOSOPHY

The University of Texas Medical Branch

October, 2016.

Dedication

Acknowledgements

First and foremost I would like to thank my graduate school mentor, Dr. Darren Boehning. Dr. Boehning is a great example of an amazing mentor, scientist, teacher and person. Thanks for being a good mentor and for guiding me through my graduate school career.I will always be grateful to you for your support. I also want to thank my committee members Dr. Muge N.Kuyumcu-Martinez, Dr. David W. Niesel, Dr. Gracie Vargas and Dr. KartikVenkatachalam. Their comments helped me tremendously to shape my project into the form that is today. I would also like to thank the members of Dr. Boehning's lab. Specially, I would like to thank Dr. Askar Akimzhanov, Dr. Serena Clark Hedgepeth, Dr. MostafaBorahay and Jessica Chen. Particularly, I would like to thank Askar who was always extremely helpful not only on the technical aspect but also he helped me scientifically with always very insightful advice. Serena, Mostafa and Jessica were a great support system and I have no words to thank you for the amazing time we spent in lab together. I also would like to thank my friendsNallely, Gerardo, Sam and Javier and my entire family for supporting me throughout all this years. I couldn't have done this without them! Last but not least, I would like to thank Joseph J. Shearer. You were my support system when times were rough. You are basically the reason I survived the ups and downs of grad school. Thank you for been an amazing boyfriend and thank you for being by my side all this years.

Sincerely I thank you all.

Control of Cardiac Hypertrophic Signaling by Inositol 1,4,5-Trisphosphate Receptors

Martha Iveth Garcia, PhD

The University of Texas Medical Branch, 2016

Supervisor: Darren F. Boehning

Calcium plays an integral role to many cellular processes including contraction, energy metabolism, gene expression, and cell death. The inositol 1,4,5-trisphosphate receptor (IP_3R) is a calcium channel expressed in cardiac tissue. There are three IP_3R isoforms encoded by separate genes. In the heart, the IP_3R-2 isoform is reported to being most predominant with regards to expression levels and functional significance. The functional roles of IP_3R-1 and IP_3R-3 in the heart are essentially unexplored despite measureable expression levels. Here we show that genetically encoded calcium indicators are an excellent tool to study calcium dynamics *in* vitro. As well we explore whether immortalized cell models can be used as an alternative to primary cells to study cardiac hypertrophy. Additionally, we show that all three IP_3R proteins were expressed throughout the cardiomyocyte sarcoplasmic reticulum in neonatal and adult rat ventricular cardiomyocytes and in the human heart tissue. Mechanistically, IP_3Rs specifically contribute to activation of the hypertrophic program by mediating the positive inotropic effects of endothelin-1 leading to downstream activation of nuclear factor of activated T-cells (NFAT). Our findings highlight previously unidentified functions for IP_3R isoforms in the heart with significant implications for hypertrophic signaling in animal models and human disease.

TABLE OF CONTENTS

List of Tables ..... **xii**

List of Figures ..... **xiii**

List of Illustrations ..... **xv**

List of Abbreviations ..... **xvi**

Chapter 1: Introduction **1**
Cardiac hypertrophy, Heart Failure and Endothelin-1 3
Cardiac Hypertrophy 9
Inositol 1,4,5-Trisphosphate Receptor 10
Allosteric Regulators Of IP_3-induced Calcium Release 10
Isoform-Specific Function 12
IP_3Rs and Calcium Homeostasis In The Heart 14
Re-Evaluating IP_3R Expression And Function In The Heart 29

Chapter 2: Experimental Method **30**
Materials and Antibodies 32
Cell lines 33
Transfections of H9c2, HeLa,HEK 293T and AR42J cells 34
Histamine-induced Calcium Release Measurments 34
Staurosporine-Induced Calcium Release Measurements 35
Caspase-3 Enzymatic Assays 35
Preparation of primary neonatal cardiomyocytes 36
Preparation of primary adult cardiomyocytes 36
Immunofluorescence labeling of isolated cardiomyocytes 37
Immunofluorescent labeling of human heart failure samples 37
Cell size determination 38
Cytosolic and nuclear calcium imaging 38
NFAT Luciferase assay 39

Chapter 3: Genetically Encoded Calcium Indicators for Studying Long-Term Calcium Dynamics During Apoptosis **40**
Introduction 42
Results 46
Histamine-Induced Calcium Release Measurments using Fura-2, GCaMP6s, and GCaMP6f 47
Long-term Imaging of Apoptotic Calcium Release Induced by Staurosporine. 49
Discussion 52

Chapter 4: The H9c2 cell line as an alternative for modeling cardiac hypertrophy **55**
Introduction 56
Results 56
Expression and function of the different IP_3R isoforms in ET-1 treated H9C2 cells 56
Discussion 59

Chapter 5: Functionally Redundant Control of Cardiac Hypertrophic Signaling by Inositol 1,4,5-Trisphosphate Receptors **61**
Introduction 63
Results 65
Expression of IP_3R protein in neonatal and adult ventricular cardiomyocytes 66
Altered contractility induced by ET-1 is attenuated by decreasing IP3R expression 69

Attenuating IP_3R expression inhibits ET-1 induced NFAT activation and hypertrophy 72
Calcium release induced by ET-1 is not restricted to the nuclear compartments 79
Discussion 82

Chapter 6: Conclusion and Future Directions 85
GCaMP6 Proteins to Study Calcium Dynamics 87
H9c2 Cells are not a Suitable Model to Study Cardiac Disease 88
IP_3R Expression and Localization in Ventricular Cardiomyocytes 89
ET-1 Inotropic Response is Attenuated in IP_3R Knockdowns 90
IP_3R Triple Knockdown inhibits ET-1 Induced NFAT Activation and Hypertrophy 92
IP_3R are not Restricted to Nuclear Compartments 93
General Conclusions and Significance 94

References 97

Biographical Sketch 117

List of Tables

Table 1: **Expression of the different IP_3R isoforms in the heart.** 28

Table 2: **Properties of Fura-2, GCaMP6s and 6f [147, 155, 175]** 52

Table 3: **Clinical characteristics of patient's samples.** 75

List of Figures

Figure 3-1: Comparison of Fura-2 to GCaMP6s and GCaMP6f in measuring agonist-induced calcium release. 49

Figure 3-2: Changes in cytosolic calcium during cell death. 51

Figure 4-1: NFAT nuclear translocation after ET-1 treatment. 58

Figure 4-2: Expression of IP_3R isoforms H9C2 cells. 58

Figure 4-3: IP_3R-1 an important mediator of calcium release in response to ET-1. 59

Figure 5-1: Expression and distribution IP_3R isoforms in primary neonatal and adult ventricular cardiomyocytes. 67

Figure 5-2: Expression and distribution of IP_3R, SERCA2, and RYR in primary ventricular cardiomyocytes. 68

Figure 5-3: siRNA-mediated knockdown of IP3R-1, -2, and -3. 70

Figure 5-4: All three IP_3R isoforms contribute to hypertrophic signaling by ET-1. 71

Figure 5-5: IP_3Rs expression during ET-1 induced hypertrophy. 73

Figure 5-6: Expression of IP_3R isoforms in non-failing and end stage heart failure 75

Figure 5-7: IP_3R triple knockdown inhibits ET-1 induced NFAT activation and hypertrophy 77

Figure 5-8: Histogram of cardiomyocytes size distribution after ET-1 stimulation 78

Figure 5-9: Nuclear and cytosolic calcium in response to ET-1 stimulation..... 81

Figure 5-10: Plot of cytosolic GCaMP6s versus Fura-2 oscillations frequency 82

Figure 6-1: IP_3R localization adult rat and human samples 90

List of Illustrations

Illustration 1: Schematic of signaling pathways involved in ET-1-induced cardiomyocyte hypertrophy. 8

Illustration 2: Different roles of IP_3R in the heart. 20

Illustration 3: Genetically encoded calcium indicator GCAMP6. 46

List of Abbreviations

AngII	Angiotensin II
ANP	Atrial natriuretic peptide
AP	Action potential
BAPTA	1,2-bis(o-aminophenoxy)ethane-N,N,-N',N'-tetraacetic acid
BNP	Brain natriuretic peptide
CaM	Calmodulin
CaMKII	Ca2+ /calmodulin-dependent protein kinase II
CaN	Calcineurin
CICR	Calcium-induced calcium release
DAG	Diacylglycerol
ECC	Excitation-contraction coupling
ECE	ET-converting enzymes
ER	Endoplasmic reticulum
ERK1/2	Extra cellular signal-regulated kinase 1/2
ET	Endothelin
ET1	Endothelin-1
ETA	Endothelin receptor A
ETB	Endothelin receptor B
F0	Baseline fluorescence
FRET	Förster resonance energy transfer
GECI	Genetically encoded calcium indicators
GFP	Green fluorescent Protein
GPCR	G protein coupled receptor
GSK3	Glycogen synthase kinase 3
HDAC	Histone deacetylase
HF	Heart failure
IICR	IP_3 induced calcium release
IP_3	Inositol 1,4,5-trisphosphate
IP_3R	Inositol 1,4,5-trisphosphate receptor
M13	Myosin light chain kinase
MEF2	Myocyte enhancer factor-2
NCX	Sodium-calcium exchanger
NFAT	Nculear factor activated T cell
NO	Nitric Oxide
opt	Opisthotonos
PKA	Cyclic AMP-dependent protein kinase
PKC	Protein kinase C
PKD	Protein kinase D
PLC	Phospholipase C
PM	Plasma membrane
RYR	Ryanodide Receptor
SCA	Spinocerebellar ataxia

SERCA2	Sarco/endoplasmicreticulumcalciumATPase
SMG	Submandibular gland
SR	Sarcoplasmic reticulum
STS	Staurosporine
TAC	Transverse aortic constriction
TGF-beta	Transforming necrotic factor-β
ΔF/F0	Change in fluorescence/baseline fluorescence

Chapter 1:Introduction

Cardiac Inositol 1, 4, 5-Trisphosphate Receptors

Modified in part from:

Cardiac Inositol 1,4,5-Trisphosphate Receptors

M. IvethGarcia[a,b] and Darren Boehning[b]

[a]Cell Biology Graduate Program, University of Texas Medical Branch, Galveston, TX 77555; [b]Department of Biochemistry and Molecular Biology, McGovern Medical School at UTHealth, Houston, TX 77030

Published in:
BiochimicaetBiophysicaActa (BBA)-Molecular Cell Research

CARDIAC HYPERTROPHY, HEART FAILURE AND ENDOTHELIN-1

Heart failure (HF) is characterized by the inability of the heart to maintain adequate blood flow. As a result the heart is unable to provide enough blood flow to different organs such as the brain and kidneys. Currently, there is an estimated 5.7 million Americans ≥20 years of age that live with HF [1]. Risk factors for HF include hypertension, diabetes, and low socioeconomic status. Overall, African Americans have the highest risk of developing HF, followed by Hispanic and white Americans [1]. Some of the most common causes of HF are long standing hypertension, myocardial infarction, coronary artery disease and congenital heart defects.

In patients with HF there is an increase in the endothelin-1 (ET-1) plasma levels, which has been associated with worsening HF and increased mortality [2, 3]. As well,ET-1 and its receptor ETA are known to beupregulated during other cardiovascular diseases including, hypertension,cardiac hypertrophy, atherosclerosis, and diabetes [4, 5]. ET-1 is responsible for maintaining vascular tone and allows the heart to responds to increased workload caused by cardiovascular diseases [6, 7]. However, if ET-1 signaling cascade persist beyond the “compensatory state”, ventricular remodeling and cardiac hypertrophy may occur. One of the major predictors of HF is sustained pathological hypertrophy [8]. Since the discovery of ET-1 there have been many attempts to target it as a treatment for hypertension and HF, however currently there are no therapeutics targeting this pathway. The only antihypertensive agents that target the ET system arebosentan and ambrisentan, whichtreat pulmonary arterial hypertension and

digital ulcers in scleroderma [9, 10]. A large body of evidence suggests that ET-1 is a key player in diverse pathways that trigger cardiovascular diseases and at the same time is essential for normal cardiac function which demonstrates the complex relationship between ET-1 system and pathological remodeling of cardiomyocytes. Perhaps one of the major reasons ET-1 related therapeutics have remained largely ineffective is due to the complex molecular mechanisms behind the function of the endothelin (ET) family. Composed of three peptide ligands, ET-1, ET-2 and ET-3, members of the ET family are known to play an important role in the cardiovascular system. ET-1 is the most potent vasoconstrictor and most studied in the ET peptide family. ET-1 is a 21-amino acid peptide that is synthesized by endothelial cells, cardiac myocytes, smooth muscle, and fibroblasts [4, 11]. ET-1 is derived from a 212 amino acid prepro peptide preproendothelin-1 that is later cleaved by furin proteases to yield inactive big-ET-1. Big-ET-1 is later processed by ET-converting enzymes (ECE-1 and ECE-2) to yield the bioactive peptide ET-1.

ET-1 transcription is tightly regulated and alterations in ET system expression have been linked to progression of pathogenesis including a range of cardiovascular diseases [4, 12, 13]. Several biological and pharmacological factors such as angiotensin II (AngII), transforming necrotic factor-β (TGF-β), hypoxia, and shear stress have been utilized to control ET-1 transcription [14-16]. Vasodilators such as natriuretic peptides or nitric oxide (NO) have also been shown to reduce ET-1 expression [17, 18]. The ET family has two main receptors ETA and ETB, which belong to the G protein coupled receptor (GPCR) family [19, 20]. Generally found at the plasma membrane of cardiomyocytes, the ETA

receptor is known to be the most predominant isoform making up nearly 90% of ET receptors [4, 21]. These receptors have key differences including affinity toward the different ET isoforms. For example, ETA has higher affinity to ET-1, where ETB binds non-selectively to either ET isoform. Aside from differences in binding affinity and expression patterns, ET receptors activate different downstream signaling pathways. ETA is coupled to G-protein $G\alpha_q$ which leads to inositol 1, 4, 5-trisphosphate (IP_3) and diacylglycerol (DAG) production [22]. ETA receptor has been implicated in playing a key role in vasoconstriction, cardiac remodeling and extracellular matrix production. ETB receptor couples with $G\alpha_q$ and $G\alpha_i$ which is known to promote ET-1 clearance, nitric oxide production and production of other vasodilators [22, 23].

As the predominant isoform expressed in cardiomyocytes our focus is to better understand the downstream effects and activation of different pro-hypertrophic signals from ETA. IP_3 binds to the inositol 1, 4, 5-trisphosphate receptor (IP_3R) leading to increases in cytosolic calcium which stimulates cardiomyocyte contractility or activation of different pro-hypertrophic pathways. The calcium sensor calmodulin (CaM) is activated in response to calcium released from IP_3Rs, which in turn activates the phosphatase calcineurin (CaN). CaN activates nuclear factor of activated T cell (NFAT) by dephosphorylation leading to the translocation of NFAT to the nucleus. Nuclear NFAT initiates transcription of different pro-hypertrophic genes. The role of NFAT in hypertrophy will be discussed in greater detail below. Similar to NFAT, calcium/calmodulin-dependent protein kinase II (CaMKII) is activated in response to IP_3-induced calcium release

in response to CaM activation (sometimes abbreviated IICR) [24]. CaMKII activation leads to phosphorylation of class II histone deacetylase 4 (HDAC4) leading to HDAC4 translocation out of the nucleus. Myocyte enhancer factor-2 (MEF2), a transcription factor whose activation is attenuated by interacting with HDAC4 in the nucleus, is activated upon HDAC4 phosphorylation. An increase in MEF2 activity has been associated with the regulation of genes expressed during cardiac hypertrophy and with pathological remodeling in response to ET-1 stimulation in cardiomyocytes [25, 26]. DAG production in response to ET-1 binding to GPCR leads to activation of protein kinase C (PKC). PKC proteins are ubiquitously expressed and are important signaling transducers. In the heart, PKC activation has been linked to development cardiac hypertrophy by regulating several downstream targets including extracellular signal-regulated kinase 1/2 (ERK1/2) and protein kinase D (PKD) signaling [16, 27-29]. PKC activation of Raf1 leads to activation of MEK and ERK1/2 in response to ET-1. ERK1/2 phosphorylation leads to the phosphorylation of cytoplasmic proteins and subsequent translocation of ERK1/2 into the nucleus which leads to activation of different transcription factors. Dominant negative Raf1 mutants have been shown to have an attenuated response to pressure overload [30]. Similar a variety of MEK inhibitors have been shown to reduce hypertrophy induced by ET-1 treatment [31-33]. The Raf/MEK/ERK1/2 axis has been implicated in pathological and physiological cardiac hypertrophy [34-36]. PKC also mediates activation of PKD which mediates nuclear export of transcriptional repressor HDAC5. PKD repression correlates with suppression of HDAC5 shuttling and cardiomyocytes

growth [37, 38]. The pathways mentioned above have been implicated in cardiomyocytes hypertrophy (**Illustration 1**). Overall the primary inducers of hypertrophy are not clear, however the neurohormonal factor ET-1 is likely linked to hypertrophy. ET system is an important regulator of physiological cardiac and vascular functions and tightly regulation of this complex system is essential for its normal function [6, 39]. Understanding the molecular processes that lead to cardiac hypertrophy is extremely important and may play a critical role in the development of therapeutic innervations against hypertrophic-induced arrhythmias, heart failure and death.

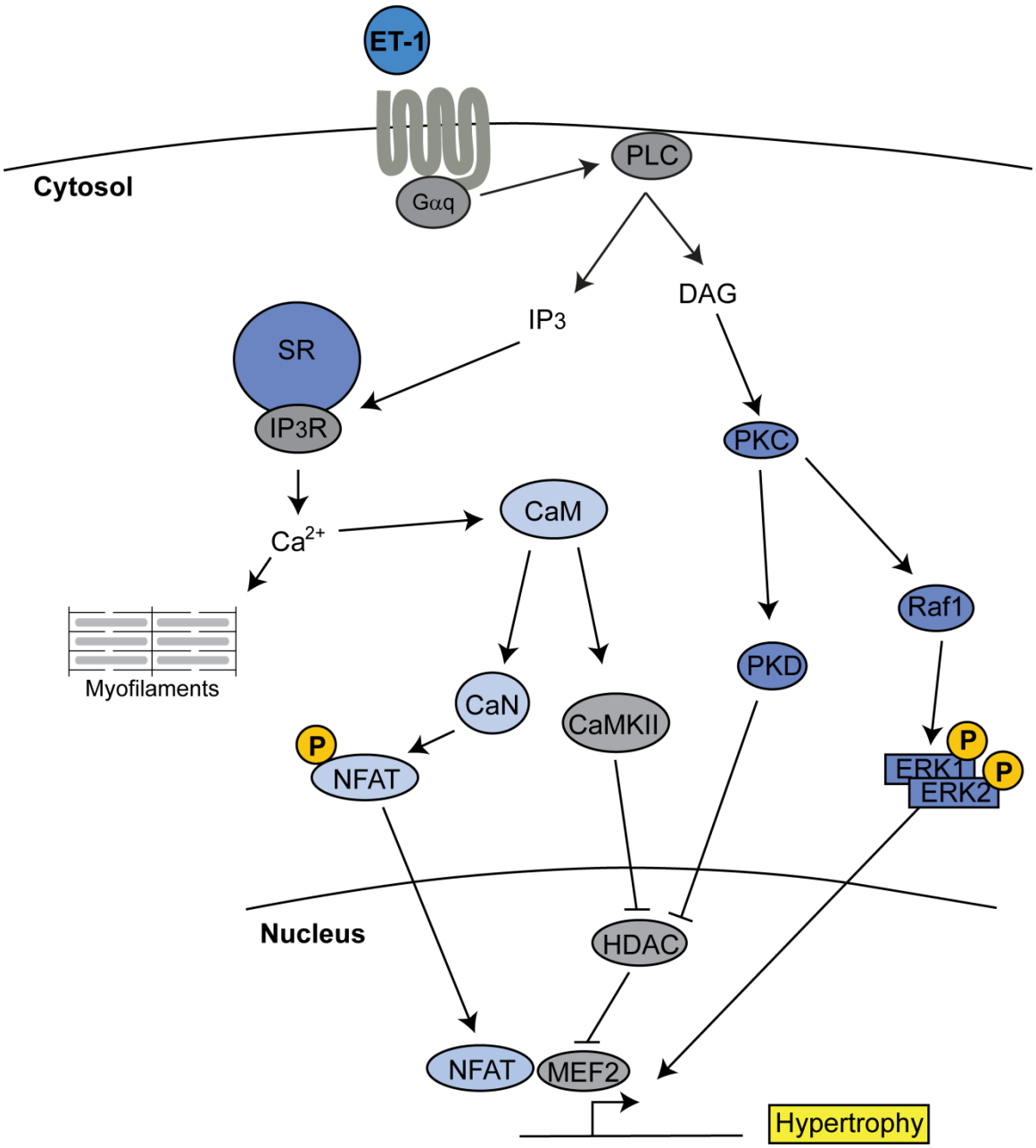

Illustration 1: Schematic of signaling pathways involved in ET-1-induced cardiomyocyte hypertrophy.
Cardiac hypertrophic agonist endothelin-1 acts through its receptor and activates phospholipase C (PLC) leading to the production of IP_3 and DAG. Activation of second messengers IP_3 and DAG lead to activation of several downstream pathways that are known to induce cardiac hypertrophy.

CARDIAC HYPERTROPHY

Cardiac hypertrophy is an adaptive response to a wide variety of cardiovascular diseases such as hypertension, ischemic insults, and cardiomyopathy [40-42]. Ventricular hypertrophy can occur in either the right or left ventricle and usually occurs as a compensatory mechanism to maintain normal contractility. Ventricular hypertrophy is characterized by increased ventricular wall thickness as a means to decrease wall tension and cardiac stress. Sustained pathological hypertrophic remodeling can lead to arrhythmias, heart failure, and sudden death [43].

Hormonal factors such as endothelin-1 (ET-1) are known to contribute to the development of cardiac hypertrophy. ET-1 is a potent vasoconstrictor known to increase in the circulation with age and during cardiac stress [4, 5, 16, 44]. In the heart ET-1 regulates cardiac muscle function by modulating contractility, cardiomyocyte size, and cardiac gene expression [13, 45]. ET-1 binds and activates the G-protein coupled receptor endothelin receptor type A (ET_A) localized on the cardiomyocyte plasma membrane, leading to activation of phospholipase C (PLC) and production of inositol 1,4,5-trisphosphate (IP_3) and diacylglycerol (DAG) [46-48]. An increase in cytosolic IP_3 leads to calcium release *via* the IP_3R calcium channel. Increases in cytosolic calcium *via* the IP_3R can lead to modulation of cardiomyocyte contraction and activation of signaling pathways that modulate gene expression. Nuclear factor of activated T cells (NFAT) is a transcription factor that is well known to be one of the targets of the ET-1/ IP_3R signaling cascade [49-51]. Calcium release through IP_3Rs leads to activation of calcineurin, which is a

calcium-activated phosphatase. Dephosphorylation of cytosolic NFAT by calcineurin leads to the translocation of NFAT to the nucleus, where it initiates transcription of different genes that contribute to hypertrophic remodeling. The ET-1 signaling cascade has been extensively studied and it is known to play a crucial role during pathological hypertrophic remodeling of the heart [45, 49].

In the heart IP_3Rs are thought to play an important role by modulating calcium signals in response to extracellular stimulation. IP_3R expression levels have been shown to be increased in cardiac hypertrophy, failing myocardium, atrial fibrillation, ischemic dilated cardiomyopathy, and hypertension [52-54]. Cardiomyocyte IP_3R expression is less abundant compared to the main calcium release channel of the heart, the ryanodine receptor (RYR). However, during cardiac hypertrophy IP_3R expression and function is increased, and this is thought to contribute to cardiac remodeling [52, 53, 55]. To what extent IP_3Rs specifically contributes to the hypertrophic remodeling is not completely understood and somewhat controversial.

REGULATION OF INOSITOL 1,4,5-TRISPHOSPHATE RECEPTOR

The IP_3R is a ligand-gated calcium channel that is primarily localized to the endoplasmic/sarcoplasmic reticulum (ER/SR). In some cell types, the IP_3R may also be found at the plasma membrane, Golgi apparatus, secretory vesicles, and perinuclear/nuclear membrane [46, 53, 56]. The IP_3R family is comprised of three isoforms that are encoded by three distinct genes. Each IP_3R isoform is about 300kDa and they form homo- and hetero- tetramers when co-expressed in different

tissues [57-59]. The IP_3R N-terminus contains the ligand (IP_3) binding domain and the suppressor domain. The C-terminal domain has six transmembrane alpha helices that forms an ion conduction pore and a C-terminal tail that is thought to modulate gating by interacting with the ligandbinding domain from an adjacent subunit [60]. The C-terminal tail is also the site of binding of multiple proteins that modulate channel function, as well as being targeted for post-translational modifications such as phosphorylation [61]. Between the N-terminal ligand binding domain and the C-terminal channel domain the IP_3R has a modulatory domain, which is an additional site of interaction for a variety of proteins and molecules that regulate channel function [62]. The modulatory domain is also a site for post-translational modifications that are thought to further modulate IP_3-induced calcium release [63-65]. The three IP_3R isoforms share ~60% overall sequence identity, with the N- and C- terminal domains sharing the highest homology between isoforms [66, 67]. As expected, the three IP_3R isoforms also share similarities in gating and conductance characteristics consistent with their high sequence homology [68, 69]. IP_3R-1 is the main isoform expressed in the central nervous system (and in particular the cerebellum), and is critical for proper central nervous system function as evidenced by the hereditary spinocerebellar ataxias 15/16 and 29 that are caused by deletions/mutations in one allele of the *ITPR1* gene [70, 71]. IP_3R-2 is expressed at high levels in the heart, pancreas, liver, and salivary glands. Similar to IP_3R-2, IP_3R-3 is also highly expressed in the pancreas and salivary glands [71]. IP_3R isoform expression is presumed to be regulated in a cell and tissue specific manner [71, 72], however the mechanisms regulating differential

expression are unclear. Practically speaking, most tissues have detectable levels of all three IP_3R isoforms that can form both homo and heterotetramers[57, 59, 71, 73]. Thus, evaluating or interpreting isoform-specific function *in vivo* is a daunting task.

Allosteric Regulators Of IP_3-induced Calcium Release

Signal transduction pathways leading to calcium release classically originate at the plasma membrane (PM). Activation of PM receptors can lead to generation of the signaling molecules IP_3 and diacylglycerol through the action of phospholipase C (PLC). IP_3 binding to the IP_3R causes a conformational change that leads to calcium release from intracellular calcium stores. [74]. IP_3-induced calcium release (sometimes abbreviated IICR) can be allosterically regulated by calcium, ATP, and many proteins [75-82]. It has been shown using a wide variety of techniques that the different IP_3R isoforms are differentially regulated by IP_3[66, 72]. It was later confirmed by single channel recording in planar lipid bilayers that IP_3R-2 has the highest affinity for IP_3, followed by IP_3R-1 and IP_3R-3 [68, 83]. Much of what we know about IP_3R function, including isoform-specific function, has been elucidated in the DT40 chicken B cell line in which each IP_3R isoform has been knocked out using homologous recombination either singly or in combination [83, 84]. B-cell receptor mediated calcium release in DT40 cells exclusively expressing IP_3R-2 was characterized by calcium oscillations that were more robust and longer-lasting compared to those observed in wild-type cells [83]. On the other hand, IP_3R-1 mediated calcium release was characterized by an initial monophasic

calciumresponse that was followed by irregular calcium oscillations with smaller amplitude compared to IP_3R-2. The IP_3R-3 mediated calcium response was characterized by a single calcium release event, and in contrast to IP_3R-1 and -2, there were no additional calcium oscillations [83]. These studies depict the different functional characteristics of calcium release events mediated by each isoform, at least in the DT40 cell system in response to B cell receptor stimulation. Similar results were obtained using concatenated homo- and heterotetramers[85]. The ligand IP_3 is not the only regulator of IP_3R-mediated calcium release. It has been shown that calcium functions as a co-agonist for IP_3R calcium release at low concentrations while at higher calcium concentrations IP_3R activity is inhibited [86-90]. Therefore, calcium has the ability to bi-phasically regulate IP_3R function. These positive and negative feedback loops contribute to the complex spatio-temporal aspects of calcium release.

The crucial event that activates IP_3R calcium release is the binding of IP_3 to the IP_3R. IP_3R activation by IP_3 is known to be modulated by ATP. Binding of ATP to the IP_3R results in an increase in IP_3R open probability and this modulation is isoform specific [68, 75, 77, 91, 92]. Accordingly, each receptor has different affinities for ATP. IP_3R-2 is known to have the highest affinity, approximately 10 fold-higher compared to IP_3R-1. Interestingly, IP_3R-2 is modulated by ATP only at submaximal IP_3 concentrations [77]. IP_3R-3 is known to have a lower affinity compared to the other two isoforms [77]. ATP binds to a glycine rich region (GXGXXG) on the IP_3R that is commonly found in several ATP binding proteins and is known as a Walker motif. IP_3Rs have two of these motifs named ATP-

binding motif A and B (ATPA/ATPB) [93]. It is known that the ATPA binding motif is exclusively found on IP_3R-1, while ATPB binding motif is conserved among all three isoforms. Using mutagenesis experiments, it was shown that mutation of the ATP binding motifs on IP_3R-1, ATPA and ATPB, does not abrogate ATP's positive effect on IP_3R-1. Similarly, mutation of IP_3R-3 ATPB binding motif does not affect IP_3R-3 open probability in response to ATP. Thus, available evidence suggests that IP_3R-1 and IP_3R-3 have other still unknown ATP binding sites. In contrast, mutagenesis experiments done on IP_3R-2 show that ATPB is essential for ATP modulation of IP_3R-2 [77, 93]. Interestingly, a recent report using recombinant concatemeric IP_3R constructs has shown conclusively that at least two subunits of IP_3R-2 is sufficient to confer ATP sensitivity [94]. In contrast, other functional aspects such as IP_3 sensitivity display an intermediate phenotype. Thus, the difference in IP_3R activation/modulation by IP_3, calcium, and ATP highlights the unique characteristics of each IP_3R isoform that is further enriched by heterotetramer formation. However, the three IP_3R isoforms have been shown to be at least partially functionally redundant *in vivo*.

Isoform-Specific Function

It is difficult to assess the importance and role of an individual IP_3R isoform because they are co-expressed in almost all tissues [71, 72]. As noted above, *in vitro* studies using DT40 cells revealed differences in IP_3R function between isoforms, and this is likely mediated by distinct regulation by IP_3, calcium, and ATP. DT40 experiments with concatenated receptors also revealed unique properties of

heterotetrameric channels [94]. Mutations in IP_3R channels causing human disease have been very instructive for establishing isoform-specific function *in vivo*. Heterozygous mutations of the *ITPR1* gene cause spinocerebellar ataxia (SCA) 15 and 29 [95-99], which are progressive neurodegenerative disorders characterized by cerebellar ataxia and tremors. SCA16 is also caused by mutations in *ITPR1,* and it is now clear that SCA15 and SCA16 are clinically indistinguishable. As such, SCA16 is now considered a "vacant SCA" [100]. SCA15 is an autosomal dominant disorder characterized by a decrease in IP_3R-1 expression that leads to slow degeneration of Purkinje cells of the cerebellum where normally IP_3R-1 is highly expressed [96, 101]. Lower amounts of IP_3R-1 cause Purkinje cell degeneration, possibly by the dysregulation of intracellular calcium homeostasis in these cells. The related disorder SCA29 is distinguished clinically by earlier age of onset and cognitive impairment [98, 99]. At the molecular level, it is associated with a missense mutation in the regulatory domain. However, the functional consequences at the cellular level of the mutation observed in SCA29 disorder have yet to be determined [99]. Missense, nonsense, and in-frame deletion mutations in *ITPR1* are also the cause of a very rare disease associated with ataxia known as Gillespie Syndrome [102, 103]. Interestingly, some Gillespie Syndrome patients have homozygous truncating mutations in the IP_3R protein resulting in what would be predicted to be a complete loss IP_3R-1 calcium release function [103]. Other mutants might function as dominant-negative subunits to inhibit channel function [103]. Thus, the loss of IP_3R-1 function appears to be compatible with life in humans. A homozygous missense mutation in *ITPR2*

is a rare cause of isolated anhidrosis with normal sweat glands [104]. The mutation is within the putative selectivity filter of the IP_3R pore, substituting glycine 2498 for serine. This mutation results in normal levels of IP_3R-2 expression in clear cells of the sweat gland, but loss of IP_3R-2 mediated calcium release. Thus the complete loss of IP_3R-2 calcium release function, like IP_3R-1, is compatible with life in humans. Currently, there are no known human diseases definitively linked to mutations in the IP_3R-3 protein, however single nucleotide polymorphisms in the *ITPR3* gene are associated with increased risk of type 1 diabetes [105] and systemic lupus erythematosus[106].

Several mouse models have been used to explore the role of IP_3Rs *in vivo*. One example is the spontaneous mouse mutant *opisthotonos (opt),* which has an in-frame deletion of exon 43 and 44 of the *itpr1* gene (IP_3R^{opt}). These two exons encode a portion of the modulatory domain that includes a key site that is essential for ATP binding and modulation of IP_3R-1 [107]. *Opt* mice display a severe phenotype characterized by seizures that can range from body tremors to tonic-clonic seizures. Homozygous *opt* mice show lower levels of functional IP_3R-1 expression [108]. Furthermore, using single channel recording it was shown that the IP_3R-1 *opt* mutant has a lower single channel conductance compared to the wild type channel [107].ATP and conductance alterations in the *opt* mutant may help explain the severe phenotype observed in *opt* mouse. Furthermore, a heterozygous knockout ($IP_3R\text{-}1^{-/+}$) mice model of the *itpr1* exhibits impaired motor coordination manifested primarily on the Rota-Rod test [109]. Interestingly, this mouse model is mostly undistinguishable from WT mice. Double knockout (IP_3R-

$1^{-/-}$) mice have a more severe phenotype that is mostly embryonic lethal, though a few mice survive to birth and display severe ataxia with seizures until death before weaning[70]. In both cases, $IP_3R\text{-}1^{-/-}$*and* $IP_3R\text{-}1^{-/+}$ mice show no significant anatomical differences in any organs including the brain, heart, and spleen when compared to wild-type littermates. Overall the clinical phenotype observed in both human and animal models with mutations on the IP_3R-1 is mainly due to high expression of this specific receptor in the cerebellum, with very important differences between the two models.

Global homozygous knockout of *itpr2* in mice does not results in any obvious phenotypic abnormalities [110]. Similar to a loss of function *ITPR2* mutation in patients, *itpr2* double knockout mice exhibit reduced sweat production and diminished sweat gland responses to acetylcholine [104]. Homozygous knockout mice retain residual sweat secretionthat was attributed to the expression of the other two IP_3R isoforms in mice [104], whereas in humans the IP_3R-2 isoform appears to be the primary isoform expressed in eccrine sweat glands.

Using double *itpr2* and *itpr3* knockout mice, it was found that these mice lack salivary secretion leading to low weight and eventually death caused by starvation [110]. Interestingly, *itpr2* or *itpr3* single mutants were indistinguishable from control showing functional redundancy of the two isoforms. Using submandibular glands of wild type, $itpr2^{-/-}$, $itpr3^{-/-}$ or $-3^{-/-}$, and$itpr2^{-/-}3^{-/-}$mice, it was shown that double mutants exhibit impaired cholinergic and beta-adrenergic responses. The impairment of this response led to a decrease in the salivary secretion[110]. Furthermore, $itpr2^{-/-}3^{-/-}$mice also showed deficits in exocrine

pancreas function leading to alterations in lipase, amylase, and trypsinogen secretion in pancreatic tissue. IP_3R-2 and IP_3R-3 single knockout mice were phenotypically indistinguishable from wild type mice, which would suggest that the overlapping function of these channels compensate for the lack of one IP_3R subtype, and that IP_3R-2 and IP_3R-3 may have redundant roles *in vivo* in mouse models[111, 112].

Double knockout of the *itpr1* and *itpr2* genes in mice leads to embryonic development defects of the ventricular myocardium, and as expected based upon the *itpr1* knockout phenotype, the double knockouts die *in utero* [113]. Interestingly, the double knockout mouse model phenocopies NFAT triple knockout mice, including thin myocardial walls, poor trabeculation of the ventricles, poor ventricular cell proliferation and decreased NFAT nuclear translocation [113]. In contrast, single IP_3R mutants do not have the same physiological abnormalities that are seen in the double knockout, suggesting that during heart development IP_3R-1 and IP_3R-2 have redundant roles in regulating NFAT activation [113]. In general, both mouse studies and human diseases associated with IP_3R mutations support the notion that the different IP_3R isoforms have at least partially functional redundant roles *in vivo*, and the phenotypes observed in the knockout mice are due to restricted tissue-specific expression of the isoforms.

IP_3Rs and Calcium Homeostasis In The Heart

Calcium is a critical regulator of cardiac function. Cardiomyocyte contraction and relaxation is directly regulated by cytosolic calcium. Contraction is initiated by

the activation of L-type voltage gated calcium channels (also known as the dihydropyridine receptor or Cav1.2 calcium channel). Calcium entry through L-type channels activates SR-localized ryanodine receptor (RYR) calcium channels *via* a process known as calcium-induced calcium release (CICR) [114]. Gating of the RYR allows SR calcium to be released into the cytoplasm where it binds to troponin C to initiate contraction. Relaxation is promoted when calcium is cleared from the cytoplasm primarily by the plasma membrane-localized sodium-calcium exchanger (NCX) and sarco/endoplasmic reticulum calcium ATPase (SERCA2), however other pumps, exchangers, and buffers can modulate relaxation [115]. In addition to the RYR, cytosolic calcium levels are modulated by IP_3Rs in the heart. IP_3R expression levels are thought to be relatively low compared to RYR, typically 50-fold less abundant than RYR2 [55, 116-118]. However, an important caveat is that these studies rely almost exclusively on the quantification of mRNA levels, not protein levels. Despite apparently low expression levels, IP_3Rs have been linked to modulation of cardiac contraction and activation of cardiac gene expression. Importantly, it has been reported that IP_3R expression and localization pattern are altered during heart failure and cardiac ventricular hypertrophy. IP_3R overexpression has been linked to cardiac remodeling in response to multiple stressors

that lead to hypertrophy [119]. Overall, there is strong evidence that that IP_3Rs play an important role in the heart physiology in health and disease (**Illustration 2**).

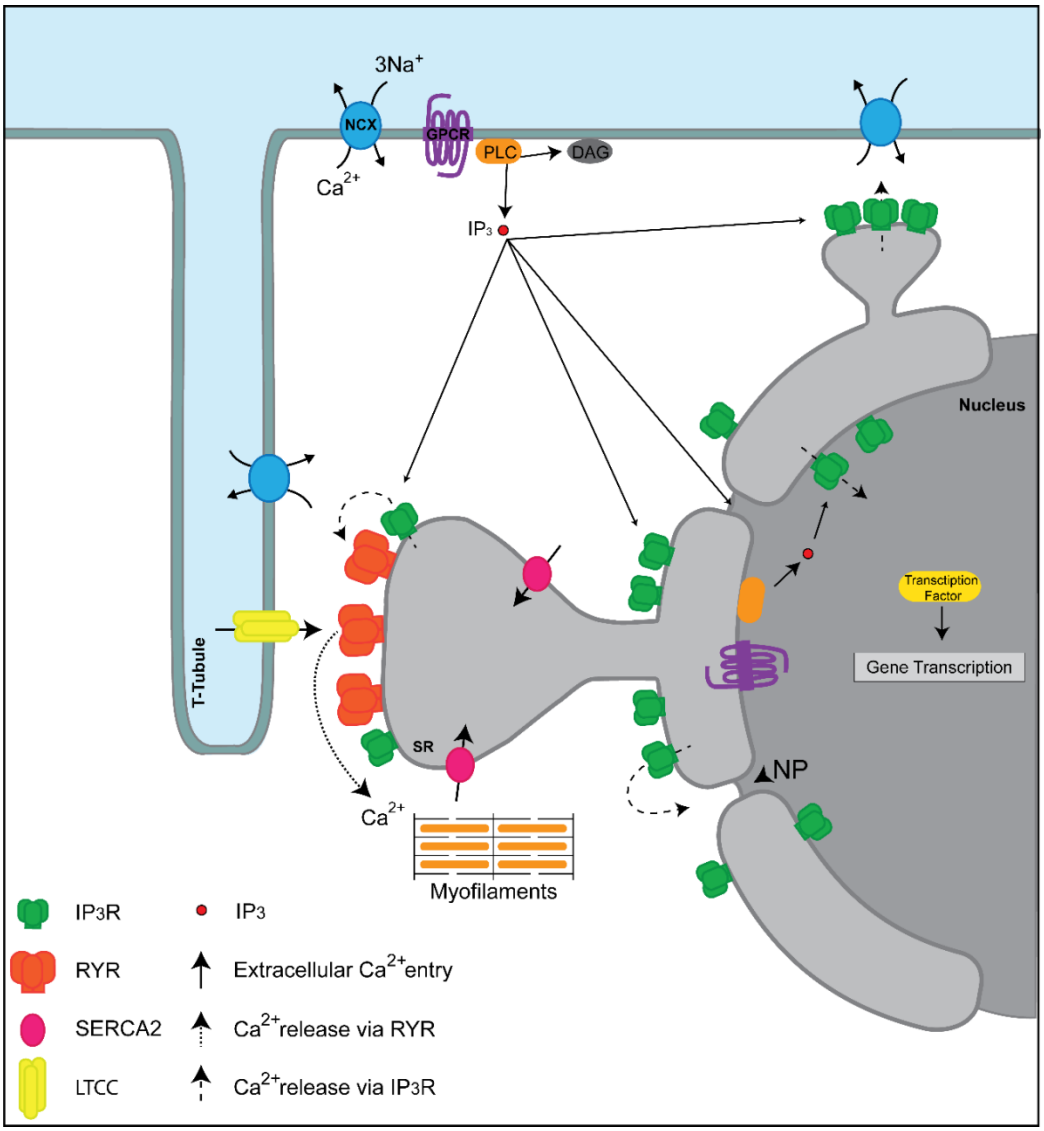

Illustration 2:Different roles of IP_3R in the heart.
Activation of GPCRs coupled to PLC such as the ET_A receptor lead to the production of IP_3 and diacylglycerol. IP_3 then diffuses through the cytosol to bind and activate IP_3R channels. IP_3-mediated calcium release can modulate CICR and muscle contraction via modulation of RYR activity. Nuclear/perinuclear IP_3Rs are tough to modulate gene transcription.

IP_3R-2 is thought to be the predominant isoform found in the heart. Consequently, most of the studies that focus on the role of IP_3R in the heart have focused solely on IP_3R-2 function [118, 119]. Global genetic knockout of the IP_3R-2 in mice does not cause any significant difference in the hypertrophic response in pressure overload or dilated cardiomyopathy mouse models [120]. However, the potential involvement of IP_3R-1 and IP_3R-3 activity was not investigated further. Another group showed that global knockout of IP_3R-2 eliminates the positive inotropic effects of endothelin-1 (ET-1) in the atria and protects against arrhythmias [121]. In support of a role of IP_3R-2 in regulating cardiac hypertrophy, transgenic overexpression of the channel in the heart was sufficient to induce mild hypertrophy and exaggerated responses to ET-1 [50]. Targeted inducible overexpression of the IP_3-binding site of the IP_3R-1, also known as the IP_3"sponge", was used to block cardiac signaling through all IP_3R channels [50, 122]. The IP_3 sponge acts by sequestering IP_3 generated by PLC-coupled agonists and preventing the activation of endogenous IP_3R channels. The IP_3 sponge inhibited hypertrophy in response to isoproterenol and angiotensin-II, but not a pressure overload model (transverse aortic constriction) [50]. Using an ischemic model (left anterior descending artery ligation), cardiac-specific deletion of the IP_3R-2 lead to improved cardiac function, reduced cell death, and reduced cardiac fibrosis [123], but did not reduce mitochondrial calcium overload and dysfunction [124]. Thus, there are numerous conflicting reports in mouse models that suggest that IP_3R-2 may (or may not) contribute to cardiac physiology and dysfunction in

disease. However, there is a general consensus that the IP_3R-2 protein contributes at the very least to signaling downstream of ET-1 stimulation.

There have been few attempts to elucidate the role of IP_3R-1 and IP_3R-3 in the heart, either *in vitro* or *in vivo*, despite measureable expression levels [53, 54, 71, 116, 118, 120, 125, 126]. This may lead to erroneous conclusions regarding IP_3R function in the heart using IP_3R-2 mouse models, as several groups have reported that all three IP_3R isoforms are expressed in the heart with detectable mRNA and protein levels in mouse, rat and human ventricular cardiomyocytes (**Table 1**). In addition to total expression levels, the subcellular localization and precise aspects of how IP_3Rs regulate spatio-temporal aspects of calcium release in the contracting myocyte is an area of debate. In particular, how IP_3R signals are decoded to regulate processes such as transcriptional activation in the beating cardiomyocyte is unclear. IP_3Rs are known to be mainly localized at the ER/SR membranes in most cells, however in the heart it is thought to be concentrated at the nuclear and perinuclear membranes, where it is thought to play a key role in gene transcription [45, 125, 127, 128]. There is an abundant amount of evidence that suggests that the IP_3R and IP_3 producing machinery is localized in or adjacent to the nucleus of several cell types including cardiomyocytes [129-132], and this localization is thought to be important for spatially restricting calcium transients mediated by this channel to the nuclear matrix. It has been shown that IP_3 and ET-1 can trigger nuclear calcium sparks and nuclear localized calcium transients [125, 127, 128, 133, 134]. However, other studies argue against this notion and suggest that IP_3Rs are localized at the perinuclear membrane area, and IP_3-induced

calcium transients from the cytosol can diffuse into the nucleus to increase nuclear calcium[45, 86, 135, 136]. Indeed, as the nuclear pore is freely permeable to calcium it is unclear why an intranuclear IP_3R channel would be required. The IP_3R has been shown to activate different transcription factors that initiate hypertrophic remodeling induced by hormonal stimulation such as ET-1 and angiotensin II (AngII) [45, 50, 137]. In turn, IP_3R calcium release activates calcium sensitive proteins such as calcineurin and CamKII leading to activation of transcription factors that are known to be localized in the cytoplasm such as NFAT or the nucleus such as HDAC5 [45, 127]. The role of NFAT in hypertrophic remodeling has been well studied [49, 50, 128, 138] and it has been shown that NFAT de-phosphorylation and nuclear translocation leads to expression of different genes and microRNAs (miRs) that modulate hypertrophic remodeling of the heart such as atrial natriuretic peptide (ANP), brain natriuretic peptide (BNP), and miR-23a [45, 138, 139]. As mentioned previously, the IP_3R nuclear/perinuclear localization is proposed as a mechanism by which IP_3Rsare able to specifically activate nuclear calcium transients without the disruption of the cytosolic calcium signals that are mediated by the RYR [45]. Experiments using calcium chelators targeted to the nucleus have shown quite definitely that nuclear calcium is required for hypertrophic gene expression [45], however this does not discriminate whether the calcium signal originated in the cytosolic compartment. Studies using a combination of nuclear and cytosolic chelators support the notion that IP_3R-dependent calcium transients originate in the cytosol and translocate to the nucleus [140]. It should be noted that most studies have relied on confocal imaging

to infer “nuclear only” calcium transients, which is indirect at best. The use of genetically encoded calcium indicators targeted to the nucleus is a much more direct method, and has already been used to evaluate nuclear transients evoked by various stimuli [140]. However, additional experimental work needs to be done in order to completely understand how nuclear calcium is regulated in the healthy and diseased heart.

Calcium is directly responsible for cardiac contraction and relaxation. RYRs are the main modulators of the SR calcium release mediating excitation-contraction coupling (ECC) in cardiomyocytes. ECC is a process by which an action potential triggers a contraction via L-type calcium channel opening and subsequent RYR activation. IP_3Rs have been also shown to modulate ECC both in ventricular and atrial cardiomyocytes [118, 141]. However, the role of IP_3Rs in ventricular ECC is controversial due to lower expression levels in ventricular cardiomyocytes (at least as determined by mRNA levels) compared to other cell types such as atrial cardiomyocytes [55, 118]. Indeed, it has been suggested that IP_3R signaling does not contribute to the positive inotropic effects of ET-1 in ventricular cardiomyocytes [119]. In atrial cardiomyocytes the role of IP_3Rs has been extensively studied. It has been shown that after neurohormonal stimulation, IP_3R can modulate ECC by increasing action potential (AP) amplitude, calcium spark frequency, and by creating spontaneous calcium transients [118, 142]. In healthy ventricular cardiomyocytes, IP_3R is found in perinuclear/nuclear areas and near the RYRs at the dyadic cleft. IP_3R localization at the SR/dyadic cleft is believed to also modulate ECC in ventricular cardiomyocytes, and is characterized

by increasing AP amplitude, increasing spontaneous calcium transient frequency, and decreasing resting membrane potential [53, 54, 141]. It is well established that IP_3R expression is increased in cardiac hypertrophy, heart failure, dilated cardiomyopathy, spontaneously hypertensive rats, and in transverse aortic constriction (TAC) models [52-55]. It was found that the increase in IP_3R expression was observed mainly in the dyadic cleft of salt hypertensive rats, and that IP_3Rs may contribute to ECC during disease by sensitizing nearby RYR for activation [53]. In disease states there are alterations in t-tubule morphology that compromise L-type channel/RYR coupling, and therefore an increase in IP_3Rs expression could be a way to compensate for the decreased coupling in failing heart by promoting CICR. A more recent study showed that failing human ventricular cardiomyocytes have a reduction in the resting membrane potential and AP prolongation, and suggested that IP_3Rs might modulate ECC using an alternative mechanism [54]. This report found that IP_3Rs are localized to specific domains in the cardiomyocyte that lack RYR, and IICR results in direct activation of NCX leading to AP prolongation and alterations in electric properties of cardiomyocytes [54]. Overall these studies indicate that IP_3R localization to the SR/ER leads to modulation of ECC in ventricular cardiomyocytes, providing a potential explanation for left ventricular arrhythmias.

Table 1

Isoform studied	Species or cell type used	Localization	Isoform (mRNA)	Isoform (protein)	Method of detection	Year Published	Comments	Ref
1	ARVM	ND	IP_3R-1	IP_3R-1	mRNA: In situ hybridization Protein: Immunohistochemistry	1993		[116]
1 **2** **3**	Adult rat heart	ND		IP_3R-1 IP_3R-2 IP_3R-3	Protein: Western blot	1995		[71]
1	HLV myocardium (Healthy and CHF)	ND	IP_3R-1		mRNA: In situ hybridization HLV myocytes Northern blot of HLV, HRV and septum	1995		[55]
1 **2** **3**	Adult mouse heart	ND	IP_3R-1 IP_3R-2 IP_3R-3		mRNA: RT-PCR	1997	Relative expression of each isoform: P_3R-1 (6.1%) IP_3R-2 (78.0%) IP_3R-3 (15.9%).	[143]
1 **2** **3**	Rat and ferret isolated ventricular myocytes	ND	IP_3R-1 IP_3R-2 IP_3R-3		mRNA: RT-PCR Protein: Immunoblotting	1997	Relative expression of each isoform: P_3R-1 (1.9%) IP_3R-2 (84.6%) IP_3R-3 (13.5%). At the protein level they looked at IP_3R-1 expression and it wasn't found in rat cardiac myocytes	[117]
1 **2** **3**	3 week old rats with cardiac hypertrophy	ND	IP_3R-1 IP_3R-2		mRNA: in situ hybridization	1998		[144]
1 **2** **3**	ARVM and atrial cardiomyocytes	IP_3R-2 localized near the sarcolemma	IP_3R-1 IP_3R-2 IP_3R-3	IP_3R-1 IP_3R-2	mRNA: RT-PCR Protein: Western blot	2000	At the mRNA level IP3R-2 is the most predominant isoform. At the protein level IP_3R-1 and -2 are the most abundant in ARVM.	[118]

		and RYR in atrial myocytes						
1 **2**	Neonatal Mouse cardiomyocytes	Striated localization SR pattern		IP_3R-1 IP_3R-2	Protein: Immunofluorescence	2002		[126]
2 **3**	Rabbit atrial and ventricular myocytes	ND		IP_3R-2 IP_3R-3	Protein: Western blot	2007	IP_3R-2 and -3 are more abundant in atrial myocytes compared to ventricles.	[142]
1 **2** **3**	NRVM	IP_3R-2 found at the nuclear envelop IP_3R-3 found at the cytosol	IP_3R-1 IP_3R-2 IP_3R-3	IP_3R-2 IP_3R-3	mRNA: RT-PCR Protein: Western blot and immunofluorescence	2008	All the IP_3R isoforms were detected at the mRNA level. Only IP_3R-2 and -3 were detected at the protein level.	[125]
2	NRVM and ARVM	Perinuclear localization in NRVM Surrounding the nuclei and sarcoplasmic reticulum in ARVM		IP_3R-2	Protein: immunofluorescence	2009		[45]
1 **2** **3**	ASHR, normotensive WKY. HLV failing hearts	In WKY mainly nuclear and sarcoplasmic localization. In ASHR mainly localized at the SR, and co-localized with RYR2	IP_3R-2	IP_3R-2	mRNA: RT-PCR Protein: Immunofluorescence and Western blot	2009/2010	They looked at IP_3R-1 and IP_3R-3 protein expression by western blot. IP_3R-1 and -3 is not found in ASHR or WKY cardiac myocytes	[52, 53]
2	AMVM	Sarcoplasmic localization		IP_3R-2	Protein: Immunofluorescence and western blot	2010		[50]
1 **2** **3**	AMVM		IP_3R-1 IP_3R-2 IP_3R-3	IP_3R-2	mRNA: RT-PCR Protein: Western blot	2013		[120]

1 **2** **3**	HLV myocytes and MLV myocytes	IP_3R-1 IP_3R-2 IP_3R-3	IP_3R-2	mRNA: RT-PCR Protein: Western blot	2013	They used a pan-antibody to look at the protein expression of all 3 IP3R isoforms	[54]

ARVM, adult rat ventricular myocytes; HLV, Human left ventricle; CHF, Congestive heart failure; ND; Not determined; NRVM, Neonatal rat ventricular myocytes; ASHR, Adult spontaneously hypertensive rat; WKY, normotensive Wistar-Kyoto; AMVM, Adult mouse ventricular myocytes; MLV, Mice left ventricle.

Table 1: Expression of the different IP_3R isoforms in the heart.

RE-EVALUATING IP_3R EXPRESSION AND FUNCTION IN THE HEART

IP_3Rs are the primary regulators of intracellular calcium release in many cells. However, the dominant role of RYR in modulating calcium changes in the heart has made investigating the role of IP_3R signaling challenging. IP_3R was first shown to be expressed in cardiac myocytes over 20 years ago [116]. This seminal study was the first to show that IP_3R-1 was expressed in the heart. It was subsequently shown that IP_3R-1 is upregulated in human chronic heart failure tissue, whereas RYR2 expression was significantly reduced [55]. It was concluded that IP_3R-1upregulation might be an alternative pathway to stabilize calcium homeostasis in end-stage heart failure [55]. Despite these early reports suggesting IP_3R-1 may have a functional role in the heart a series of studies emerged indicating that, at least at the mRNA level, IP_3R-2 predominates in both atrial and ventricular cardiomyocytes (**Table 1**).

More recently, the mRNA expression levels of the different IP_3R isoforms have been re-evaluated in both human and mouse tissue [54]. It was found that the relative expression level of the receptors varies between both species (human IP_3R-3>IP_3R-1>IP_3R-2 and mouse IP_3R-2> IP_3R-1> IP_3R-3). As mentioned above, a large amount of work using transgenic/knockout animals have suggested that IP_3R-2 plays at least some role in cardiac physiology [50, 121, 123], however this is quite controversial [120, 124]. This leads to the question as to whether IP_3R-1 or -3 are able to compensate for IP_3R-2 deficiency in mouse models. Unfortunately IP_3R-1/2 double knockout mice are lethal; however it is theoretically possible to make a conditional knockout of all three IP_3Rs in the heart. In addition, *in vitro*

studies with targeted knockdown or knockout of individual isoforms in cardiomyocytes would be a useful endeavor to elucidate the potential functional redundancy of these isoforms in regulating cardiomyocyte physiology.

Finally, it is also important to note that some of the literature evaluating cardiomyocyte function *in vitro* use 2-APB and Xestospongins as dubious pharmacological inhibitors of IP_3R-mediated calcium release. It is now very well established that 2-APB has many off target effects and is a poor inhibitor of the IP_3R [145, 146] and Xestospongins do not inhibit the channel at all [146]. Thus, interpretation of studies using these agents needs to be approached with extreme reservation. Indeed, the significant number of studies demonstrating that Xestospongins have an effect on IICR in cardiomyocytes is somewhat concerning. Future studies using transgenic, RNAi, or CRISPR approaches will allow more specific elucidation of the phenotype of loss of IP_3R channels in cardiomyocyte signaling events.

Chapter 2: Experimental Method

Modified in part from:

Functionally redundant control of cardiac hypertrophic signaling by inositol 1,4,5-trisphosphate receptors

M. IvethGarcia[a, b], Anja Karlstaedt[c], Javier Amione-Guerra[d], Keith A. Youker[d], Heinrich Taegtmeyer[c], and Darren Boehning[b]

[a]Cell Biology Graduate Program, University of Texas Medical Branch, Galveston, TX 77555; [b]Department of Biochemistry and Molecular Biology, McGovern Medical School at UTHealth, Houston, TX 77030; [c]Department of Internal Medicine, Division of Cardiology, McGovern Medical School at UTHealth, Houston, TX 77030. [d]Houston Methodist Hospital, Houston, TX 77030.

And

Genetically Encoded Calcium Indicators for Studying Long-Term Calcium Dynamics During Apoptosis.

M. IvethGarcia[a,b] , Jessica J. Chen[b] , Darren F. Boehning[b]

[a]Cell Biology Graduate Program, University of Texas Medical Branch, Galveston, TX 77555, [b]Department of Biochemistry and Molecular Biology, McGovern Medical School at UTHealth, Houston, TX 77030.

MATERIALS AND ANTIBODIES

Rabbit polyclonal antibody against type-1 IP_3R was developed in-house and is specific for the type-1 isoform [78]. The rabbit polyclonal antibody against type-2 IP_3R have been described elsewhere [71] and was kindly provided by Dr. Richard Wojcikiewicz (SUNY Upstate). Mouse monoclonal anti-IP_3R type-3 was purchased from BD Bioscience. Mouse monoclonal anti-α-actinin and anti-ryanodine receptor antibody was purchased from Sigma-Aldrich. Mouse anti-SERCA2 antibody was from ThermoFisher and rabbit anti-ANP was purchased from Abcam. Anti-alpha-fodrin was purchased from EMD Millipore. Secondary antibodies conjugated to Alexa-488 and Alexa-555 were from Molecular Probes, and peroxidase-conjugated antibodies were from Jackson ImmunoResearch. Expression constructs 9X NFAT-apha-MHC-Luc was a gift from Jeffery Molkentin (Addgene plasmid # 51941), pGP-CMV-GCaMP6s and 6f was a gift from Douglas Kim ([147]; Addgene plasmid # 40753 and 40755), and Tol2-elavl3-H2B-GCaMP6s was a gift from Misha Ahrens (Addgene plasmid # 59530). Endothelin-1 was purchased from Bachem. Silencer pre-design siRNAs were purchased from Ambion. Lipofectamine 2000 and 3000 were purchased from Invitrogen. Fura-2 AM was purchased from Molecular Probes, and the dual luciferase reporter assay kit was from Promega. All other reagents were purchased from Sigma-Aldrich.

CELL LINES

HeLa, H9c2,HEK 293T and AR42J cells were purchased from ATCC and maintained in DMEM supplemented with 10% FBS and 1% penicillin/streptomycin and kept in an incubated atmosphere maintained at 37°C and 5% CO_2.

TRANSFECTIONS OF H9C2, HELA,HEK 293T AND AR42J CELLS

HeLa cells were transfected usinglipofectamine 2000 following manufacturer's instructions. The total amount of GCaMP6 cDNA transfected into HeLa cells was 2µg per 400,000 cells. Experiments were carried out 24 hrs after transfection. H9c2 cells were transfected using lipofectamine 3000 following manufacturer's instructions. H9c2 were transfected with total amount of siRNA targeting each specific IP_3R's (12.5 pmol per 400,000 cells). HEK 293T and AR42J cells were transfected with lipofectamine 3000 with specific siRNAtargeting each IP_3R total amount of siRNA 12.5 pmol per 400,000 cells.

HISTAMINE-INDUCED CALCIUM RELEASE MEASURMENTS

HeLa cells were incubated with 5 µM Fura-2 AM (Molecular Probes) in imaging solution (1% BSA, 107mM NaCl, 20 mM HEPES, 2.5 mM $MgCl_2$, 7.5 mMKCl, 11.5mM glucose, and 1 mM $CaCl_2$) for 30 min at RT. The solution was replaced with imaging solution without Fura-2 AM for an additional 20 min. Images were acquired using a Nikon TiS inverted microscope as previously described [79]. After transfection, responses to 0.1µM, .5µM, 1µM, and 10µM of histamine were recorded via excitation at 340 nm, 380 nm (Fura-2 AM) and 480 nm (GCAMPs) in 3 seconds intervals during continuous recording. GCaMP6 calcium traces are expressed as the ratio relative to resting fluorescence ($\Delta F/F_0$). Fura-2 calcium traces are expressed as the ratio of fluorescence emitted at two different excitations wavelengths (340/380 nm).Percent responders and peak release was determined manually. A calcium transient was counted when the Fura-2 ratio rose

10% above the baseline ratio. Similar to Fura-2, a calcium transient was counted when GCaMP6 fluorescence rose above 5% from baseline fluorescence. All measurements are representative of a minimum of three independent experiments.

Staurosporine-Induced Calcium Release Measurements

Coverslips with GCaMP6s transfected HeLa cells were mounted in an imaging chamber and bathed in Leibovitz's L-15 media at room temperature and allowed to rest for 30 min. Images were captured every 60 seconds on a Nikon TiS inverted microscope with a 40x oil objective. Baseline fluorescence (F_0) was determined by using the average intensity of the first 20 images before treatment. Cells were imaged for up to 10 hrs after treatment with 10μM staurosporine (or DMSO for control). A calcium release event was defined as a 1.5-fold rise in fluorescence intensity over the baseline ($\Delta F/F0>1.5$).

Caspase-3 Enzymatic Assays

HeLa cells were treated with 10μM staurosporine or DMSO in L-15 media with 10% FBS and 1% penicillin/streptomycin at room temperature (25°C) for 2-12 hrsto recapitulate the conditions used to image long-term calcium. Cell lysates were collected every 2 hours and enzymatic determination of DEVDase (caspase-3-like) activity was performed as described previously [47]. All results are presented as means±SEM. Statistical comparisons were performed using an unpaired t-test. A p value of < 0.05 was considered statistically significant.

PREPARATION OF PRIMARY NEONATAL CARDIOMYOCYTES

Neonatal rat ventricular cardiomyocytes (NRVM) were obtained from 1 to 2 day old Sprague-Dawley rat hearts as previously described, with minor modifications [148]. Cardiomyocytes were plated into fibronectin-coated culture dishes and incubated at 37°C in 5% CO_2 incubator. Two days after plating, media was replaced with 50% Ham's F10 - 50% DMEM culture medium with β-D-arabinofuranoside (ARA-C; 1 µM) to inhibit growth of fibroblasts. NRVMs were transfected using Lipofectamine 3000 following manufacturer's instructions. All experiments were carried out 48 hours after transfection. All vertebrate animal procedures were approved by the Animal Welfare Committee (AWC) at UTHealth.

PREPARATION OF PRIMARY ADULT CARDIOMYOCYTES

Calcium-tolerant adult rat ventricular myocytes (ARVM) were isolated from hearts of wildtype Sprague-Dawley rats (300 – 320 g) as described by Louchet. al.[149]. Briefly, animals were anesthetized with chloralhydrate (400mg/kg b.w. i.p.) and heparinized (5,000 U/kg b.w.) via direct injection into the vena cava inferior. The hearts were aseptically removed and directly placed in ice-cold Krebs-Henseleit (KH) buffer (133.5 mMNaCl, 4 mMKCl, 1.2 mM NaH2PO4, 10 mM HEPES, 1.2 mM MgSO4, 10 mM BDM) containing glucose (5.5 mM) before being perfused with a Langendorff preparation. Perfusion (3 min) with KH buffer at 37°C lacking Ca2+ was followed by perfusion with recirculating KH buffer containing 2% BSA (wt/vol), 50 µM Ca2+ and type II collagenase. After 20 minutes of perfusion, hearts were minced, and undigested tissue was separated with a 230 µm mesh sieve. The cell

suspension was allowed to settle with gravity within 5 to 7 min, and the cell pellet was re-suspended in KH containing 2% BSA (wt/vol), and calcium was slowly reintroduced to a final concentration of 1 mM. Cardiomyocytes were plated and culture under 5% carbon dioxide.

IMMUNOFLUORESCENCE LABELING OF ISOLATED CARDIOMYOCYTES

Adult and neonatal cardiomyocytes were plated at a density of 300 cells per mm^2 on glass coverslips coated with fibronectin. On day 4 the medium was exchanged and the cells were treated with 100 nM ET-1 for 48 hrs. Cells were fixed with 4% paraformaldehyde in PBS. Briefly, cells were incubated with either rabbit polyclonal anti-IP_3R-1 (1:250), rabbit polyclonal anti-IP_3R-2 (1:250), mouse monoclonal anti-IP_3R-3 (1:250), mouse monoclonal anti-α-actinin (1:250), mouse anti-SERCA2 (1:250), or mouse anti-ryanodine2 (1:250), overnight at 4°C. Followed by incubation with secondary antibodies conjugated to Alexa-488 and Alexa-555 for 1 hr.

IMMUNOFLUORESCENT LABELING OF HUMAN HEART FAILURE SAMPLES

Disease heart tissue was obtained from patients undergoing heart transplantation due to advanced heart failure. Immediately after explant the tissue is flash frozen with liquid nitrogen for future analyses. Control heart tissue was obtained from organs that were declined for transplantation due to non-cardiac reasons. Frozen left ventricular cardiac tissues were cryo-sectioned onto charged glass slides. The

sections were fixed with 4% paraformaldehyde in PBS. Tissue was stained with anti-IP_3R-1 (1:100), anti-IP_3R-2 (1:100), anti-IP_3R-3 (1:100), or anti-α-actinin (1:100), for 1hr at 37°C. Subsequently, slides were washed and incubated with secondary antibodies conjugated to Alexa-488 and Alexa-555 for 1 hr. All experiments on human samples were approved by the Institutional Review Board (IRB) of UTHealth.

CELL SIZE DETERMINATION

NRVM were plated on glass coverslips. Two days after plating cells were transfected with control siRNA or triple IP_3R siRNA. Following transfection cells were treated with ET-1 for 48 hours. After treatment cells were fixed with 4% paraformaldehyde in PBS. Subsequently, coverslips were stained with anti-α-actinin and secondary antibodies conjugated to Alexa-555. For measurement of cell area, at least 30 fields randomly chosen were analyzed in each coverslip. Cardiomyocytes area was measured in captured images using ImageJ software.

CYTOSOLIC AND NUCLEAR CALCIUM IMAGING

NRVM were plated on fibronectin-coated glass coverslips and were transfected with triple IP_3R siRNA targeting rat IP_3R-1, IP_3R-2 and IP_3R-3. The total amount of siRNA transfected was 12.5 pmol per 350,000 cells. Transfected cells were identified by co-transfection with cDNA for YFP (0.25pmol per 350,000 cells). Cells were imaged after 48 hrs. For imaging, cardiomyocytes were incubated with 5 μM

Fura-2 AM in imaging solution (1% BSA, 107mM NaCl, 20 mM HEPES, 2.5 mM $MgCl_2$, 7.5 mMKCl, 11.5mM glucose, and 1 mM $CaCl_2$) for 30 min at RT. The solution was replaced with imaging solution without Fura-2 AM for an additional 20 min. Images were acquired using a Nikon TiS inverted microscope as previously described [79]. Responses to 100 nM ET-1 were recorded on YFP only positive cells. In order to specifically look at nuclear calcium transients we used GCaMP6s fused to a sequence encoding human histone H2b at the 5′ end [150]. We sub-cloned H2b-GCAMP6s into the mammalian expression vector pcDNA 3.1(+).NRVM were transfected with different siRNAs (IP_3R-1, IP_3R-2 or IP_3R-3) and with H2b-GCAMP6s two days after plating. Cells were loaded with Fura-2 AM in imaging solution 48 hrs after transfection. Responses to 100nM ET-1 were acquired at 1 Hz during continuous recording. Oscillation frequency was determined manually. An oscillation was counted when the Fura-2 ratio rose 10% above the baseline ratio. Similar to Fura-2, an oscillation was counted when GCaMP6s fluorescence rose above 5% from baseline fluorescence

NFAT LUCIFERASE ASSAY

For assessment of NFAT activation cells were co-transfected with 9xNFAT-TATA luciferase plasmid [151] and pRL-TK control vector (2:1). All experiments were performed 48 hours after transfection. Cells were harvested and cell extracts were assayed using dual luciferase reporter assay as specified by manufacturer's protocol (Promega). All data are shown as mean ± SEM, with statistical significance determined at $p < 0.01$ vs control using an unpaired Student's t-test.

Chapter 3: Genetically Encoded Calcium Indicators for Studying Long-Term Calcium Dynamics During Apoptosis

Modified in part from:

Genetically Encoded Calcium Indicators for Studying Long-Term Calcium Dynamics During Apoptosis.

M. IvethGarcia[a,b] , Jessica J. Chen[b] , Darren F. Boehning[b]

[a]Cell Biology Graduate Program, University of Texas Medical Branch, Galveston, TX 77555, [b]Department of Biochemistry and Molecular Biology, McGovern Medical School at UTHealth, Houston, TX 77030.

INTRODUCTION

Calcium is a secondmessenger that is widely involved in almost all cellular processes, including orchestrating apoptotic signaling[62, 152, 153]. To investigate the spatial and temporal regulation of intracellular calcium signals, many fluorescent calcium indicators have been developed. The firstfluorescent calcium indicators were based on the highly selective calcium chelator 1,2-bis(o-aminophenoxy)ethane-N,N,-N',N'-tetraacetic acid (BAPTA) [154]. Identification of derivatives that exhibit a shift in excitation wavelength upon binding calcium was advantageous since taking the ratio of fluorescence intensity at each excitation wavelength corrected for differences in dye loading and allowed for more

quantitative measurements. Many of such “ratiometric”calcium indicators have been developed, including Fura-2, Indo-1 and Fura Red, each with different affinities for calcium and excitation/emission wavelengths [155-157]. Some of the major limitations of ratiometric indicators include the low temporal resolution resulting from the requirement to monitor at two excitation or emission wavelengths and relatively small dynamic ranges [157]. To resolve these problems, single-wavelength indicators, including fluo-3 and 4, rhod-2 and Oregon Green BAPTA, were developed [158, 159]. These indicators show large changes in fluorescence intensity upon binding of calcium and exhibit a wide variety of kinetic and spectral properties.

To study calcium transients in distinct cell types or in subcellular organelles, researchers developed genetically encoded fluorescent calciumindicators. These indicators are based upon conferring calcium sensitivity to green fluorescent protein (GFP) variants using eitherFörster resonance energy transfer (FRET) pairs or circularly permutated GFP mutants[160-163]. GCaMPs are among the most widely used genetically encoded indicators and consist of circular permutated green fluorescent protein, calmodulin, and a calmodulin binding motif derived from skeletal muscle myosin light chain kinase (M13 peptide)[162, 164]. Once bound to calcium, GCaMPundergoes a conformational change that leads to an increase in fluorescence intensity [162]. There have been several iterations of GCaMP to optimize the sensitivity and kinetics [165-167]. Among the most recent GCaMP derivatives are GCaMP6s, 6m and 6f (for slow, medium and fast kinetics), all of

which have greatly improved brightness andlarger dynamic ranges compared to their predecessors [147, 168].

Given the wide variety of calciumindicators it is important to choose the most suitable indicators based on the magnitude and duration of calcium transients, which depends heavily on the type of cell and the stimuli presented. Many factors, including affinity, kinetics, sensitivity and signal-to-noise ratio contribute to the choice of calcium indicator for a specific study. As an example, high affinity indicators tend to buffer calcium transients and show a slow rise to peak and a prolonged signal. Therefore, to detect rapid calcium transients such as those in neurons, indicators with faster kinetics and lower affinity to calcium are preferred [169] such as afforded by GCaMP6f[147]. However, indicators with higher sensitivity and brighter fluorescence such as GCaMP6s may have more utility in detecting small changes in calcium or in those cases where fast kinetics are not necessary such as during the relatively slow process of apoptotic calcium release [78]. The timing from the initiation of apoptosis to completion spans over several hours [47, 78, 84, 170-172]. Therefore, long-term imaging is required to monitor calcium release during apoptosis. To perform long-term imaging using synthetic calcium dyes, previous studies had to sequentially image multiple coverslips every 30 min to account for photobleaching and artifacts arising from UV illumination of living cells[78, 172]. In theory, genetically encoded calcium indicators would overcome most of these limitations and facilitate monitoring of intracellular calcium over protracted time courses.

In this study, we found that GCaMP6s and 6f perform as well as Fura-2 in reporting intracellular calcium elevations induced by histamine stimulation of HeLa cells. The indicator GCaMP6s outperformed Fura-2 in detecting release events induced by low concentrations of agonist. We next used GCaMP6s to monitor staurosporine-induced calcium transients over the course of 10 hours. We were able to continuously monitor cytosolic calcium during cell death revealing the kinetics of calcium release and surprising heterogeneity in the responses to staurosporine. Our results support of the utility of GCaMP6s as a general purpose calcium indicator protein with several properties superior to dye-based methodologies, especially for long-term imaging.

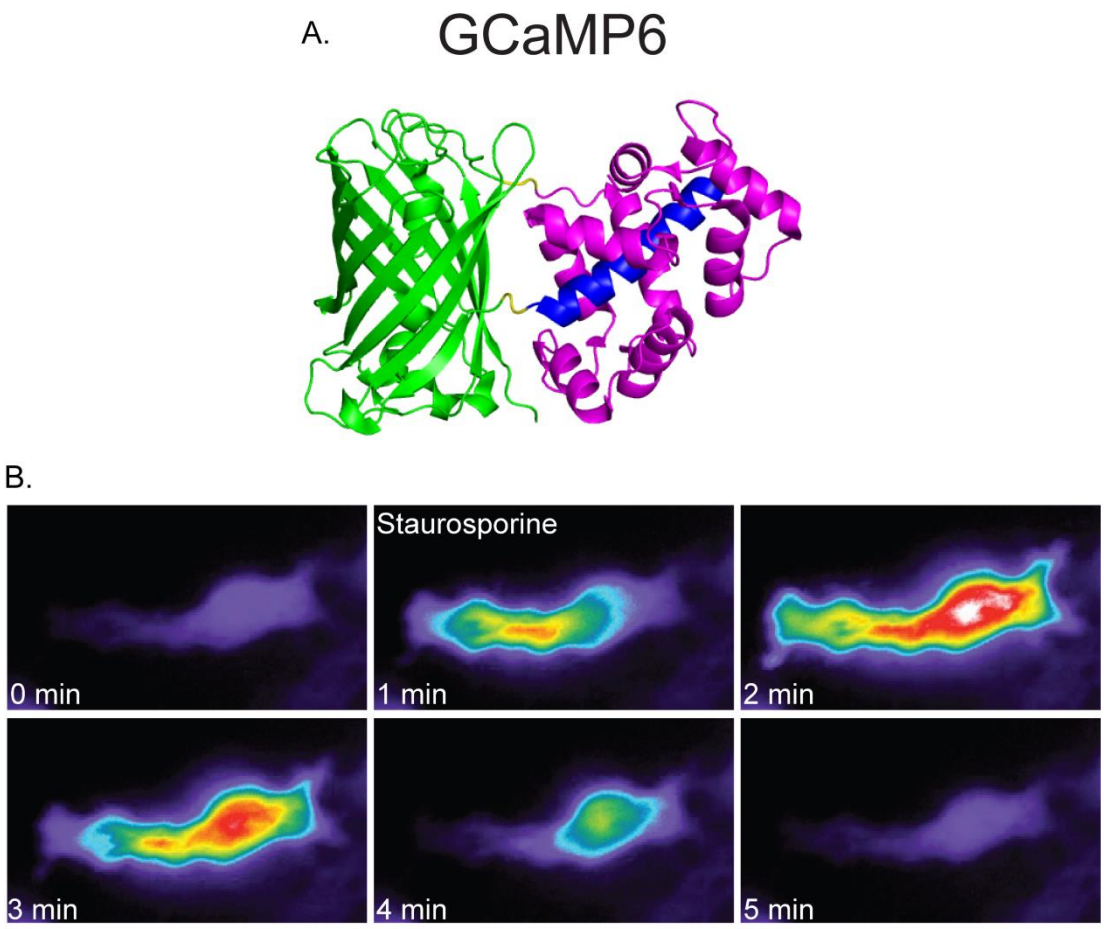

Illustration 3: Genetically encoded calcium indicator GCAMP6.
A.Schematic of GCAMP6 structure colored by domains: green, circular permutated GFP; yellow, linker 1 and linker 2; magenta, CaM; blue, M13 peptide. **B**. Time lapse images of a single cell which shows an increase in fluorescence intensity after binding of calcium in response to STS.

RESULTS

Histamine-Induced Calcium Release Measurments using Fura-2, GCaMP6s, and GCaMP6f

We first compared the performance of GCaMP6s and GCaMP6f with Fura-2 in HeLa cells. We quantified the calcium release kinetics in response to a dose response of histamine ranging from 0.1µM to 10µM. In general, both GCaMP6 indicator proteins performed similarly to Fura-2 at detecting calcium transients in the cytosol evoked by histamine (**Fig. 3-1A**). Quantitatively, GCaMP6s was more efficient at detecting calcium release events evoked by low (0.1µM) concentrations of histamine in HeLacells compared to GCaMP6f and Fura-2 (**Fig 3-1D**). Fura-2 has moderately better performance at detecting events evoked by 0.5µM and 1µM histamine (**Fig 3-1B-D**). The indicator GCaMP6f was the least sensitive reporter at detecting release events at all concentrations of histamine. To compare peak calcium release induced by histamine stimulation between the three indicators, we normalized calcium release at subsaturating concentrations of histamine as a percentage of the response to a saturating histamine (10µM, **Fig 3-1F-G)**. In those cells that responded to histamine, Fura-2 detected larger release events compared to both GCaMP6 proteins. GCaMP6s performed similarly to Fura-2 at all concentrations except 0.1µM. The indicator GCaMP6f performed significantly worse that the other two indicators at reporting peak release of calcium. These data indicate that GCaMP6s performs similarly to Fura-2 at detecting agonist-induced calcium release, and may outperform Fura-2 at detecting small release events at subsaturating concentrations of agonist

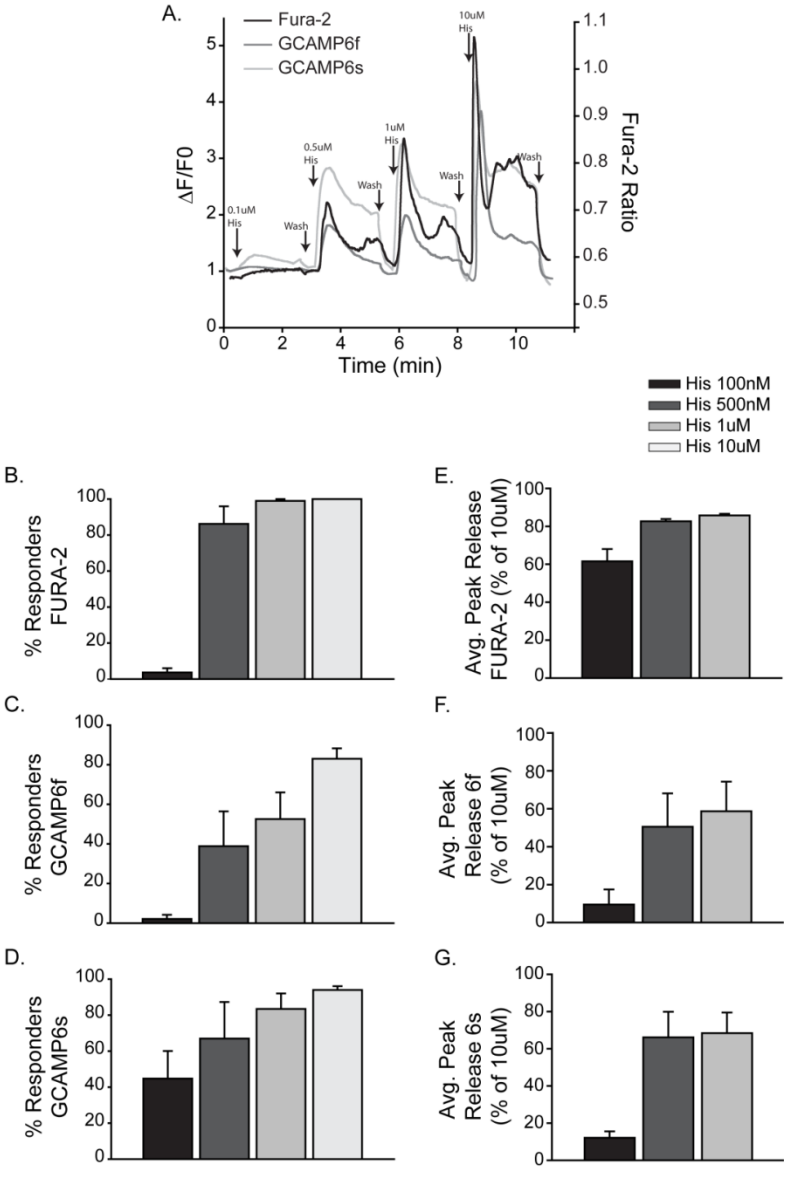
A.
Fura-2
GCAMP6f
GCAMP6s
ΔF/F0
Fura-2 Ratio
Time (min)
0.1uM His
Wash
0.5uM His
Wash
1uM His
Wash
10uM His
Wash
His 100nM
His 500nM
His 1uM
His 10uM
B.
% Responders FURA-2
C.
% Responders GCAMP6f
D.
% Responders GCAMP6s
E.
Avg. Peak Release FURA-2 (% of 10uM)
F.
Avg. Peak Release 6f (% of 10uM)
G.
Avg. Peak Release 6s (% of 10uM)

Figure 3-1: Comparison of Fura-2 to GCaMP6s and GCaMP6f in measuring agonist-induced calcium release.
A. Representative single cell traces showing calcium changes in HeLa cells incubated with Fura-2 or expressing GCAMP6f/GCAMP6s in response to increasing concentrations of histamine (0.1µM, 0.5µM, 1µM and 10µM). Fluorescence signals are scaled as $\Delta F/F_0$ (GCaMP6 proteins) and Fura-2 fluorescence signals are presented as the 340/380nm ratio. **B-D**. Bar graphs show percent of cells that show a change in fluorescence in response to increasing concentrations of histamine (% responders). The total number of cells quantified is as follows: Fura-2 (n=92), GCaMP6f (n=103) and GCaMP6s (n=179). **E-G.** Peak release in response to different concentration of histamine (0.1µM, 0.5µM and 1µM) was analyzed for each calcium indicator. Peak release is reported as percent of saturating dose of histamine (10µM histamine). All data are shown as mean ± SEM, *p< 0.05 vs control.

Long-term Imaging of Apoptotic Calcium Release Induced by Staurosporine.

To study calcium dynamics during apoptosis, we induced cell death in HeLa cells by using the broad-spectrum kinase inhibitor staurosporine (STS)[173, 174]. First we determined the conditions under which STS-treated cells show elevated caspase activity, a relatively late event in apoptosis, while the control cells did not undergo cell death. Using air-buffered Leibovitz's L-15 media at room temperature, STS-treated cells showed a significant increase in caspase activity starting from 6hr to 12hrs, whereas there was no significant caspase activity in control cells(**Fig. 3-2A**).Therefore, we chose to image calcium release inHeLa cells continuously for 10 hours after STS treatment, a time at which the majority of STS-treated cells had undergone apoptosis but no cell death was observed in control cells.

Based upon the performance of GCaMP6s in Figure 1, we performed long-term calcium imaging using this indicator in control and STS-treated cells. In control cells treated with DMSO, we found that 78% of the cells (n=42) did not undergo morphological changes and had infrequent low amplitude spontaneous

intracellular calciumtransients during the 10 hourimaging period(**Fig. 3-2B,D**). In STS-treated cells, over 90% of the cells went through distinct morphological changes including cell shrinkage and blebbing at the cell surface. In 76% of STS-treated cells (n=35),there were significant calcium release events including oscillations and slow waves induced by STS (**Fig. 3-2C,D**). Interestingly, we observed extensive variability in the frequency, duration and timing of calciumrelease in each individual cell following STS treatment. To better characterize such variability, we categorized the pattern of calcium release into three types: oscillations, gradual increase (no significant oscillatory behavior but increased basal calcium), and a combination of both oscillations and gradual increase. We found that 41.1% of the STS-treated responders show oscillations only, 7.4% showed gradual increase, and 51.5% showed a combination of both patterns (**Fig. 3-2E**). Previous studies using Fura-2 and averaging traces from multiple cells demonstrated that STS-treated cells showed gradual increases in basal calcium levels that correlates with cell death [78, 172]. To assess whether we observe a similar trend using GCaMP6s, we calculated the average of all cells in one representative experiment and found a similar trend of increased calcium levels in STS-treated cells, while no increase was observed in control cells (**Fig. 3-2F**). Together, our results suggest that GCaMP6s is an excellent tool to monitor long-term calcium dynamics during apoptosis.

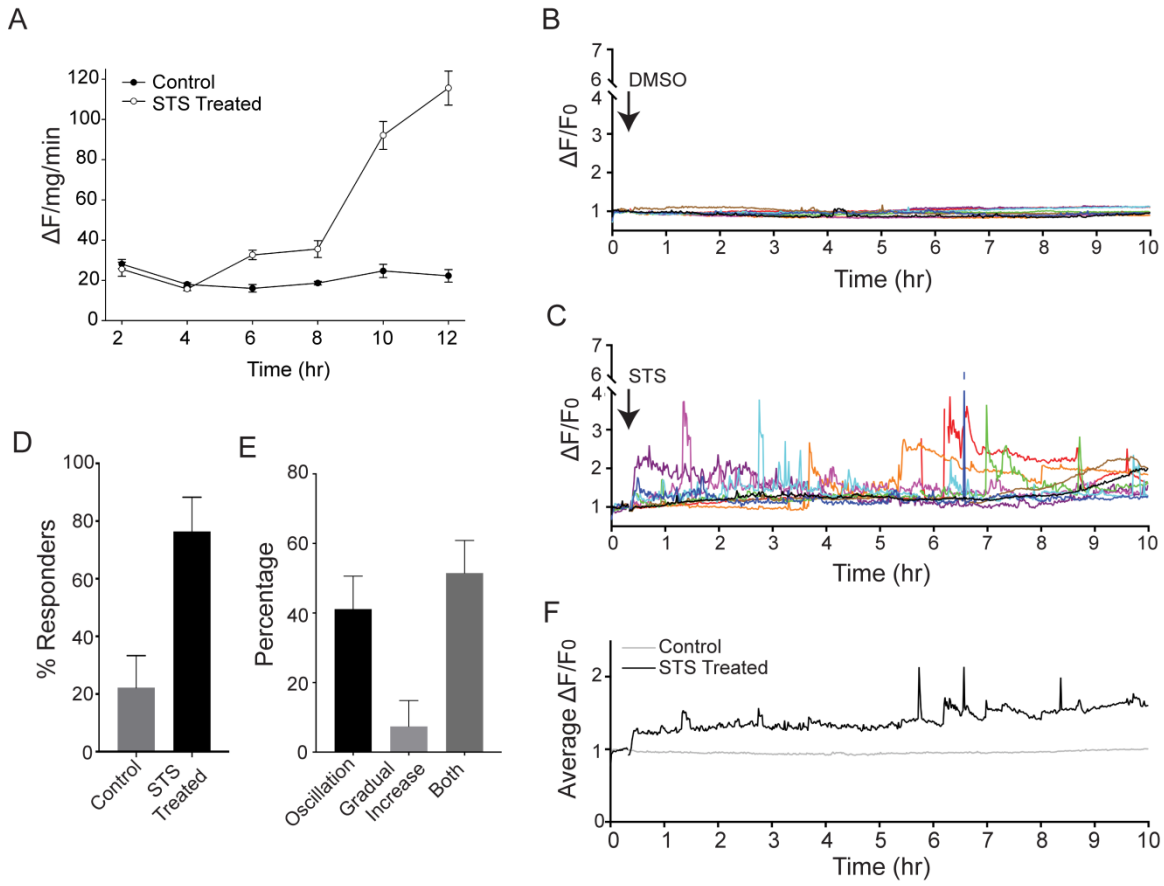

Figure 3-2: Changes in cytosolic calcium during cell death.
A. Caspase-3-like activity (DEVDase activity) in HeLa cells treated with 0.1% DMSO (control) and 10uM staurosporine (STS) were measured every 2hr from zero to 12 hours post treatment. **B-C.** GCaMP6s transfected HeLa cells were treated with DMSO or 10µM STS and imaged for 10 hours. Traces of GCaMP6s fluorescence in individual cells are shown (n=9 for one experiment). Cells treated with DMSO showed rare low amplitude changes in cytosolic calcium level throughout the experiment, with individual events not obvious at this scale (B).**D.** Bar graph showing percent responders in control (n=42) and STS-treated cells (n=35). **E.** Bar graph showing the type of calcium signals in individual STS-treated cells. Cells with release events that go above baseline and have ending calcium levelsreturn to baseline are categorized as an *oscillation*. Cells with no rapid and obvious release events above baseline but show a gradual increase towards the end of 10 hours are categorized as *gradual increase*. Cells showing both oscillation and gradual increase patterns are categorized as both. **F.** Traces of the average fluorescence of all cells in one representative experiment (n=10).

Indicator	K_d (nM)	Quantum Yield	K_{on} (x 10^7 M^{-1} s^{-1})	K_{off} (s^{-1})
Fura-2	135-224	0.49	10	23
GCaMP6s	144±4	0.61	0.78	1.12
GCaMP6f	375±14	0.59	1.05	3.93

Table 2: Properties of Fura-2, GCaMP6s and 6f[147, 155, 175]

DISCUSSION

Investigating calcium over extended time periods such as during cell death requires specialized approaches. Ideally, a fluorescence calcium indicator needs to have high sensitivity and be extremely photostable over a period of hours or even days. In the present study we found that GCaMP6s exhibited improved performance over Fura-2 when used to monitor calcium transients induced by histamine and during apoptosis induced by staurosporine. The expression patternof GCaMP6s is well distributed throughout the cell and can readily be used *in vitro* or *in vivo*[147]. Compared to GCaMP6f, GCaMP6s has a higher affinity to calcium and slower kinetics, but with higher brightness (**Table 2**)[147]. Both GCaMP6 proteins are significantly slower than Fura-2 (**Table 2**), which may limit their utility for imaging fast events.

Imaging calcium during cell death can be technically demanding. Previous approaches used by our group and others required loading and imaging sequential coverslips or taking static measurements every few hours or days after stimulation [47, 78, 171, 172]. These limitations precluded the possibility of following calcium dynamics in a single cell throughout the entire apoptotic process. We found

remarkable heterogeneity in the calcium responses after STS stimulation which were previously uncharacterized. Previous studies have shown that cytochrome c release is coordinated after STS stimulation [176, 177],and this process is likely mediated by calcium [78, 178]. In HeLa cells under similar conditions reported here, this occurs between 6 and 8 hours [78, 176]. We find that there is an increase in oscillatory activity around 6-8 hours in some cells (**Fig. 3-2C**), however this is clearly not observed in all cells. Thus, we conclude there must be another factor which functions alongside with calcium to induce coordinated cytochrome c release during cell death. Future studies examining RFP-cytochrome c release simultaneously with GCaMP6s imaging would help to resolve this apparent discrepancy and to further interrogate the role of calcium as a coordinating factor driving cytochrome c release during cell death.

Although we have highlighted the advantages of GCaMP6 proteins in this report, there are certain advantages to using dye-based reporters. Fura-2 is a ratiometric dye, which controls for heterogeneity in indicator loading and facilitates relatively easy quantification of absolute calcium levels [155]. Using specific loading techniques designed to intentionally cause compartmentalization of AM ester dyes, organelle calcium dynamics can also be interrogated using dye-based reporters [179]. Genetically encoded indicators rely upon transfection or viral transduction of plasmid DNA into the cell type to be investigated. Some cell types, and in particular primary cells such as adult cardiomyocytes and neurons, are refractory to transfection/transduction and thus dye-based methods are preferred. As mentioned previously, GCaMP6s and GCaMP6f are much slower than dye-

based approaches, and thus would not be preferred for doing high-speed imaging. Indeed, the wide variety of calcium indicators with different spectra, affinities, quantum yield, and other characteristics allows for tailoring the dye to the exact experiment preparation and functional readout.

Finally we would like to highlight a technical note about potential artifacts associated with long-term imaging. We found that the choice of buffer and incubation conditions have dramatic effects on the viability of cells mounted on the microscope stage. We found that imaging in Leibovitz's L-15 media was highly suitable for controlling pH when imaging in air and preserved cellular integrity for up to 12 hours (**Fig. 3-2A-B**). Importantly, long-term calcium imaging with GCaMP6s demonstrated that it overcame the limitations that conventional calcium indicators have such as poor photostability and leakage and is ideal for recording calcium dynamics during apoptosis for hours and possibly days.

Chapter 4:The H9c2 cell line as an alternative for modeling cardiac hypertrophy

INTRODUCTION

H9c2 cells are immortalized ventricular rat cardiomyocytes derived from embryonic BD1X rat heart tissue [180]. H9c2 cells have been shown to have similar characteristics to cardiomyocytes such as expression of ET, Angiotensin II receptors, also their capability to undergo hypertrophy and they share similar energy metabolism patterns [181-184]. For that reason, we decided to use H9c2 cells to investigate the expression and function of the different IP_3R isoforms in response to ET-1 induced hypertrophy. In our study we found readily detectable levels of expression of all three IP_3R isoforms. We also observed that there is a significant decrease in expression of IP_3R-1 and -3 after treatment with ET-1 for 48 hrs. Lastly, we show that knocking down IP_3R-2 in H9C2 cells do not alter H9C2 calcium dynamics in response to ET-1.

RESULTS

Expression and function of the different IP_3R isoforms in ET-1 treated H9C2 cells

It has been previously reported that H9c2 cells are a good alternative model to study cardiac hypertrophy [182]. Therefore, our first step was to confirm whether ET-1 can induce hypertrophy in H9c2 cells. As shown in fig 1A, we fail to see a significant increase in average cell area after treatment with ET-1 for 48 hrs. However, we were able to confirm that there was an increase in translocation of endogenous NFAT into the nucleus (**Fig. 4-1B** red arrows). NFAT activation

implies that there is an increase in transcription activity after ET-1 treatment in H9c2 cells. NFAT activity is known to be downstream of IP_3Rs activity [49-51]. As well several studies have previously reported that expression IP_3R-2 is modified during hypertrophy and heart failure [52, 53, 55]. Therefore, we decided to determine whether a change in IP_3R expression after treating H9c2 cells with ET-1. After treatment we observed a significant reduction in the protein expression in IP_3R-1 and -3 (**Fig. 4-2A, B**), but there was not a significant change in expression of IP_3R-2. In order to further understand the function of IP3Rs in H9c2 cells we used siRNA to knockdown the expression of each IP_3R isoform. After treatment with ET-1 we can see rapid increase in cytosolic calcium in H9c2 cells. However, when we knockdown IP_3R-1 we observed that the intracellular calcium response is almost abolished, as less than 10% of the cells responded to ET-1 treatment (**Fig. 4-3A**). Fo-3r IP_3R-2 or -3 knockdowns, we see a significant number of cells that responded to ET-1 (**Fig. 4-3A**). Suggesting that, at least in H9c2 cells, IP_3R-1 is a key mediator of the ET-1 response. Interestingly when comparing average peak release in IP_3R-2 and -3 knockdowns, we can see that there is a significant decrease in the average peak release in cells with IP_3R-2 knockdown (**Fig. 4-3B**) suggesting that IP_3R-2 might also play a role in ET-1 induced calcium release. However, IP_3R-2 implication is not as significant as IP_3R-1. Overall our results suggest that IP_3R-1 is an important mediator of calcium release after ET-1 stimulation in H9c2 cells.

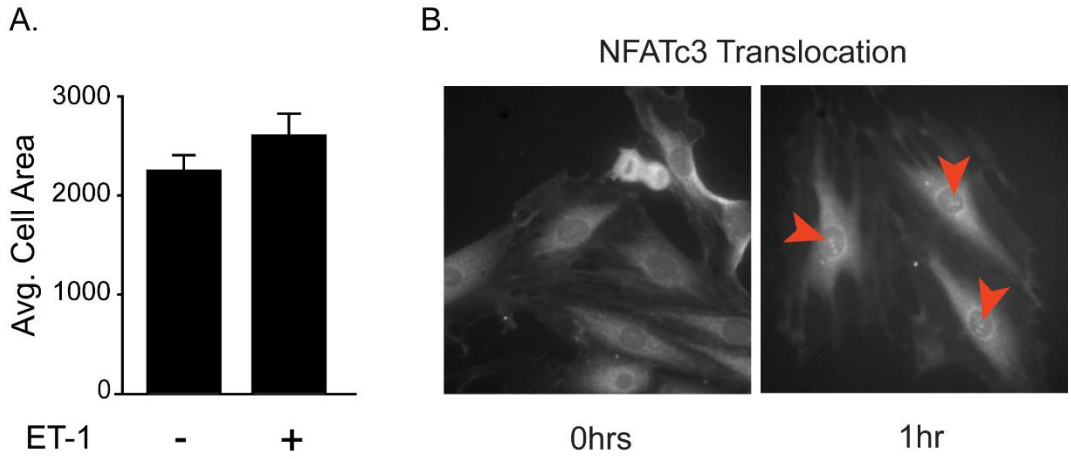

Figure 4-1: NFAT nuclear translocation after ET-1 treatment.
Average cell area of cells treated with ET-1 for 48 hrs (n=80) and no treatment (n=91). All data are shown as mean ± SEM, *P < 0.05 vs control.

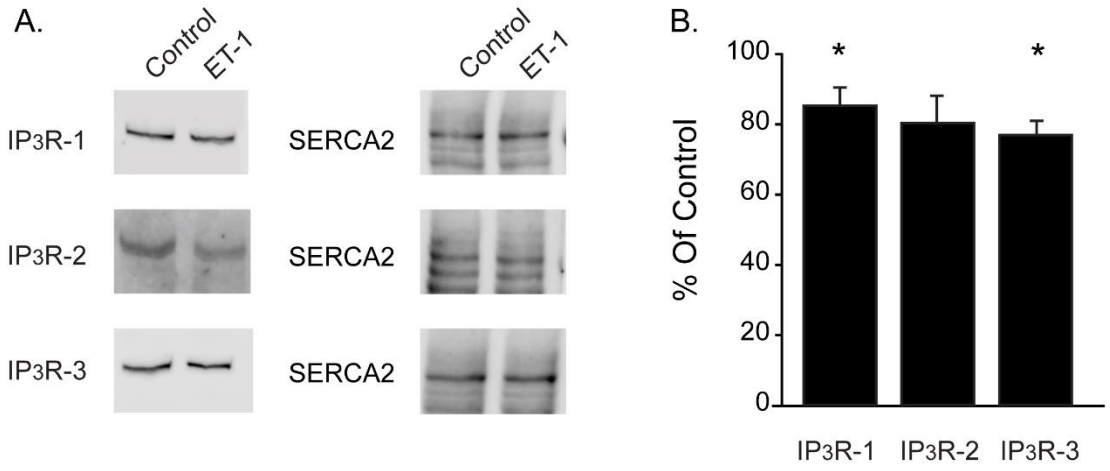

Figure 4-2: Expression of IP_3R isoforms H9C2 cells.
A. Western blot analysis of rat H9C2 cells treated with or without 100nM ET-1 for 48 hrs. The membranes were probed with specific anti-IP3R-1, anti-IP3R-2, and anti-IP3R-3 antibodies. Anti-SERCA2 antibody was used as loading control. Data shown are representative of three experiments. **B**. Change in IP_3R-1, -2 and -3 expression levels after treatment with ET-1 for 48 hrs compared to control. All data are shown as mean ± SEM, *P < 0.05 vs control.

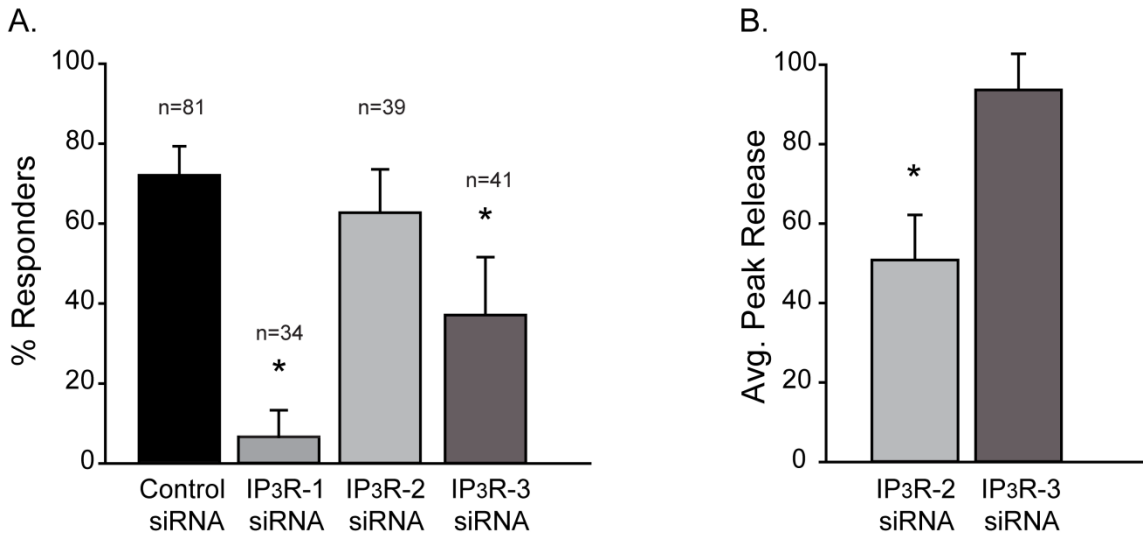

Figure 4-3: IP_3R-1 an important mediator of calcium release in response to ET-1.

A. Percentage of cells which responded to 100nM ET-1 challenge, control RNAi (n=81), IP_3R-1 RNAi (n=34), IP_3R-2 (n=39) and IP_3R-3 RNAi (n=41). **B**. Average peak release of H9c2 transfected with IP_3R-2 and IP_3R-3 siRNA. All data are shown as mean ± SEM, *P < 0.05 vs control.

DISCUSSION

Endothelin-1 is a critical player mediating the cardiac hypertrophic response and the maladaptive remodeling of the heart. It has been suggested that IP_3R-2 is the dominant isoform expressed in cardiomyocytes, and that it plays an essential role in this signaling cascade by specifically mediating nuclear calcium transients. In our study, we show that all three IP_3R isoforms are expressed in H9c2 cells. It has been previously shown that H9c2 cells show enhanced hypertrophy following ET-1 infusion [182]. However, in our study we show that there is not a significant increase in average cell area after ET-1 treatment. Still, we observed an increase in nuclear translocation of endogenous transcription factor NFAT. For our next set of experiments we decided to look upstream NFAT activation and look at IP_3R role in ET-1 response. We saw that ET-1 treatment downregulates the expression of IP_3R-1 and -3 in H9c2 cells. Using H9c2 cells as a model to study hypertrophy we do not see that expression of IP_3R-2 is significantly incresed which contradicts previous reports which show that expression of IP_3R-2 is altered during hypertrophy. As well we observed that IP_3R-1 knockdown abolishes intracellular calcium release in response to ET-1, suggesting that IP_3R-1 is a key mediator of the ET-1 response at least in H9c2 cells. We found that H9c2 cells are a good model to study intracellular calcium changes in response to ET-1. Based on our observations the H9c2 cell do not undergo hypertrophy in response to ET-1, we conclude that H9c2 cells are not a good model to study hypertrophy *in vitro*. Overall we conclude that H9c2 cells should not be used as a substitution for primary cardiomyocytes to study hypertrophy *in vitro*.

Chapter 5:Functionally Redundant Control of Cardiac Hypertrophic Signaling by Inositol 1,4,5-Trisphosphate Receptors

Modified in part from:

Functionally redundant control of cardiac hypertrophic signaling by inositol 1,4,5-trisphosphate receptors

M. IvethGarcia[a, b], Anja Karlstaedt[c], Javier Amione-Guerra[d], Keith A. Youker[d], Heinrich Taegtmeyer[c], and Darren Boehning[b]

[a]Cell Biology Graduate Program, University of Texas Medical Branch, Galveston, TX 77555; [b]Department of Biochemistry and Molecular Biology, McGovern Medical School at UTHealth, Houston, TX 77030; [c]Department of Internal Medicine, Division of Cardiology, McGovern Medical School at UTHealth, Houston, TX 77030. [d]Houston Methodist Hospital, Houston, TX 77030.

INTRODUCTION

Calcium is an essential modulator of a wide variety of cellular functions including cardiomyocyte excitation-contraction coupling (ECC) and gene expression. Cardiomyocyte function is modulated by neuro-hormonal agonists to

accommodate cardiac demand. One example is endothelin-1 (ET-1), which is a potent vasoconstrictor that plays an important role in modulating muscle contractility, vascular tone, cardiomyocyte growth, and survival [13, 45]. Plasma levels of ET-1 are also increased during pathological conditions such as chronic heart failure, myocardial infarction, cardiac hypertrophy and in hypertension [5, 44]. As such, ET-1 has been linked to pathological remodeling of the heart [45, 49]. ET-1 signaling is initiated by ET-1 binding to G-protein coupled receptors at the plasma membrane leading to the activation of phospholipase C (PLC). PLC catalyzes the hydrolysis of phosphatidylinositol 4,5-bisphosphate (PIP_2) which leads to increased production of the second messengers inositol 1,4,5-trisphosphate (IP_3) and diacylglycerol. IP_3 then acts as a second messenger that binds inositol 1,4,5-trisphosphate receptors (IP_3Rs), activating IP_3-induced calcium release (IICR).

IP_3Rs are a family of calcium channels involved in a variety of cellular functions. There are three different IP_3R isoforms encoded by separate genes. The three IP_3Rs share a high degree of sequence homology and are found in a variety of tissues including the heart [71, 117]. Cardiac IP_3Rs are implicated in regulating the progression of cardiac hypertrophy [53, 54]. Within the cardiomyocyte, IP_3Rs are known to localize in the dyadic cleft, sarcoplasmic reticulum and at the outer/inner nuclear membrane [45, 53, 54, 128]. Several lines of evidence have also implicated nuclear calcium transients as a significant contributor to cardiomyocyte hypertrophy. Nuclear or perinuclear IP_3Rs may promote nuclear-restricted calcium release events that initiate gene transcription[128]. Nuclear calcium transients are involved in the activation of transcription factors such as

histone deacetylase 5 (HDAC5) [45, 127]. However, the mechanism by which cardiomyocytes can discriminate between calcium signals from ECC and calcium signals that target gene transcription it still unclear, as calcium release events mediated by ECC are also efficiently transmitted to the nuclear matrix. Hypertrophic agents such as ET-1 also increase contractility [53, 141], which may afford a mechanism for decoding IP_3-dependent signals without requiring subcellular compartment-specific IP_3R activation.

The IP_3R-2 isoform is considered the predominant isoform in the heart [118, 144]. Transgenic IP_3R-2 rodent models have either supported [50, 121], or contradicted [120, 124] the role of IP_3R channels in cardiac hypertrophy. As such, it is still unclear whether IP_3R channels are significant contributors to cardiac physiology and pathologic remodeling such as hypertrophy [185]. It has been shown that all three IP_3R isoforms, at least at the mRNA level, are expressed in the heart of humans and mice [54]. This opens the question of whether IP_3R-1 and -3 are able to functionally compensate for IP_3R-2 deficiencies in these models.

We now show that all three IP_3R isoforms are expressed in cardiomyocytes and that they are essential for the progression of ventricular hypertrophy induced by ET-1. IP_3R-dependent activation of the hypertrophic program was not dependent upon nuclear-specific calcium transients, but instead was mediated by increased contractility induced by ET-1. Lastly, these results were independent of increased IP_3R expression both in vitro and in vivo.

RESULTS

Expression of IP_3R protein in neonatal and adult ventricular cardiomyocytes

Previous studies have indicated that IP_3R-2 mRNA is predominant compared to other IP_3R isoforms in ventricular cardiomyocytes[118, 144]. Using highly specific antibodies we analyzed the protein expression and localization of the three IP_3R isoforms in primary neonatal and adult rat cardiomyocytes. In neonatal ventricular cardiomyocytes all three IP_3R isoforms were expressed throughout the cell (**Fig. 5-1A-C**, second column). Expression was more prominent in the perinuclear region consistent with previous reports[45]. Similarly, all three IP_3R isoforms are expressed throughout the cell in adult rat cardiomyocytes (**Fig. 5-1 D-F**, second column). In contrast to neonatal ventricular cardiomyocytes, IP_3R expression in adult cardiomyocytes was more equally distributed throughout the cell with no obvious concentration in the perinuclear region. This expression pattern overlaps with SERCA2 localization indicating is it present throughout the sarcoplasmic reticulum in both neonatal and adult cardiomyocytes (**Fig. 5-2A, C**). As expected, IP_3R localization was distinct from the localization with RYR ([45]; **Fig. 5-2B, D**). These results indicate that in addition to IP_3R-2, IP_3R isoforms type 1 and 3 are expressed in rat neonatal and adult ventricular cardiomyocytes

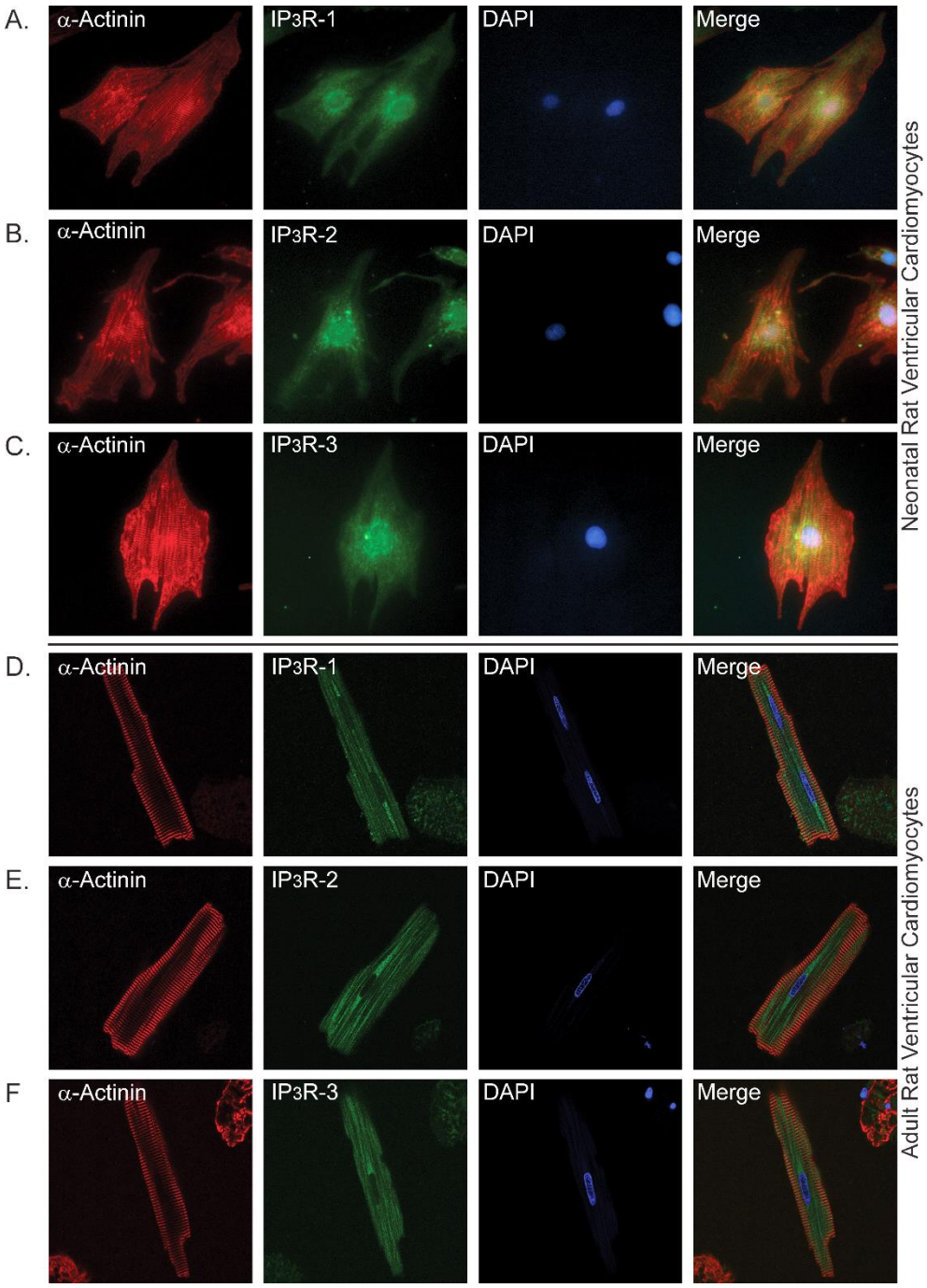

Figure 5-1: Expression and distribution IP_3R isoforms in primary neonatal and adult ventricular cardiomyocytes.
Immunofluorescence staining of neonatal (rows A-C) and adult (rows D-F) ventricular cardiomyocytes. Column 1 is stained with α-actinin to label sarcomeres. Column 2 is stained with indicated IP_3R antibodies. Column 3 is DAPI staining of the nucleus. Column 4 is the merged images of each row.

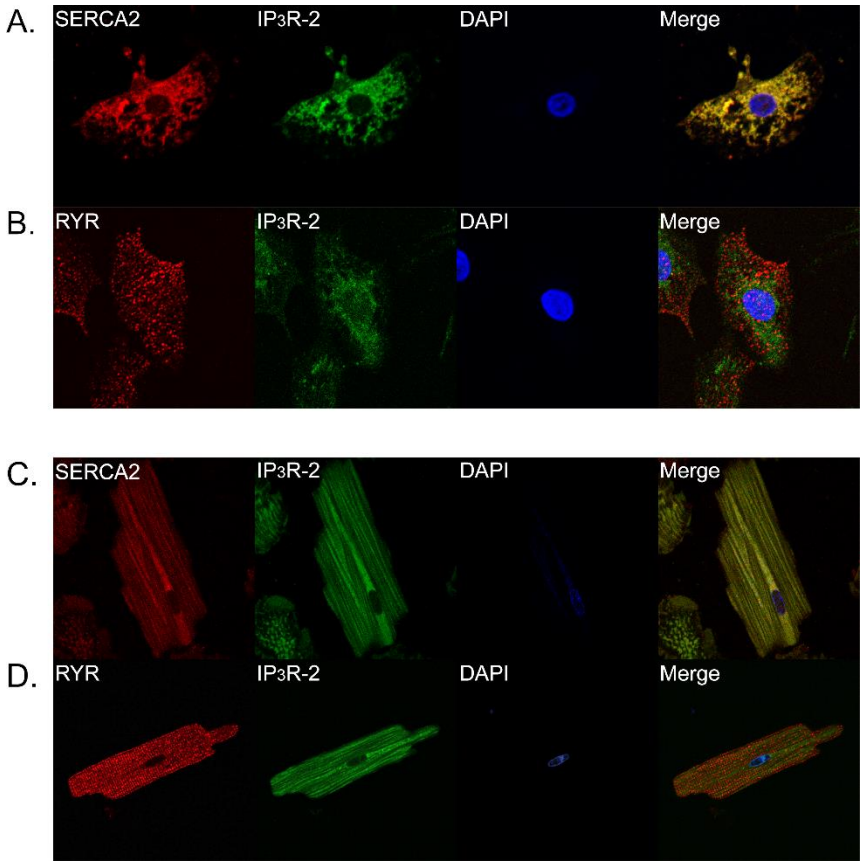

Figure 5-2: Expression and distribution of IP_3R, SERCA2, and RYR in primary ventricular cardiomyocytes.
Immunofluorescence staining of neonatal ventricular cardiomyocytes stained with SERCA2 and IP3R-2 (A); RYR2 and IP3R-2 (B). Immunofluorescence staining of adult ventricular cardiomyocytes with SERCA2 and IP3R-2 (C); RYR2 and IP3R-2 (D).

Altered contractility induced by ET-1 is attenuated by decreasing IP3R expression

ET-1 is known act as a positive inotropic agent in cardiomyocytes[53, 141]. We monitored intracellular calcium in spontaneously contracting neonatal ventricular cardiomyocytes treated with ET-1. As shown in **Fig. 5-4** (control bars) there is an increase in the calcium oscillation frequency in neonatal cardiomyocytes stimulated with 100 nM ET-1. Previous studies using overexpression of IP_3 5'-phosphatase to inhibit IP_3 signaling suggested that IP_3R channels do not play a role in this response to ET-1[45]. To evaluate the role of IP_3R channels in the process more specifically, we used siRNA knockdown of each individual IP_3R isoform. Western blot analysis confirmed efficient and specific knockdown of each of the three IP_3R isoforms (**Fig. 5-3**). Knockdown of individual IP_3R isoforms did not have significant effects on the increased oscillation frequency induced by ET-1 stimulation (**Fig. 5-4**). Next, we used double knockdowns (IP_3R 1/2, 2/3 and 1/3) and determined their effect on the response to ET-1. Similar to single knockdown, double knockdown did not have a significant effects on the increased oscillation frequency induced by ET-1 stimulation. Triple knockdown of all three IP_3R isoforms completely suppressed the response of cardiomyocytes to ET-1 (**Fig. 5-4**). Thus, the increased contractility in response to ET-1 requires IP_3R activity, and furthermore all three IP_3Rs are expressed and play a functionally redundant role in the response to ET-1 stimulation.

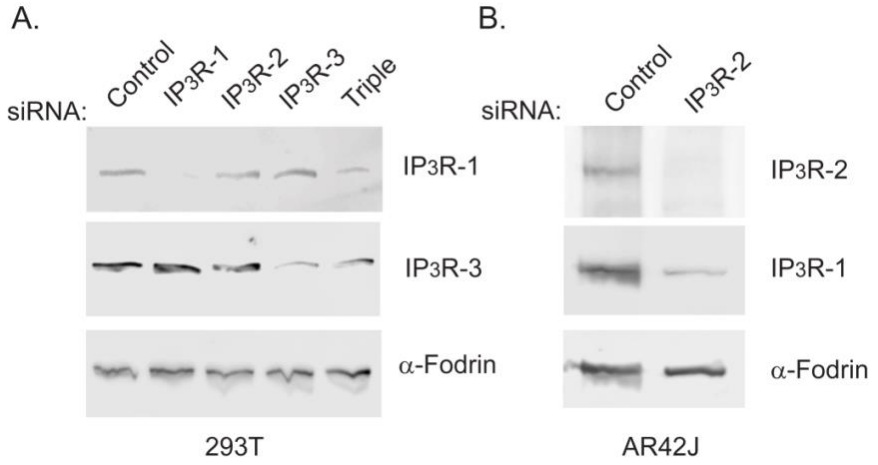

Figure 5-3: siRNA-mediated knockdown of IP3R-1, -2, and -3.
Western blot analysis of 293T (A) and AR42J (B) cell lines transfected with control siRNA and siRNAoligos specific for each IP_3R isoform as indicated. IP_3R-1 siRNA significantly reduced endogenous IP_3R-1 expression in 293T where control siRNA did not. Similarly IP_3R-3 siRNA significantly reduced IP_3R-3 expression. Both siRNAs were specific for the individual isoforms. Triple IP_3R siRNA transfection inhibited the expression of both IP_3R-1 and -3 in 293T cells (A). IP_3R-2 expression was below detection levels in 293T cells. To probe the efficiency of IP_3R-2 siRNA, we used AR42J cells which express high amounts of this isoform (B). IP_3R-2 siRNA completely inhibited IP_3R-2 expression, and also partially reduced IP_3R-1 levels. IP_3R-3 expression was below detection levels in AR42J cells. In both panels, alpha-fodrin was used as loading control.

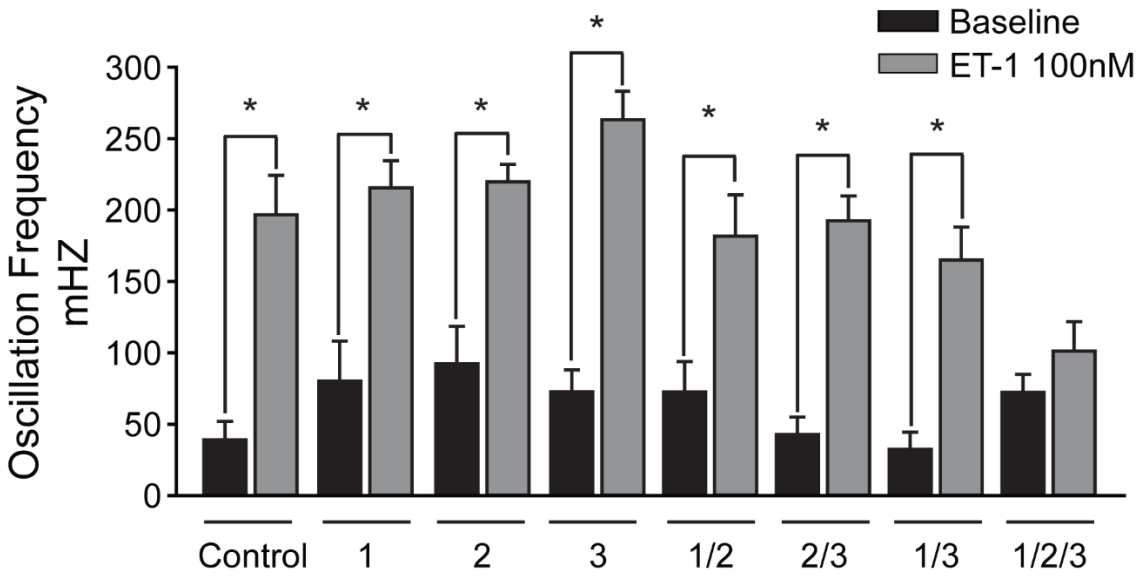

Figure 5-4: All three IP_3R isoforms contribute to hypertrophic signaling by ET-1.

Neonatal cardiomyocytes were transfected with control or IP_3R siRNA as indicated. Cells were treated with ET-1 and oscillation frequency was quantified from at least 4 separate experiments (control n=6, 1 n=6, 2 n=7, 3 n=6, 1/2 n=6, 2/3 n=5, 1/3 n=5 and 1/2/3 n=4). All data are shown as mean ± SEM, *P < 0.01 vs control.

Attenuating IP_3R expression inhibits ET-1 induced NFAT activation and hypertrophy

At the cellular level cardiac hypertrophy is characterized by activation of the hypertrophic transcriptional program by NFAT ultimately leading to increased cardiomyocyte cell size. ET-1 is one of the best described neuro-hormonal factors known to induce cardiomyocyte hypertrophy [50, 128]. As mentioned previously, IP_3R mRNA levels are altered during hypertrophy [117, 118], however the effect on IP_3R protein levels is not clear. In order to assess whether IP_3R protein expression is altered during ET-1 induced hypertrophy, we treated neonatal cardiomyocytes with ET-1 for 48 hours and 6 days. Using this paradigm, protein expression of all three IP_3R isoforms is unchanged compared to non-treated controls (**Fig. 5-5A-B**) despite robust induction of the hypertrophic marker protein atrial natriuretic peptide (**ANP; Fig. 5-5C**). It has also been shown that IP_3R mRNA levels are altered in both animal models [53, 120] and in the human failing heart[54]. We examined IP_3R expression level in left ventricular heart tissue from one control and two end stage heart failure patients. Protein expression of all three IP_3R isoforms could be readily detected in the three human heart samples. We found no significant differences in the protein expression level of IP_3R isoforms in human failing hearts relative to control (**Fig.5-6 and Table 3**).

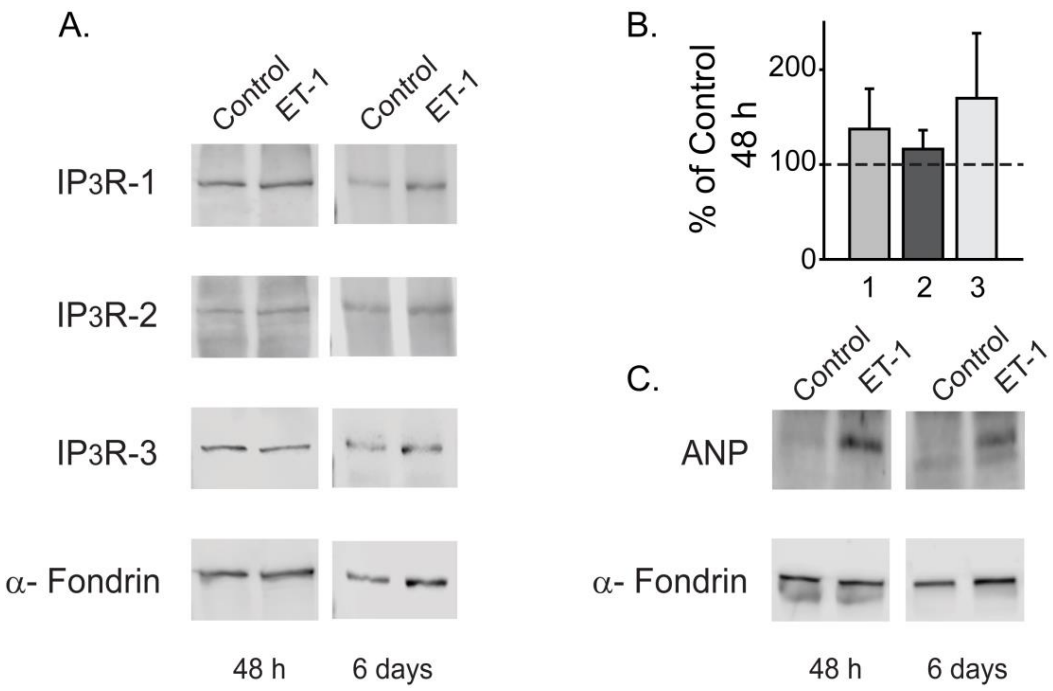

Figure 5-5: IP_3Rs expression during ET-1 induced hypertrophy.

A. Western blot of indicated proteins after 48 hours or 6 days treatment with 100 nM ET-1. **B**. Quantification of IP_3R levels after ET-1 treatment for 48 hours expressed as percent of control. C. Atrial natriuretic peptide (ANP) levels after 48 hours and 6 days treatment with ET-1. Blotting with alpha-Fodrin was used as control.

A. **Non-Failing Left Ventricle**

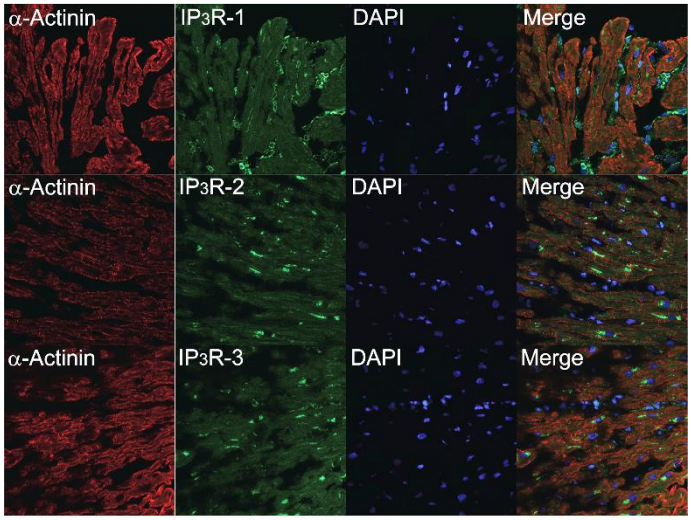

B. **Failing Left Ventricle-Patient 1**

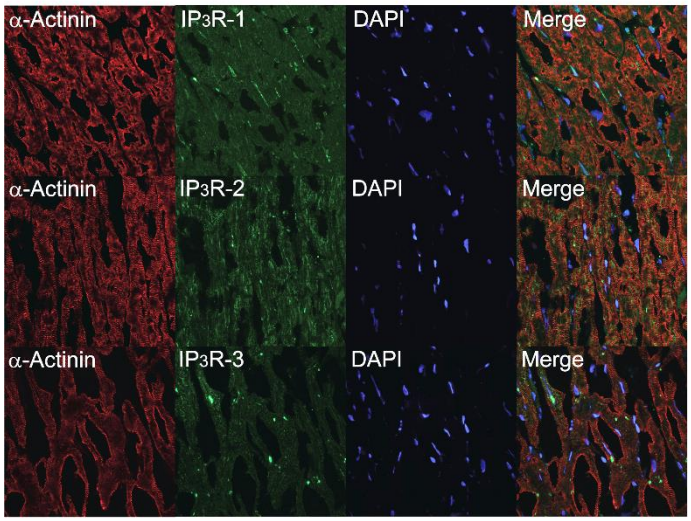

C. **Failing Left Ventricle-Patient 2**

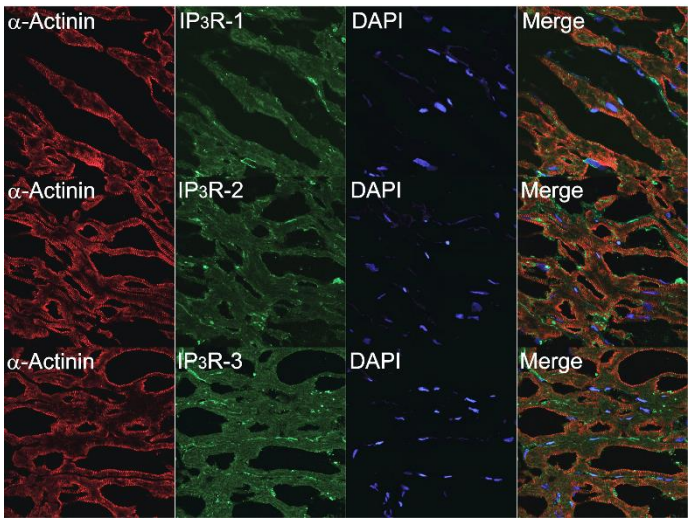

Figure 5-6: Expression of IP_3R isoforms in non-failing and end stage heart failure

Immunofluorescence staining of non-failing human left ventricle (A). Left ventricular heart failure patient 1(B) and patient 2 (C). Column 1 is stained with α-actinin to label sarcomeres. Column 2 is stained with indicated IP_3R antibodies. Column 3 is DAPI staining of the nucleus. Column 4 is the merged images of each row.

	Control	Patient 1 ICM	Patient 2 ICM
NYHA Class	0	4	3.5
Age	43	57	64
Sex	F	M	M
Hypertension	-	Stage 1	Stage 1
LVEDD	-	7.2	6.7
LVPWd	-	1.4	1.3
EF	60%	20%	20%

Table 3: Clinical characteristics of patient's samples.

Control sample was obtained from a heart that was declined for transplantation due to non-cardiac reasons. Patient 1 and 2 samples were obtained from patients that suffered with end stage heart failure. NYHA indicates New York Heart Association; Stage 1 hypertension, systolic pressure ranging from 140 to 159 mm Hg or a diastolic pressure ranging from 90 to 99 mm Hg; LVEDD, left ventricular end diastolic diameter- normal range 4.2-5.9 cm; EF, Ejection Fraction, normal EF ranges from 55-70%; LVPWd, Left ventricular posterior wall end diastole and end systole-normal range 0.6-1.1 cm.

Next we determined whether IP_3R expression is essential for activation of the hypertrophic program downstream of ET-1 stimulation. Treatment of cells with ET-1 led to significant NFAT activation within 12 hours as determined by a luciferase reporter assay (**Fig. 5-7A**). Triple knockdown of all three IP_3R isoforms completely abrogated NFAT activation in response to ET-1 stimulation (**Fig. 5-7A**), a finding consistent with our observation that triple IP_3R knockout suppresses the increased calcium oscillation frequency in response to ET-1 (**Fig. 5-4**). Treatment of cardiomyocytes with ET-1 leads to an increase in cell size, the cardinal feature of hypertrophy ((1, 5); **Fig. 5-7B**). Triple knockdown of all three IP_3R isoforms completely abrogates the increased cell size induced by to ET-1 treatment (**Fig. 5-7B** and **Fig. 5-8**). Thus, all three IP_3Rs contribute to signaling downstream of ET-1 in cardiomyocytes and are essential for activation of the hypertrophic program.

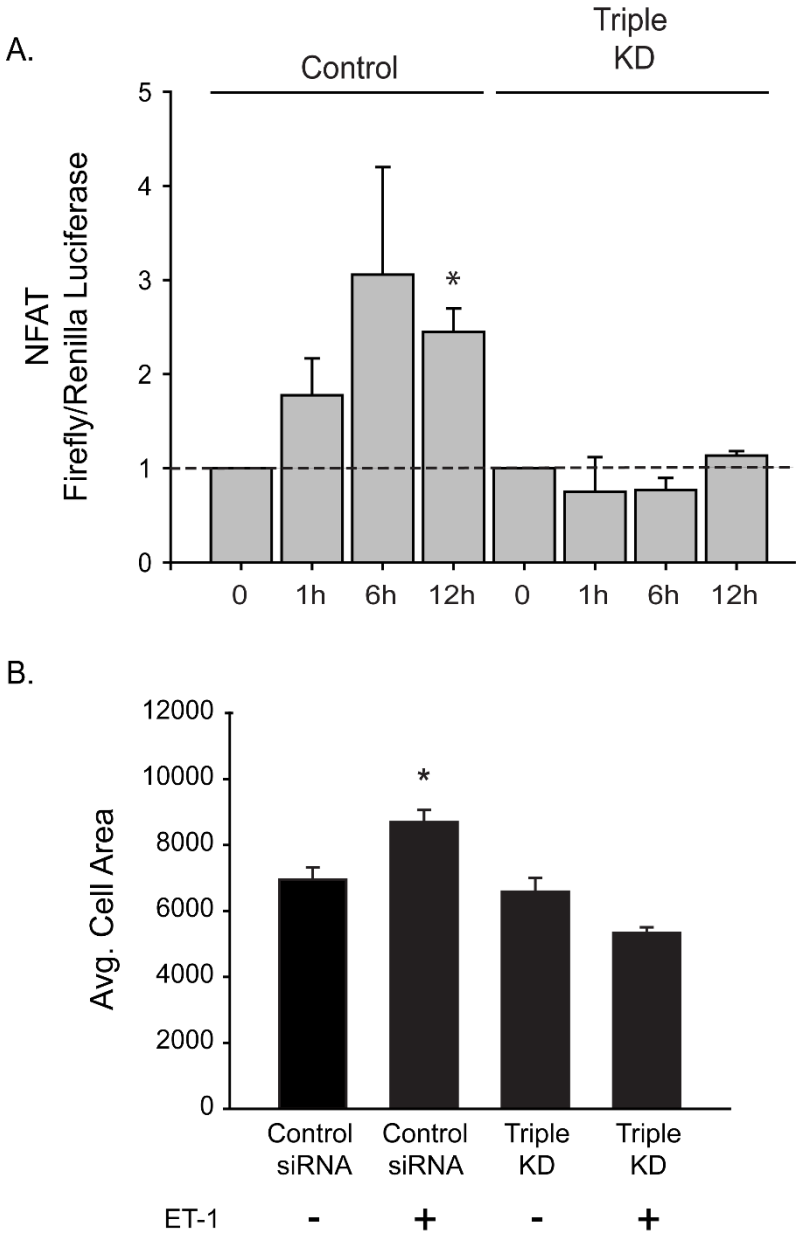

Figure 5-7: IP_3R triple knockdown inhibits ET-1 induced NFAT activation and hypertrophy

A. NFAT activity using luciferase reporter construct after ET-1 treatment for the indicated times in control siRNA and triple IP_3R siRNA transfected cardiomyocytes. **B**. Average cell area before and after 48 hours treatment with ET-1. Neonatal cardiomyocytes were transfected with control siRNA and triple IP_3R siRNA. All data are shown as mean ± SEM, *P < 0.01 vs control.

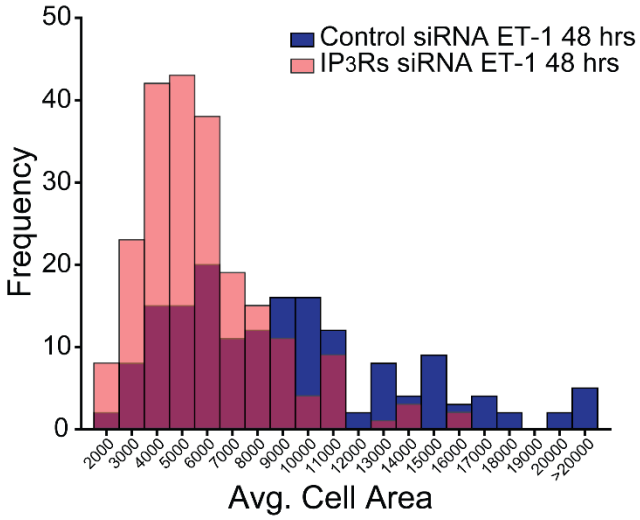

Figure 5-8: Histogram of cardiomyocytes size distribution after ET-1 stimulation

Histogram of neonatal ventricular cardiomyocytes cell size distribution showing control (n=166) and triple IP_3R siRNA (n=218) transfected cells treated with ET-1 for 48 hrs.

Calcium release induced by ET-1 is not restricted to the nuclear compartments

Rhythmic contraction of the heart is mediated by intracellular RyR calcium channels in a process termed calcium-induced calcium release (CICR). An important question is how IP_3R-mediated calcium transients could be "decoded" in the constant background of CICR in the beating heart. One prevalent model is that nuclear-compartment specific IP_3R calcium transients mediate gene expression in response to hypertrophic agents[128]. However, as CICR calcium transients also diffuse into the nucleus the specific mechanism is not clear. Furthermore, NFAT is a cytosolic protein in the inactive state, and translocates to the nucleus in response to elevations in cytosolic calcium [49]. To resolve these discrepancies, we used the genetically encoded calcium indicator GCaMP6s targeted to the nucleus in order to measure nuclear calcium transients unambiguously (**Fig. 5-9A-B**). Using the spectrally separated indicator Fura-2 to measure cytosolic calcium, we were able to quantify calcium release in both nuclear and cytosolic compartments with high specificity. As shown in **Fig. 5-9C-D**, calcium release was detectable in both compartments of spontaneously beating cardiomyocytes. After ET-1 stimulation there is an increase in the oscillation frequency consistent with the positive inotropic effects of ET-1 (**Fig.5-9C-D**), which we showed is absolutely dependent upon IP_3R expression (**Fig. 5-4**). Visual observation of Fura-2 versus H2b-GCaMP6s traces revealed essentially overlapping plots (**Fig. 5-9C-D**), however

the H2b-GCaMP6s signal had lower resolving power at higher oscillation frequencies. Expression of cytosolic GCaMP6s revealed that this was due to a buffering effect of the indicator, not an intrinsic property of the nuclear matrix (**Fig. 5-10**). In order to compare the cytosolic versus nuclear oscillations more quantitatively, we calculated the oscillation frequency over the course of the experiment in 20 second bins in both the cytosolic and nuclear compartments (**Fig. 5-9E**). Data points above the line in **Fig. 5-9E** would indicate a higher frequency in the nucleus (thus highlighting nuclear only events). Conversely, data points below the line are representative of events that occur in the cytosol but were not detectable in the nucleus. Presented in this way, we were unable to visualize any "nuclear only" release event either before or after ET-1 stimulation. We did, however, note a few "cytosol only" events at various frequencies. This may be due to either a cytosol restricted transient or insufficient sensitivity of the GCaMP6s sensor. Regardless, if there are nuclear restricted calcium transients they are either rare or low amplitude events. The results presented herein are also entirely consistent with the large body of evidence indicating that NFAT is activated by changes in calcium release frequency, not amplitude[186-188].

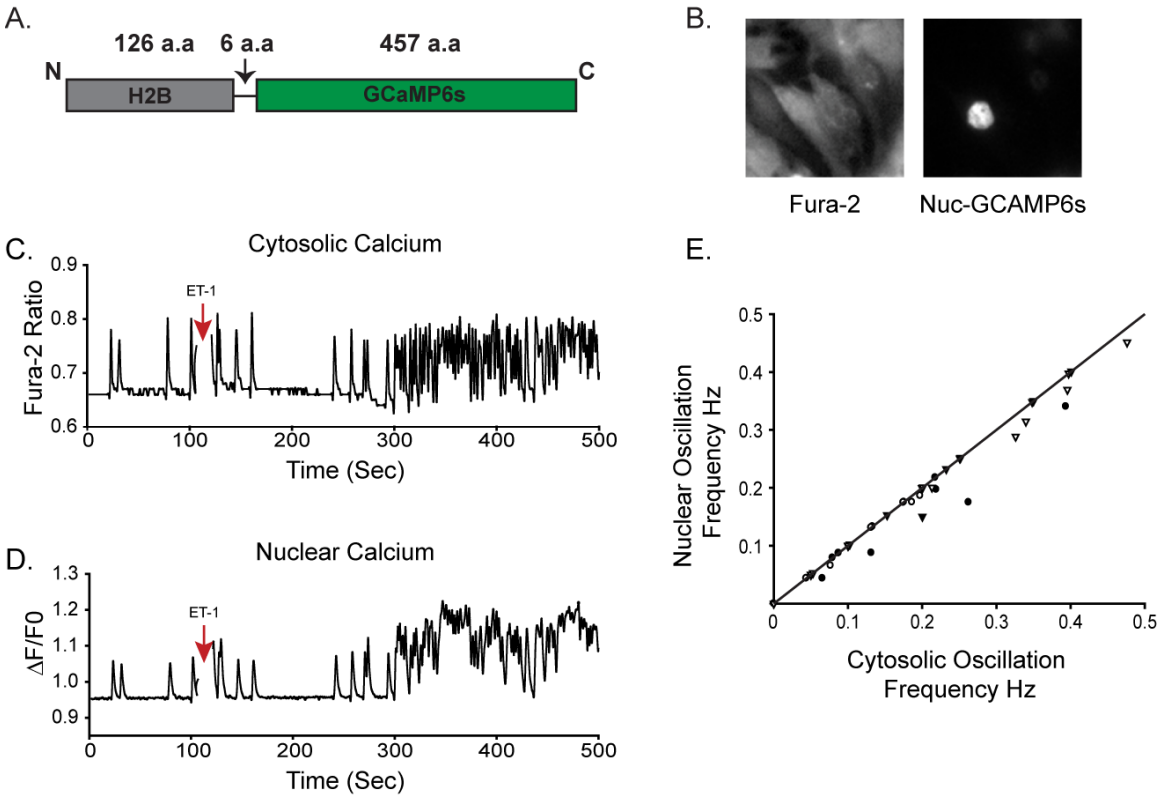

Figure 5-9: Nuclear and cytosolic calcium in response to ET-1 stimulation
A. Schematic cartoon of H2B-GCaMP6s. **B**. Representativeimage of neonatal cardiomyocytes expressing H2B-GCaMP6s loaded with Fura-2 AM. **C**. Single cell imaging of a neonatal cardiomyocyte treated with 100 nM ET-1 at indicated time. **D**. H2b-GCaMP6s signal in the same cell as in C. **E**. Plot of cytosolic vs. nuclear oscillation frequency. Each symbol represents a single coverslip averaging 5-10 cells for a total of four separate coverslips. Frequency data was quantified from 20 seconds bins.

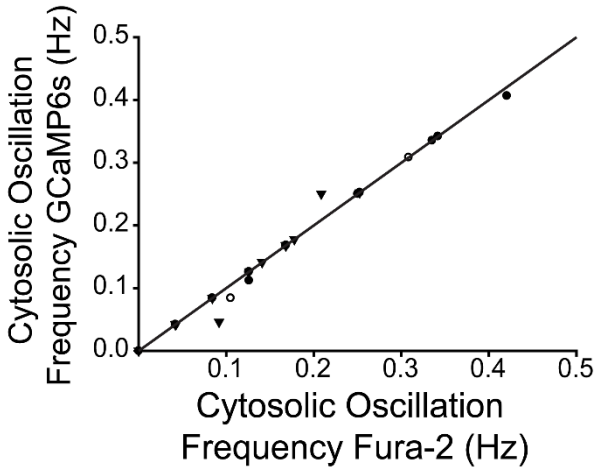

Figure 5-10: Plot of cytosolic GCaMP6s versus Fura-2 oscillations frequency Cytosolic GCaMP6s was imaged simultaneously with cytosolic Fura-2 oscillation in neonatal cardiomyocytes and relative oscillation frequencies from each indicator were quantified. Each symbol represents a single coverslip averaging 5-10 cells for a total of three separate experiments. Frequency data was quantified from 20 seconds bins.

DISCUSSION

IP_3Rs likely play a key role in the progression of hypertrophy[45, 50, 53]. However, the majority of the studies on the role of IP_3Rs in hypertrophy have focused solely on IP_3R-2, despite the fact that the other two isoforms are also expressed in the heart [54, 120]. We show here that all three IP_3R channels are expressed at readily detectable levels in cardiomyocytes in both rodent and human heart. Furthermore, all three channels contribute to calcium release and activation of the hypertrophic program in a functionally redundant manner. Lastly, our findings indicate that IP_3Rs contribute to activation of the hypertrophic program after ET-1 stimulation primarily by mediating the increase in calcium release frequency/contractility. We do not find evidence, at least in this model, for nuclear-specific calcium events.

Our finding that IP_3Rs play functionally redundant roles in ventricular cardiomyocytes may resolve some controversies regarding transgenic models of IP_3R function in the heart. Previously, the IP_3R-2 was thought to be the predominant isoform expressed in the heart. Consequently, most of the studies that focus on the role of IP_3R in the heart have focused solely on IP_3R-2 function [118, 119]. Global genetic knockout of the IP_3R-2 in mice does not cause any significant difference in the hypertrophic response in pressure overload or dilated cardiomyopathy mouse models[120]. However, the potential involvement of IP_3R-1 and IP_3R-3 activity has not been investigated further. Another group has showed that global knockout of IP_3R-2 eliminates the positive inotropic effects of endothelin-1 (ET-1) in the atria and protects against arrhythmias [121]. Overexpression of the ligand binding domain of the IP_3R inhibits signaling through

the channel by buffering IP_3 levels (so called "IP_3 sponge" [122]). Targeted inducible overexpression of the IP_3 sponge in the heart inhibited hypertrophy in response to isoproterenol and angiotensin-II[50]. As the IP_3 sponge would inhibit signaling through all three IP_3R channels, these findings are consistent with our results suggesting that all three IP_3Rs can contribute to hypertrophic signaling in cardiomyocytes.

The subcellular localization and precise aspects of how IP_3Rs regulate spatio-temporal aspects of calcium release in the contracting myocyte is an area of debate. In particular, how IP_3R signals are decoded to regulate processes such as transcriptional activation in the beating cardiomyocyte is unclear. IP_3Rs are known to be primarily localized at the ER/SR membranes in most cells, however in the heart it is thought to be concentrated at the nuclear and perinuclear membranes, where it is thought to play a key role in gene transcription [45, 125, 127, 128]. Nuclear localized IP_3R would thus facilitate spatially restricted calcium transients to the nuclear matrix. It has been shown that IP_3 and ET-1 can trigger nuclear calcium sparks and nuclear localized calcium transients [125, 128, 133, 134], however it is unclear whether these transients originate from the cytosol/perinuclear area. We show now that all three IP_3Rs are expressed throughout the SR of the cardiomyocyte in both isolated rat cardiomyocytes and human tissue. Using nuclear-localized GCaMP6s to unambiguously monitor nuclear calcium, our results simultaneously imaging nuclear and cytosolic calcium indicate that nuclear-only calcium transients, if present, are an exceedingly rare events. Rather, our results indicate unequivocally that IP_3Rs mediate the positive

inotropic effects of ET-1 in a functionally redundant manner. The increase calcium release frequency would then result in activation of NFAT and activation of the hypertrophic program.

Chapter 6: Conclusion and Future Directions

IP_3R is a calcium channel that is ubiquitously expressed and plays a key role in different cellular processes. However, the role that IP_3R plays in ventricular cardiomyocytes is poorly understood. We aimed to examine the expression and

role of all three IP_3R isoforms in cardiomyocytes. While there are several studies focusing on the role of IP_3R-2 in the heart, little is known about IP_3R-1 and -3. Our study describing the role of all three IP_3R isoforms in ET-1 induced hypertrophy reveals completely new functions for this class of proteins in regulating cardiac physiology.

GCaMP6 Proteins to Study Calcium Dynamics

Genetically encoded calcium indicators have improved over the years. GCaMP6 variants are some of the more advanced calcium indicators due to their low baseline fluorescence, large dynamic range, and medium to high affinity to calcium [147]. In our study we compared GCAMP6s, GCAMP6f and Fura-2 to determine a suitable method to study calcium dynamics during cell death. Our results show that GCAMP6s has similar kinetics compared to Fura-2 in response to different concentrations of histamine, an IP_3-coupled stimulus in HeLa cells. However, our results also demonstrated that GCaMP6s is capable of detecting small cytosolic calcium changes in response to low concentrations of histamine. Importantly, our study demonstrated that GCaMP6s overcame the limitations that conventional calcium indicators have with regards to long-term imaging. Fura-2 requires that the coverslip is changed every 30 min due to photobleaching, dye leakage and UV-induced damage to the cells [78]. This scenario limits our ability to follow calcium dynamics in a single cell throughout the entire experiment. Using GCaMP6s allowed us to understand that calcium responses are heterogeneous throughout a single experiment. On the other hand bulk measurements of cell

death, such as Fura-2 and caspase assays, dilute these valuable information in the cell death process. Overall our findings demonstrated that GCaMP6 indicators are an excellent tool to study small calcium changes and long term calcium dynamics using live cell imaging.

H9C2 CELLS ARE NOT A SUITABLE MODEL TO STUDY CARDIAC DISEASE

In order to study the role of the IP_3R in ventricular cardiomyocytes we decided to use the immortalized cell line H9c2. H9c2 is a cell line derived from rat myocardium that has been shown to be a useful alternative for neonatal cardiomyocytes [182, 183]. We studied the expression and function of the different IP_3R isoforms in H9c2 cells. We demonstrated that all three different IP_3R isoforms are expressed. However, we fail to see an increase in cell area after ET-1 treatment. On the other hand we observed an increase in nuclear translocation of transcription factor NFAT. Finally, we showed that knocking down IP_3R-2 in H9c2 cells does not alter H9c2 calcium dynamics in response to ET-1. Our results show that IP_3R-1 knockdown abolishes intracellular calcium release in response to ET-1, suggesting that IP_3R-1 is a key mediator of ET-1 calcium release in H9c2 cells. Altogether, our results suggest that IP_3R-1 is the key contributor to the physiologic response of H9c2 cells to ET-1 exposure. However, as explained in the previous chapters, all IP_3R isoforms contribute to cardiac function and the hypertrophic response due to ET-1 exposure in isolated neonatal rat cardiomyocytes. The discrepancy between our results indicates that immortalized cells might not be an

appropriate model to study the molecular mechanisms of calcium dynamics in cardiovascular diseases.

IP_3R Expression and Localization in Ventricular Cardiomyocytes

In chapter 5 we examined the expression pattern of all three IP_3R isoforms. We used highly specific antibodies to confirm the protein expression of the different IP_3R isoforms in neonatal rat, adult rat and human ventricular cardiomyocytes from non-failing and failing hearts. IP_3R-1 antibody is a homemade antibody that has been validated by us and others. IP_3R-1 antisera antibody was raised against a peptide corresponding to the C-terminus of the type I receptor [78, 189]. Similar to IP_3R-1, IP_3R-2 antibody was homemade at State University of New York Health Science Center by Dr. Richard J. H. Wojcikiewicz. IP_3R-2 antisera was raised against a peptide that corresponds to the C-terminal end of rat type 2 receptor [71]. IP_3R-3 antibody was raised against the N-terminal of the type 3 receptor (aa. 22-230). IP_3R-3 is commercially available and it has been extensively validated.

Immunostaining of neonatal rat cardiomyocytes showed that all three IP_3R isoforms are expressed in the heart. Expression of IP_3R was prominent at the perinuclear membrane (**Fig. 5-1A-C**, second column). Interestingly, we can see that IP_3R is also expressed in a reticular pattern that was later confirmed to be the SR (**Fig. 5-2**). In contrast to neonatal cardiomyocytes, immunostaining of adult rat cardiomyocytes showed that IP_3Rs are distributed throughout the cell and there is no concentration of IP_3Rs at the perinuclear membrane (**Fig. 5-1 D-F**, second column). Similar to neonatal cardiomyocytes, IP_3R in adult cardiomyocytes also

co-localize with SERCA2 in the SR. Lastly, we looked at IP_3R expression and localization in human samples obtained from left ventricle of our control patient (**Table 1**).Immunostaining revealed that all three IP_3R isoforms are found in the healthy heart. Interestingly, the localization of IP_3R in human heart resembled IP_3R localization in the adult rat (**Fig 6-1.**white arrows). Other groups have shown IP_3Rs are expressed and functional in the human heart [54, 116]; however most of the studies focus on IP_3R-2 expression or look at IP_3R only at the message level. For the first time we are able to confirm the expression of all three IP_3R isoforms in rodents and humans.

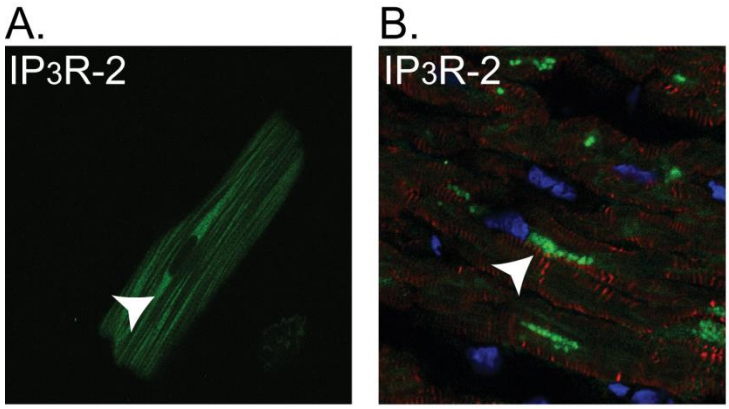

Figure 6-1: IP_3R localization adult rat and human samples **A**. IP_3R localization in adult rat ventricular cardiomyocyte. **B**. IP_3R localization in adult human non-failing left ventricle.

ET-1 Inotropic Response is Attenuated in IP_3R Knockdowns

Next we decided to examine the functional role of all IP_3R is cardiomyocytes. Transgenic models have shown that IP_3R-2 plays a major role in the progression of cardiac hypertrophy [50, 121]. Conversely, it has also been

shown that IP_3R-2 knockout models have normal progression to hypertrophy, suggesting that IP_3R-2 does not play a role in hypertrophy [120, 124]. The majority of the studies focused on understanding the role of IP_3R-2 in cardiomyocytes, leaving IP_3R-1 and -3 largely unexplored. Using neonatal rat cardiomyocytes we found that knocking down individual IP_3Rs is the heart had no functional implication in the inotropic effect induced by ET-1. Similar results were observed when we knockdown IP_3Rs in pairs. When we knockdown IP_3R-1 and 2 simultaneously we observed a decrease in the contraction frequency after ET-1 addition. However, there was still an increase in contractility compared to baseline when this cells were exposed to ET-1. Overall our observations suggest that cardiomyocytes expressing a single isoform of IP_3R are able to respond to ET-1. Lastly, we looked at ET-1 inotropic response in triple knockdowns. Interestingly, there was a complete inhibition of the ET-1 response only when all three IP_3R isoforms were knocked down in cardiomyocytes. Our experiments support previous research that suggests that IP_3R have functional redundant roles when co-expressed in different tissues. Futatsugi*et al.* showed that *in vivo* IP_3R-2 and -3 are key in exocrine physiology in energy metabolism and animal growth. Conversely, single knockouts ($IP_3R\text{-}2^{-/-}$ or $IP_3R\text{-}3^{-/-}$) mice are indistinguishable from controls. Important to note that their study was done using pancreatic cells and submandibular glands tissue which only express IP_3R-2 and -3 [110]. Similar results were noted when the role of IP_3Rs were studied in cardiogenesis[113] . In cardiogenesis it has been suggested that only IP_3R-1 and -2 are expressed in the embryonic heart. Single knockouts are able to develop normally. On the contrary, double knockout mice

died *in utero* with developmental defects of the ventricular myocardium [113]. Other groups have shown that all three IP_3R isoforms exhibit a functional redundant role in calcium mobilization and apoptosis [84]. These data corroborates our results demonstrating that there is functional redundancy among the different IP_3R isoforms.

IP_3R Triple Knockdown inhibits ET-1 Induced NFAT Activation and Hypertrophy

Previous reports have shown that IP_3R expression is altered during hypertrophy and heart failure [53-55, 120], however those studies focused largely on IP_3R gene expression or IP_3R-2 protein expression changes. We used neonatal cardiomyocytes to determine whether there is a change in IP_3R protein expression. Following 48 hrs and 6 days treatment with ET-1 we saw an increase in the hypertrophic marker ANP. However we did not see a change in the protein expression of any of theIP_3R isoforms. Next the expression of the different IP_3R isoforms was compared using samples from non-failing myocardium (control) and failing ventricular myocardium. We found no differences in the expression pattern of any of the IP_3R isoforms (**Fig. 5-6**). Our findings suggest that the expression of the IP_3Rs remains unaffected during the disease progression. Our study in human samples further corroborates our observations suggesting the expression of the IP_3Rs stays unaffected during hypertrophy in neonatal cardiomyocytes.

Next we decided to look whether knocking down all IP_3R isoforms will affect ET-1 signaling. Cardiomyocytes which were transfected with triple IP_3R siRNA

show a decrease in activation of NFAT luciferase reporter, suggesting that all three IP_3R isoforms are essential for the activation of transcription factors. Similar, the hypertrophic response induced by ET-1 is also abolished in triple IP_3R knockdown cardiomyocytes. Overall, our study suggests that all IP_3R isoforms are essential for the ET-1 inotropic and hypertrophic response. In our study we did not look at single or double IP_3R knockdown and their implication in NFAT activation and in ET-1 hypertrophy. Based on our observations from **fig. 5-4**, we concluded that triple knockdown would be more suitable for our study. However, further experiments should look into the potential involvement of single and double knockdowns in hypertrophy.

IP_3R ARE NOT RESTRICTED TO NUCLEAR COMPARTMENTS

To further investigate the role of IP_3R in cardiomyocytes, we aimed to determine whether IP_3R calcium transients are exclusively localized in nuclear compartments of cardiomyocytes. Using genetically encoded calcium indicators we were able to discriminate nuclear calcium transients from cytosolic calcium transients (**Fig. 5-9**). Our experiments showed that there are not exclusive IP_3R calcium transients inside the nucleus of cardiomyocytes. However, in **fig. 5-9E** we can observe some cytosolic only events detected with Fura-2. Our results support our hypothesis that IP_3R are localized at the SR/outer nuclear membrane. We hypothesize that calcium release from the SR sensitizes the RYR, which increases the frequency of calcium transients leading to activation of different transcription factors including NFAT.

IP_3Rs are calcium channels that are known to be expressed in the SR/ER. However, in the heart IP_3Rs are thought to be expressed mainly in the inner nuclear membrane or in the nucleoplasmic reticulum of cardiomyocytes [45, 125, 127, 128]. One of the main roles of IP_3Rs in the heart is to induce gene transcription in response to extracellular stimuli. However, calcium release from IP_3Rs is not the only source of calcium in cardiomyocytes. Cardiomyocytes have constant fluctuations of high concentrations of calcium which is in charge of mediating cardiomyocytes contraction. Therefore, it is thought that localization of IP_3Rs at the inner nuclear membrane or the nucleoplasmic reticulum is essential for the activation of gene transcription “away” for the large changes of cytosolic calcium. However, it has also been well established that calcium changes initiated at the dyads is able to reach inside the nucleus. Therefore, the idea that IP_3Rs need to be in a different compartment is not a suitable model in cardiomyocytes

GENERAL CONCLUSIONS AND SIGNIFICANCE

The function of IP_3Rs in the heart has been a debated topic for many years. One of the main reasons for this debate is that the expression of IP_3Rs in the heart are relatively low compared to RYR (~1:50 [116]), therefore their function is thought to not be as significant as other calcium channels. However, subsequent discoveries showed that the expression of IP_3Rs is increased during cardiovascular disease, at least at the mRNA level [55]. Several groups have tried to understand the role of IP_3Rs in the progression of hypertrophy or HF. However, the majority of these studies have focused exclusively on the role of IP_3R-2. Overall

there is still a debate whether IP_3Rs play a role in cardiovascular disease. As explained previously several animal models have contradictory results on the role of IP_3R-2 in the heart [50, 120, 121, 124]. However, several studies including ours show that not only IP_3R-2 is expressed in the heart (**Table1**). Our findings that IP_3Rs are essential for hypertrophic signaling and the underlying molecular mechanisms are highly significant.

IP_3Rs are well-known mediators of calcium signaling events. Our study suggests the expression of these receptors is not altered in ET-1 induced hypertrophy or in left ventricles of failing hearts. However, the function of these receptors might be regulated by other mechanisms. One possibility is that IP_3 alone is capable of increasing IP_3R activity without needing an increase in IP_3R expression. As result of increased GPCR stimulation there is also an increase in production of secondary messenger IP_3. This observation has been noted by other groups and they showed that in response to hypertrophy and heart failure IP_3 production is increased [50]. Similarly, some studies using an IP_3 sponge suggest that decreasing IP_3 availability is enough to stop the progression of hypertrophy [50]. IP_3 sponge studies not only demonstrate that IP_3R are important mediators of hypertrophy, but also suggest that an increase in IP_3 production may play an important role in disease progression without the need of increase in IP_3R expression.

Post-translational modifications represent another mechanism for IP_3R modulation. IP_3R are known to contain several consensus sequences for post-translational modifications, such as phosphorylation, which have previously been

implemented in in modulation of IP_3R activity [190]. A variety of kinases are known to phosphorylate IP_3Rs such as cyclic AMP-dependent protein kinase (PKA), PKC, CamKII and glycogen synthase kinase 3 (GSK3) and either increase or suppress IP_3R activity [190]. In order to support cardiovascular function the sympathetic nervous system activity is increased, leading to activation of the beta-adrenergic pathway where it activates cAMP/PKA signaling in cardiomyocytes [21]. Overall PKA phosphorylation is known to increase calcium mobilization in all three IP_3R isoforms [191, 192]. Similarly PKC and CaMKII phosphorylation are known to induce an increase in IICR [193, 194]. GSK3 phosphorylation of IP_3Rs results in a detrimental effect in ischemia reperfusion. Gomez *et al.* focused on mitochondrial calcium overload and subsequent cell death as a result of ischemic reperfusion. However, they do determine that lack of phosphorylation of IP_3R by GSK3 after ischemic reperfusion reduces SR calcium mobilization which reduces the severity of infarct size. It is important to point out that GSK3 has been shown to be down regulated in response to ET-1 stimulation. However, it gives a perfect example of how IP_3R posttranslational modification can lead to severe effects on cardiomyocyte function. The majority of the studies that looked at IP_3R phosphorylation status are done in other systems. Currently, there are few studies looking at IP_3R phosphorylation or other post-translational modifications in cardiomyocytes as a result of hypertrophy or HF. Understanding the molecular basis of how IP_3Rs are modulated in different systems is vital. It will allow us to further understand the critical role this receptors play in controlling different cellular

functions in health and disease. Our study opens the opportunity for future research aimed at uncovering the role of these channels in cardiac physiology.

References

1. Mozaffarian, D., et al., *Heart Disease and Stroke Statistics-2016 Update: A Report From the American Heart Association.* Circulation, 2016. **133**(4): p. e38-360.
2. Perez, A.L., et al., *Increased mortality with elevated plasma endothelin-1 in acute heart failure: an ASCEND-HF biomarker substudy.* Eur J Heart Fail, 2016. **18**(3): p. 290-7.
3. Pousset, F., et al., *Prognostic value of plasma endothelin-1 in patients with chronic heart failure.* Eur Heart J, 1997. **18**(2): p. 254-8.

4. Serneri, G.G., et al., *Selective upregulation of cardiac endothelin system in patients with ischemic but not idiopathic dilated cardiomyopathy: endothelin-1 system in the human failing heart.* Circ Res, 2000. **86**(4): p. 377-85.

5. Yorikane, R., et al., *Increased production of endothelin-1 in the hypertrophied rat heart due to pressure overload.* FEBS Lett, 1993. **332**(1-2): p. 31-4.

6. Kurihara, Y., et al., *Elevated blood pressure and craniofacial abnormalities in mice deficient in endothelin-1.* Nature, 1994. **368**(6473): p. 703-10.

7. Piuhola, J., et al., *Endothelin-1 contributes to the Frank-Starling response in hypertrophic rat hearts.* Hypertension, 2003. **41**(1): p. 93-8.

8. Levy, D., et al., *Prognostic implications of echocardiographically determined left ventricular mass in the Framingham Heart Study.* N Engl J Med, 1990. **322**(22): p. 1561-6.

9. Korn, J.H., et al., *Digital ulcers in systemic sclerosis: prevention by treatment with bosentan, an oral endothelin receptor antagonist.* Arthritis Rheum, 2004. **50**(12): p. 3985-93.

10. Galie, N., et al., *Ambrisentan therapy for pulmonary arterial hypertension.* J Am Coll Cardiol, 2005. **46**(3): p. 529-35.

11. Brunner, F., *Tissue endothelin-1 levels in perfused rat heart following stimulation with agonists and in ischaemia and reperfusion.* J Mol Cell Cardiol, 1995. **27**(9): p. 1953-63.

12. Barton, M., T. Traupe, and C.C. Haudenschild, *Endothelin, hypercholesterolemia and atherosclerosis.* Coron Artery Dis, 2003. **14**(7): p. 477-90.

13. Shubeita, H.E., et al., *Endothelin induction of inositol phospholipid hydrolysis, sarcomere assembly, and cardiac gene expression in ventricular myocytes. A paracrine mechanism for myocardial cell hypertrophy.* J Biol Chem, 1990. **265**(33): p. 20555-62.

14. Kourembanas, S., et al., *Hypoxia induces endothelin gene expression and secretion in cultured human endothelium.* J Clin Invest, 1991. **88**(3): p. 1054-7.

15. Kurihara, H., et al., *Transforming growth factor-beta stimulates the expression of endothelin mRNA by vascular endothelial cells.* Biochem Biophys Res Commun, 1989. **159**(3): p. 1435-40.

16. Pikkarainen, S., et al., *Inverse regulation of preproendothelin-1 and endothelin-converting enzyme-1beta genes in cardiac cells by mechanical load.* Am J Physiol Regul Integr Comp Physiol, 2006. **290**(6): p. R1639-45.

17. Cheng, T.H., et al., *Nitric oxide inhibits endothelin-1-induced cardiomyocyte hypertrophy through cGMP-mediated suppression of extracellular-signal regulated kinase phosphorylation.* Mol Pharmacol, 2005. **68**(4): p. 1183-92.

18. Emori, T., et al., *Cellular mechanism of natriuretic peptides-induced inhibition of endothelin-1 biosynthesis in rat endothelial cells.* Endocrinology, 1993. **133**(6): p. 2474-80.

19. Arai, H., et al., *Cloning and expression of a cDNA encoding an endothelin receptor.* Nature, 1990. **348**(6303): p. 730-2.

20. Sakurai, T., et al., *Cloning of a cDNA encoding a non-isopeptide-selective subtype of the endothelin receptor.* Nature, 1990. **348**(6303): p. 732-5.

21. Rebsamen, M.C., et al., *Role of cAMP and calcium influx in endothelin-1-induced ANP release in rat cardiomyocytes.* Am J Physiol, 1997. **273**(5 Pt 1): p. E922-31.

22. Kelland, N.F., et al., *Endothelial cell-specific ETB receptor knockout: autoradiographic and histological characterisation and crucial role in the clearance of endothelin-1.* Can J Physiol Pharmacol, 2010. **88**(6): p. 644-51.

23. Aramori, I. and S. Nakanishi, *Coupling of two endothelin receptor subtypes to differing signal transduction in transfected Chinese hamster ovary cells.* J Biol Chem, 1992. **267**(18): p. 12468-74.

24. Zhu, W., et al., *Ca2+/calmodulin-dependent kinase II and calcineurin play critical roles in endothelin-1-induced cardiomyocyte hypertrophy.* J Biol Chem, 2000. **275**(20): p. 15239-45.

25. Kim, Y., et al., *The MEF2D transcription factor mediates stress-dependent cardiac remodeling in mice.* J Clin Invest, 2008. **118**(1): p. 124-32.

26. Chang, S., et al., *Histone deacetylases 5 and 9 govern responsiveness of the heart to a subset of stress signals and play redundant roles in heart development.* Mol Cell Biol, 2004. **24**(19): p. 8467-76.

27. Phan, D., et al., *A novel protein kinase C target site in protein kinase D is phosphorylated in response to signals for cardiac hypertrophy.* Biochem Biophys Res Commun, 2011. **411**(2): p. 335-41.

28. Braz, J.C., et al., *Targeted inhibition of p38 MAPK promotes hypertrophic cardiomyopathy through upregulation of calcineurin-NFAT signaling.* J Clin Invest, 2003. **111**(10): p. 1475-86.

29. Braz, J.C., et al., *PKC alpha regulates the hypertrophic growth of cardiomyocytes through extracellular signal-regulated kinase1/2 (ERK1/2).* J Cell Biol, 2002. **156**(5): p. 905-19.

30. Harris, I.S., et al., *Raf-1 kinase is required for cardiac hypertrophy and cardiomyocyte survival in response to pressure overload.* Circulation, 2004. **110**(6): p. 718-23.

31. Yue, T.L., et al., *Extracellular signal-regulated kinase plays an essential role in hypertrophic agonists, endothelin-1 and phenylephrine-induced cardiomyocyte hypertrophy.* J Biol Chem, 2000. **275**(48): p. 37895-901.

32. Liang, F., S. Lu, and D.G. Gardner, *Endothelin-dependent and -independent components of strain-activated brain natriuretic peptide gene transcription require extracellular signal regulated kinase and p38 mitogen-activated protein kinase.* Hypertension, 2000. **35**(1 Pt 2): p. 188-92.

33. Munzel, F., et al., *Endothelin-1 and isoprenaline co-stimulation causes contractile failure which is partially reversed by MEK inhibition.* Cardiovasc Res, 2005. **68**(3): p. 464-74.

34. Clerk, A., et al., *Peptide growth factors signal differentially through protein kinase C to extracellular signal-regulated kinases in neonatal cardiomyocytes.* Cell Signal, 2006. **18**(2): p. 225-35.

35. Wang, L. and C.G. Proud, *Ras/Erk signaling is essential for activation of protein synthesis by Gq protein-coupled receptor agonists in adult cardiomyocytes.* Circ Res, 2002. **91**(9): p. 821-9.

36. Lorenz, K., et al., *A new type of ERK1/2 autophosphorylation causes cardiac hypertrophy.* Nat Med, 2009. **15**(1): p. 75-83.

37. Harrison, B.C., et al., *Regulation of cardiac stress signaling by protein kinase d1.* Mol Cell Biol, 2006. **26**(10): p. 3875-88.

38. Haworth, R.S., et al., *Neurohormonal regulation of cardiac histone deacetylase 5 nuclear localization by phosphorylation-dependent and phosphorylation-independent mechanisms.* Circ Res, 2012. **110**(12): p. 1585-95.

39. Brunner, F., et al., *Cardiovascular endothelins: essential regulators of cardiovascular homeostasis.* Pharmacol Ther, 2006. **111**(2): p. 508-31.

40. Beach, J.M., et al., *Ventricular hypertrophy and left atrial dilatation persist and are associated with reduced survival after valve replacement for aortic stenosis.* J Thorac Cardiovasc Surg, 2014. **147**(1): p. 362-369.e8.

41. Heesen, W.F., et al., *High prevalence of concentric remodeling in elderly individuals with isolated systolic hypertension from a population survey.* Hypertension, 1997. **29**(2): p. 539-43.

42. Katholi, R.E. and D.M. Couri, *Left ventricular hypertrophy: major risk factor in patients with hypertension: update and practical clinical applications.* Int J Hypertens, 2011. **2011**: p. 495349.

43. Kannan, A. and R. Janardhanan, *Hypertension as a risk factor for heart failure.* Curr Hypertens Rep, 2014. **16**(7): p. 447.

44. Stewart, D.J., et al., *Increased plasma endothelin-1 in the early hours of acute myocardial infarction.* J Am Coll Cardiol, 1991. **18**(1): p. 38-43.

45. Higazi, D.R., et al., *Endothelin-1-stimulated InsP3-induced Ca2+ release is a nexus for hypertrophic signaling in cardiac myocytes.* Mol Cell, 2009. **33**(4): p. 472-82.

46. Khan, A.A., et al., *IP3 receptor: localization to plasma membrane of T cells and cocapping with the T cell receptor.* Science, 1992. **257**(5071): p. 815-8.

47. Wozniak, A.L., et al., *Requirement of biphasic calcium release from the endoplasmic reticulum for Fas-mediated apoptosis.* J Cell Biol, 2006. **175**(5): p. 709-14.

48. Ceccarelli, F., et al., *ETA receptor-mediated Ca2+ mobilisation in H9c2 cardiac cells.* Biochem Pharmacol, 2003. **65**(5): p. 783-93.

49. Colella, M., et al., *Ca2+ oscillation frequency decoding in cardiac cell hypertrophy: role of calcineurin/NFAT as Ca2+ signal integrators.* Proc Natl Acad Sci U S A, 2008. **105**(8): p. 2859-64.

50. Nakayama, H., et al., *The IP3 receptor regulates cardiac hypertrophy in response to select stimuli.* Circ Res, 2010. **107**(5): p. 659-66.

51. Molkentin, J.D., et al., *A calcineurin-dependent transcriptional pathway for cardiac hypertrophy.* Cell, 1998. **93**(2): p. 215-28.

52. Harzheim, D., et al., *Elevated InsP3R expression underlies enhanced calcium fluxes and spontaneous extra-systolic calcium release events in hypertrophic cardiac myocytes.* Channels (Austin), 2010. **4**(1): p. 67-71.

53. Harzheim, D., et al., *Increased InsP3Rs in the junctional sarcoplasmic reticulum augment Ca2+ transients and arrhythmias associated with cardiac hypertrophy.* Proc Natl Acad Sci U S A, 2009. **106**(27): p. 11406-11.

54. Signore, S., et al., *Inositol 1, 4, 5-trisphosphate receptors and human left ventricular myocytes.* Circulation, 2013. **128**(12): p. 1286-97.

55. Go, L.O., et al., *Differential regulation of two types of intracellular calcium release channels during end-stage heart failure.* J Clin Invest, 1995. **95**(2): p. 888-94.

56. Gerasimenko, O.V., et al., *Inositol trisphosphate and cyclic ADP-ribose-mediated release of Ca2+ from single isolated pancreatic zymogen granules.* Cell, 1996. **84**(3): p. 473-80.

57. Joseph, S.K., et al., *Factors determining the composition of inositol trisphosphate receptor hetero-oligomers expressed in COS cells.* J Biol Chem, 2000. **275**(21): p. 16084-90.

58. Joseph, S.K., et al., *Heteroligomers of type-I and type-III inositol trisphosphate receptors in WB rat liver epithelial cells.* J Biol Chem, 1995. **270**(40): p. 23310-6.

59. Monkawa, T., et al., *Heterotetrameric complex formation of inositol 1,4,5-trisphosphate receptor subunits.* J Biol Chem, 1995. **270**(24): p. 14700-4.

60. Fan, G., et al., *Gating machinery of InsP3R channels revealed by electron cryomicroscopy.* Nature, 2015. **527**(7578): p. 336-41.

61. Yule, D.I., M.J. Betzenhauser, and S.K. Joseph, *Linking structure to function: Recent lessons from inositol 1,4,5-trisphosphate receptor mutagenesis.* Cell Calcium, 2010. **47**(6): p. 469-79.

62. Patterson, R.L., D. Boehning, and S.H. Snyder, *Inositol 1,4,5-trisphosphate receptors as signal integrators.* Annu Rev Biochem, 2004. **73**: p. 437-65.

63. Khan, M.T., et al., *Akt kinase phosphorylation of inositol 1,4,5-trisphosphate receptors.* J Biol Chem, 2006. **281**(6): p. 3731-7.

64. DeSouza, N., et al., *Protein kinase A and two phosphatases are components of the inositol 1,4,5-trisphosphate receptor macromolecular signaling complex.* J Biol Chem, 2002. **277**(42): p. 39397-400.

65. Komalavilas, P. and T.M. Lincoln, *Phosphorylation of the inositol 1,4,5-trisphosphate receptor. Cyclic GMP-dependent protein kinase mediates*

cAMP and cGMP dependent phosphorylation in the intact rat aorta. J Biol Chem, 1996. **271**(36): p. 21933-8.

66. Südhof, T.C., et al., *Structure of a novel InsP3 receptor.* EMBO J, 1991. **10**(11): p. 3199-206.

67. Blondel, O., et al., *Sequence and functional characterization of a third inositol trisphosphate receptor subtype, IP3R-3, expressed in pancreatic islets, kidney, gastrointestinal tract, and other tissues.* J Biol Chem, 1993. **268**(15): p. 11356-63.

68. Tu, H., et al., *Functional characterization of mammalian inositol 1,4,5-trisphosphate receptor isoforms.* Biophys J, 2005. **88**(2): p. 1046-55.

69. Foskett, J.K., et al., *Inositol trisphosphate receptor Ca2+ release channels.* Physiol Rev, 2007. **87**(2): p. 593-658.

70. Matsumoto, M., et al., *Ataxia and epileptic seizures in mice lacking type 1 inositol 1,4,5-trisphosphate receptor.* Nature, 1996. **379**(6561): p. 168-71.

71. Wojcikiewicz, R.J., *Type I, II, and III inositol 1,4,5-trisphosphate receptors are unequally susceptible to down-regulation and are expressed in markedly different proportions in different cell types.* J Biol Chem, 1995. **270**(19): p. 11678-83.

72. Newton, C.L., G.A. Mignery, and T.C. Südhof, *Co-expression in vertebrate tissues and cell lines of multiple inositol 1,4,5-trisphosphate (InsP3) receptors with distinct affinities for InsP3.* J Biol Chem, 1994. **269**(46): p. 28613-9.

73. Joseph, S.K., et al., *Membrane insertion, glycosylation, and oligomerization of inositol trisphosphate receptors in a cell-free translation system.* J Biol Chem, 1997. **272**(3): p. 1579-88.

74. Mignery, G.A. and T.C. Südhof, *The ligand binding site and transduction mechanism in the inositol-1,4,5-triphosphate receptor.* EMBO J, 1990. **9**(12): p. 3893-8.

75. Wagner, L.E. and D.I. Yule, *Differential regulation of the $InsP_3$ receptor type-1 and -2 single channel properties by $InsP_3$, Ca^{2+} and ATP.* J Physiol, 2012. **590**(Pt 14): p. 3245-59.

76. Sienaert, I., et al., *Molecular and functional evidence for multiple Ca2+-binding domains in the type 1 inositol 1,4,5-trisphosphate receptor.* J Biol Chem, 1997. **272**(41): p. 25899-906.

77. Betzenhauser, M.J., et al., *ATP modulation of Ca2+ release by type-2 and type-3 inositol (1, 4, 5)-triphosphate receptors. Differing ATP sensitivities and molecular determinants of action.* J Biol Chem, 2008. **283**(31): p. 21579-87.

78. Boehning, D., et al., *Cytochrome c binds to inositol (1,4,5) trisphosphate receptors, amplifying calcium-dependent apoptosis.* Nat Cell Biol, 2003. **5**(12): p. 1051-61.

79. Hedgepeth, S.C., et al., *The BRCA1 tumor suppressor binds to inositol 1,4,5-trisphosphate receptors to stimulate apoptotic calcium release.* J Biol Chem, 2015. **290**(11): p. 7304-13.

80. Chen, R., et al., *Bcl-2 functionally interacts with inositol 1,4,5-trisphosphate receptors to regulate calcium release from the ER in response to inositol 1,4,5-trisphosphate.* J Cell Biol, 2004. **166**(2): p. 193-203.

81. Ando, H., et al., *IRBIT, a novel inositol 1,4,5-trisphosphate (IP3) receptor-binding protein, is released from the IP3 receptor upon IP3 binding to the receptor.* J Biol Chem, 2003. **278**(12): p. 10602-12.

82. Rong, Y. and C.W. Distelhorst, *Bcl-2 protein family members: versatile regulators of calcium signaling in cell survival and apoptosis.* Annu Rev Physiol, 2008. **70**: p. 73-91.

83. Miyakawa, T., et al., *Encoding of Ca2+ signals by differential expression of IP3 receptor subtypes.* EMBO J, 1999. **18**(5): p. 1303-8.

84. Sugawara, H., et al., *Genetic evidence for involvement of type 1, type 2 and type 3 inositol 1,4,5-trisphosphate receptors in signal transduction through the B-cell antigen receptor.* EMBO J, 1997. **16**(11): p. 3078-88.

85. Alzayady, K.J., et al., *Functional inositol 1,4,5-trisphosphate receptors assembled from concatenated homo- and heteromeric subunits.* J Biol Chem, 2013. **288**(41): p. 29772-84.

86. Boehning, D., et al., *Single-channel recordings of recombinant inositol trisphosphate receptors in mammalian nuclear envelope.* Biophys J, 2001. **81**(1): p. 117-24.

87. Mak, D.O., S. McBride, and J.K. Foskett, *Inositol 1,4,5-trisphosphate [correction of tris-phosphate] activation of inositol trisphosphate [correction of tris-phosphate] receptor Ca2+ channel by ligand tuning of Ca2+ inhibition.* Proc Natl Acad Sci U S A, 1998. **95**(26): p. 15821-5.

88. Boehning, D. and S.K. Joseph, *Functional properties of recombinant type I and type III inositol 1, 4,5-trisphosphate receptor isoforms expressed in COS-7 cells.* J Biol Chem, 2000. **275**(28): p. 21492-9.

89. Iino, M., *Biphasic Ca2+ dependence of inositol 1,4,5-trisphosphate-induced Ca release in smooth muscle cells of the guinea pig taenia caeci.* J Gen Physiol, 1990. **95**(6): p. 1103-22.

90. Bezprozvanny, I., J. Watras, and B.E. Ehrlich, *Bell-shaped calcium-response curves of Ins(1,4,5)P3- and calcium-gated channels from endoplasmic reticulum of cerebellum.* Nature, 1991. **351**(6329): p. 751-4.

91. Maes, K., et al., *Differential modulation of inositol 1,4,5-trisphosphate receptor type 1 and type 3 by ATP.* Cell Calcium, 2000. **27**(5): p. 257-67.

92. Hagar, R.E. and B.E. Ehrlich, *Regulation of the type III InsP(3) receptor by InsP(3) and ATP.* Biophys J, 2000. **79**(1): p. 271-8.

93. Betzenhauser, M.J., et al., *ATP regulation of type-1 inositol 1,4,5-trisphosphate receptor activity does not require walker A-type ATP-binding motifs.* J Biol Chem, 2009. **284**(24): p. 16156-63.

94. Chandrasekhar, R., et al., *Unique Regulatory Properties of Heterotetrameric Inositol 1,4,5-Trisphosphate Receptors Revealed by Studying Concatenated Receptor Constructs.* J Biol Chem, 2016. **291**(10): p. 4846-60.

95. Di Gregorio, E., et al., *Two Italian Families with ITPR1 Gene Deletion Presenting a Broader Phenotype of SCA15.* Cerebellum.

96. Hara, K., et al., *Total deletion and a missense mutation of ITPR1 in Japanese SCA15 families.* Neurology, 2008. **71**(8): p. 547-51.

97. Knight, M.A., et al., *Spinocerebellar ataxia type 15 (sca15) maps to 3p24.2-3pter: exclusion of the ITPR1 gene, the human orthologue of an ataxic mouse mutant.* Neurobiol Dis, 2003. **13**(2): p. 147-57.

98. Huang, L., et al., *Missense mutations in ITPR1 cause autosomal dominant congenital nonprogressive spinocerebellar ataxia.* Orphanet J Rare Dis, 2012. **7**: p. 67.

99. Sasaki, M., et al., *Sporadic infantile-onset spinocerebellar ataxia caused by missense mutations of the inositol 1,4,5-triphosphate receptor type 1 gene.* J Neurol, 2015. **262**(5): p. 1278-84.

100. Gardner, R.J., *"SCA16" is really SCA15.* J Med Genet, 2008. **45**(3): p. 192.

101. van de Leemput, J., et al., *Deletion at ITPR1 underlies ataxia in mice and spinocerebellar ataxia 15 in humans.* PLoS Genet, 2007. **3**(6): p. e108.

102. McEntagart, M., et al., *A Restricted Repertoire of De Novo Mutations in ITPR1 Cause Gillespie Syndrome with Evidence for Dominant-Negative Effect.* Am J Hum Genet, 2016. **98**(5): p. 981-92.

103. Gerber, S., et al., *Recessive and Dominant De Novo ITPR1 Mutations Cause Gillespie Syndrome.* Am J Hum Genet, 2016. **98**(5): p. 971-80.

104. Klar, J., et al., *Abolished InsP3R2 function inhibits sweat secretion in both humans and mice.* J Clin Invest, 2014. **124**(11): p. 4773-80.

105. Roach, J.C., et al., *Genetic mapping at 3-kilobase resolution reveals inositol 1,4,5-triphosphate receptor 3 as a risk factor for type 1 diabetes in Sweden.* Am J Hum Genet, 2006. **79**(4): p. 614-27.

106. Oishi, T., et al., *A functional SNP in the NKX2.5-binding site of ITPR3 promoter is associated with susceptibility to systemic lupus erythematosus in Japanese population.* J Hum Genet, 2008. **53**(2): p. 151-62.

107. Tu, H., et al., *Functional characterization of the type 1 inositol 1,4,5-trisphosphate receptor coupling domain SII(+/-) splice variants and the Opisthotonos mutant form.* Biophys J, 2002. **82**(4): p. 1995-2004.

108. Street, V.A., et al., *The type 1 inositol 1,4,5-trisphosphate receptor gene is altered in the opisthotonos mouse.* J Neurosci, 1997. **17**(2): p. 635-45.

109. Ogura, H., M. Matsumoto, and K. Mikoshiba, *Motor discoordination in mutant mice heterozygous for the type 1 inositol 1,4,5-trisphosphate receptor.* Behav Brain Res, 2001. **122**(2): p. 215-9.

110. Futatsugi, A., et al., *IP3 receptor types 2 and 3 mediate exocrine secretion underlying energy metabolism.* Science, 2005. **309**(5744): p. 2232-4.

111. Inaba, T., et al., *Mice lacking inositol 1,4,5-trisphosphate receptors exhibit dry eye.* PLoS One, 2014. **9**(6): p. e99205.

112. Fukuda, N., et al., *Decreased olfactory mucus secretion and nasal abnormality in mice lacking type 2 and type 3 IP3 receptors.* Eur J Neurosci, 2008. **27**(10): p. 2665-75.

113. Uchida, K., et al., *Gene knock-outs of inositol 1,4,5-trisphosphate receptors types 1 and 2 result in perturbation of cardiogenesis.* PLoS One, 2010. **5**(9).

114. Fearnley, C.J., H.L. Roderick, and M.D. Bootman, *Calcium signaling in cardiac myocytes.* Cold Spring Harb Perspect Biol, 2011. **3**(11): p. a004242.

115. Shareef, M.A., L.A. Anwer, and C. Poizat, *Cardiac SERCA2A/B: therapeutic targets for heart failure.* Eur J Pharmacol, 2014. **724**: p. 1-8.

116. Moschella, M.C. and A.R. Marks, *Inositol 1,4,5-trisphosphate receptor expression in cardiac myocytes.* J Cell Biol, 1993. **120**(5): p. 1137-46.

117. Perez, P.J., et al., *Identification and functional reconstitution of the type 2 inositol 1,4,5-trisphosphate receptor from ventricular cardiac myocytes.* J Biol Chem, 1997. **272**(38): p. 23961-9.

118. Lipp, P., et al., *Functional InsP3 receptors that may modulate excitation-contraction coupling in the heart.* Curr Biol, 2000. **10**(15): p. 939-42.

119. Drawnel, F.M., C.R. Archer, and H.L. Roderick, *The role of the paracrine/autocrine mediator endothelin-1 in regulation of cardiac contractility and growth.* Br J Pharmacol, 2013. **168**(2): p. 296-317.

120. Cooley, N., et al., *No contribution of IP3-R(2) to disease phenotype in models of dilated cardiomyopathy or pressure overload hypertrophy.* Circ Heart Fail, 2013. **6**(2): p. 318-25.

121. Li, X., et al., *Endothelin-1-induced arrhythmogenic Ca2+ signaling is abolished in atrial myocytes of inositol-1,4,5-trisphosphate(IP3)-receptor type 2-deficient mice.* Circ Res, 2005. **96**(12): p. 1274-81.

122. Uchiyama, T., et al., *A novel recombinant hyperaffinity inositol 1,4,5-trisphosphate (IP(3)) absorbent traps IP(3), resulting in specific inhibition of IP(3)-mediated calcium signaling.* J Biol Chem, 2002. **277**(10): p. 8106-13.

123. Santulli, G., et al., *Abstract 16984: Role of Inositol 1,4,5-Triphosphate Receptor 2 in Post-Ischemic Heart Failure.* Circulation, 2014. **130**(Suppl 2): p. A16984.

124. Santulli, G., et al., *Mitochondrial calcium overload is a key determinant in heart failure.* Proc Natl Acad Sci U S A, 2015. **112**(36): p. 11389-94.

125. Luo, D., et al., *Nuclear Ca2+ sparks and waves mediated by inositol 1,4,5-trisphosphate receptors in neonatal rat cardiomyocytes.* Cell Calcium, 2008. **43**(2): p. 165-74.

126. Mohler, P.J., A.O. Gramolini, and V. Bennett, *The ankyrin-B C-terminal domain determines activity of ankyrin-B/G chimeras in rescue of abnormal inositol 1,4,5-trisphosphate and ryanodine receptor distribution in ankyrin-B (-/-) neonatal cardiomyocytes.* J Biol Chem, 2002. **277**(12): p. 10599-607.

127. Wu, X., et al., *Local InsP3-dependent perinuclear Ca2+ signaling in cardiac myocyte excitation-transcription coupling.* J Clin Invest, 2006. **116**(3): p. 675-82.

128. Arantes, L.A., et al., *Nuclear inositol 1,4,5-trisphosphate is a necessary and conserved signal for the induction of both pathological and physiological cardiomyocyte hypertrophy.* J Mol Cell Cardiol, 2012. **53**(4): p. 475-86.

129. Guatimosim, S., et al., *Nuclear Ca2+ regulates cardiomyocyte function.* Cell Calcium, 2008. **44**(2): p. 230-42.

130. Kim, C.G., D. Park, and S.G. Rhee, *The role of carboxyl-terminal basic amino acids in Gqalpha-dependent activation, particulate association, and nuclear localization of phospholipase C-beta1.* J Biol Chem, 1996. **271**(35): p. 21187-92.

131. Faenza, I., et al., *A role for nuclear phospholipase Cbeta 1 in cell cycle control.* J Biol Chem, 2000. **275**(39): p. 30520-4.

132. Kumar, V., Y.J. Jong, and K.L. O'Malley, *Activated nuclear metabotropic glutamate receptor mGlu5 couples to nuclear Gq/11 proteins to generate inositol 1,4,5-trisphosphate-mediated nuclear Ca2+ release.* J Biol Chem, 2008. **283**(20): p. 14072-83.

133. Zima, A.V., et al., *IP3-dependent nuclear Ca2+ signalling in the mammalian heart.* J Physiol, 2007. **584**(Pt 2): p. 601-11.

134. Ibarra, C., et al., *Local control of nuclear calcium signaling in cardiac myocytes by perinuclear microdomains of sarcolemmal insulin-like growth factor 1 receptors.* Circ Res, 2013. **112**(2): p. 236-45.

135. Allbritton, N.L., et al., *Source of nuclear calcium signals.* Proc Natl Acad Sci U S A, 1994. **91**(26): p. 12458-62.

136. Genka, C., et al., *Visualization of biphasic Ca2+ diffusion from cytosol to nucleus in contracting adult rat cardiac myocytes with an ultra-fast confocal imaging system.* Cell Calcium, 1999. **25**(3): p. 199-208.

137. Escobar, M., et al., *Structural evidence for perinuclear calcium microdomains in cardiac myocytes.* J Mol Cell Cardiol, 2011. **50**(3): p. 451-9.

138. Zhou, X., et al., *Cisapride protects against cardiac hypertrophy via inhibiting the up-regulation of calcineurin and NFATc-3.* Eur J Pharmacol, 2014. **735**: p. 202-10.

139. Wang, K., et al., *Cardiac hypertrophy is positively regulated by MicroRNA miR-23a.* J Biol Chem, 2012. **287**(1): p. 589-99.

140. Nakao, S., S. Wakabayashi, and T.Y. Nakamura, *Stimulus-dependent regulation of nuclear Ca2+ signaling in cardiomyocytes: a role of neuronal calcium sensor-1.* PLoS One, 2015. **10**(4): p. e0125050.

141. Proven, A., et al., *Inositol 1,4,5-trisphosphate supports the arrhythmogenic action of endothelin-1 on ventricular cardiac myocytes.* J Cell Sci, 2006. **119**(Pt 16): p. 3363-75.

142. Domeier, T.L., et al., *IP3 receptor-dependent Ca2+ release modulates excitation-contraction coupling in rabbit ventricular myocytes.* Am J Physiol Heart Circ Physiol, 2008. **294**(2): p. H596-604.

143. De Smedt, H., et al., *Isoform diversity of the inositol trisphosphate receptor in cell types of mouse origin.* Biochem J, 1997. **322 (Pt 2)**: p. 575-83.

144. Anger, M., et al., *Cellular distribution of Ca2+ pumps and Ca2+ release channels in rat cardiac hypertrophy induced by aortic stenosis.* Circulation, 1998. **98**(22): p. 2477-86.

145. Bootman, M.D., et al., *2-aminoethoxydiphenyl borate (2-APB) is a reliable blocker of store-operated Ca2+ entry but an inconsistent inhibitor of InsP3-induced Ca2+ release.* FASEB J, 2002. **16**(10): p. 1145-50.

146. Saleem, H., et al., *Interactions of antagonists with subtypes of inositol 1,4,5-trisphosphate (IP3) receptor.* Br J Pharmacol, 2014. **171**(13): p. 3298-312.

147. Chen, T.W., et al., *Ultrasensitive fluorescent proteins for imaging neuronal activity.* Nature, 2013. **499**(7458): p. 295-300.

148. Sharma, S., et al., *Glucose phosphorylation is required for insulin-dependent mTOR signalling in the heart.* Cardiovasc Res, 2007. **76**(1): p. 71-80.

149. Louch, W.E., K.A. Sheehan, and B.M. Wolska, *Methods in cardiomyocyte isolation, culture, and gene transfer.* J Mol Cell Cardiol, 2011. **51**(3): p. 288-98.

150. Freeman, J., et al., *Mapping brain activity at scale with cluster computing.* Nat Methods, 2014. **11**(9): p. 941-50.

151. Wilkins, B.J., et al., *Calcineurin/NFAT coupling participates in pathological, but not physiological, cardiac hypertrophy.* Circ Res, 2004. **94**(1): p. 110-8.

152. Berridge, M.J., M.D. Bootman, and H.L. Roderick, *Calcium signalling: dynamics, homeostasis and remodelling.* Nat Rev Mol Cell Biol, 2003. **4**(7): p. 517-29.

153. Ivanova, H., et al., *Inositol 1,4,5-trisphosphate receptor-isoform diversity in cell death and survival.* Biochim Biophys Acta, 2014. **1843**(10): p. 2164-83.

154. Tsien, R.Y., *New calcium indicators and buffers with high selectivity against magnesium and protons: design, synthesis, and properties of prototype structures.* Biochemistry, 1980. **19**(11): p. 2396-404.

155. Grynkiewicz, G., M. Poenie, and R.Y. Tsien, *A new generation of Ca2+ indicators with greatly improved fluorescence properties.* J Biol Chem, 1985. **260**(6): p. 3440-50.

156. Kurebayashi, N., A.B. Harkins, and S.M. Baylor, *Use of fura red as an intracellular calcium indicator in frog skeletal muscle fibers.* Biophys J, 1993. **64**(6): p. 1934-60.

157. Bootman, M.D., et al., *Ca2+-sensitive fluorescent dyes and intracellular Ca2+ imaging.* Cold Spring Harb Protoc, 2013. **2013**(2): p. 83-99.

158. Minta, A., J.P. Kao, and R.Y. Tsien, *Fluorescent indicators for cytosolic calcium based on rhodamine and fluorescein chromophores.* J Biol Chem, 1989. **264**(14): p. 8171-8.

159. Maravall, M., et al., *Estimating intracellular calcium concentrations and buffering without wavelength ratioing.* Biophys J, 2000. **78**(5): p. 2655-67.

160. Miyawaki, A., et al., *Fluorescent indicators for Ca2+ based on green fluorescent proteins and calmodulin.* Nature, 1997. **388**(6645): p. 882-7.

161. Baird, G.S., D.A. Zacharias, and R.Y. Tsien, *Circular permutation and receptor insertion within green fluorescent proteins.* Proc Natl Acad Sci U S A, 1999. **96**(20): p. 11241-6.

162. Nakai, J., M. Ohkura, and K. Imoto, *A high signal-to-noise Ca(2+) probe composed of a single green fluorescent protein.* Nat Biotechnol, 2001. **19**(2): p. 137-41.

163. Nagai, T., et al., *Circularly permuted green fluorescent proteins engineered to sense Ca2+.* Proc Natl Acad Sci U S A, 2001. **98**(6): p. 3197-202.

164. Bayley, P.M., W.A. Findlay, and S.R. Martin, *Target recognition by calmodulin: dissecting the kinetics and affinity of interaction using short peptide sequences.* Protein Sci, 1996. **5**(7): p. 1215-28.

165. Tian, L., et al., *Imaging neural activity in worms, flies and mice with improved GCaMP calcium indicators.* Nat Methods, 2009. **6**(12): p. 875-81.

166. Akerboom, J., et al., *Crystal structures of the GCaMP calcium sensor reveal the mechanism of fluorescence signal change and aid rational design.* J Biol Chem, 2009. **284**(10): p. 6455-64.

167. Shindo, Y., et al., *Glutamate-induced calcium increase mediates magnesium release from mitochondria in rat hippocampal neurons.* J Neurosci Res, 2010. **88**(14): p. 3125-32.

168. Ohkura, M., et al., *Genetically encoded green fluorescent Ca2+ indicators with improved detectability for neuronal Ca2+ signals.* PLoS One, 2012. **7**(12): p. e51286.

169. Shuai, J. and I. Parker, *Optical single-channel recording by imaging Ca2+ flux through individual ion channels: theoretical considerations and limits to resolution.* Cell Calcium, 2005. **37**(4): p. 283-99.

170. Khan, A.A., et al., *Lymphocyte apoptosis: mediation by increased type 3 inositol 1,4,5-trisphosphate receptor.* Science, 1996. **273**(5274): p. 503-7.

171. Akimzhanov, A.M., et al., *T-cell receptor complex is essential for Fas signal transduction.* Proc Natl Acad Sci U S A, 2010. **107**(34): p. 15105-10.

172. Akimzhanov, A.M., J.M. Barral, and D. Boehning, *Caspase 3 cleavage of the inositol 1,4,5-trisphosphate receptor does not contribute to apoptotic calcium release.* Cell Calcium, 2013. **53**(2): p. 152-8.

173. Bertrand, R., et al., *Induction of a common pathway of apoptosis by staurosporine.* Exp Cell Res, 1994. **211**(2): p. 314-21.

174. Szalai, G., R. Krishnamurthy, and G. Hajnoczky, *Apoptosis driven by IP(3)-linked mitochondrial calcium signals.* EMBO J, 1999. **18**(22): p. 6349-61.

175. Baylor, S.M. and S. Hollingworth, *Fura-2 calcium transients in frog skeletal muscle fibres.* J Physiol, 1988. **403**: p. 151-92.

176. Goldstein, J.C., et al., *The coordinate release of cytochrome c during apoptosis is rapid, complete and kinetically invariant.* Nat Cell Biol, 2000. **2**(3): p. 156-62.

177. Bhola, P.D., A.L. Mattheyses, and S.M. Simon, *Spatial and temporal dynamics of mitochondrial membrane permeability waves during apoptosis.* Biophys J, 2009. **97**(8): p. 2222-31.

178. Garcia-Perez, C., et al., *Bid-induced mitochondrial membrane permeabilization waves propagated by local reactive oxygen species (ROS) signaling.* Proc Natl Acad Sci U S A, 2012. **109**(12): p. 4497-502.

179. Tepikin, A., *Calcium signalling : a practical approach*. 2nd ed. The practical approach series. 2001, Oxford ; New York: Oxford University Press. xix, 230 p., 10 p. of plates.

180. Kimes, B.W. and B.L. Brandt, *Properties of a clonal muscle cell line from rat heart.* Exp Cell Res, 1976. **98**(2): p. 367-81.

181. Kuznetsov, A.V., et al., *H9c2 and HL-1 cells demonstrate distinct features of energy metabolism, mitochondrial function and sensitivity to hypoxia-reoxygenation.* Biochim Biophys Acta, 2015. **1853**(2): p. 276-84.

182. Watkins, S.J., G.M. Borthwick, and H.M. Arthur, *The H9C2 cell line and primary neonatal cardiomyocyte cells show similar hypertrophic responses in vitro.* In Vitro Cell Dev Biol Anim, 2011. **47**(2): p. 125-31.

183. Hescheler, J., et al., *Morphological, biochemical, and electrophysiological characterization of a clonal cell (H9c2) line from rat heart.* Circ Res, 1991. **69**(6): p. 1476-86.

184. Zhou, H., et al., *Icariin attenuates angiotensin II-induced hypertrophy and apoptosis in H9c2 cardiomyocytes by inhibiting reactive oxygen species-dependent JNK and p38 pathways.* Exp Ther Med, 2014. **7**(5): p. 1116-1122.

185. Woodcock, E.A. and S.J. Matkovich, *Ins(1,4,5)P3 receptors and inositol phosphates in the heart-evolutionary artefacts or active signal transducers?* Pharmacol Ther, 2005. **107**(2): p. 240-51.

186. Dolmetsch, R.E., K. Xu, and R.S. Lewis, *Calcium oscillations increase the efficiency and specificity of gene expression.* Nature, 1998. **392**(6679): p. 933-6.

187. Li, W., et al., *Cell-permeant caged InsP3 ester shows that Ca2+ spike frequency can optimize gene expression.* Nature, 1998. **392**(6679): p. 936-41.

188. Tomida, T., et al., *NFAT functions as a working memory of Ca2+ signals in decoding Ca2+ oscillation.* EMBO J, 2003. **22**(15): p. 3825-32.

189. Joseph, S.K. and S. Samanta, *Detergent solubility of the inositol trisphosphate receptor in rat brain membranes. Evidence for association of the receptor with ankyrin.* J Biol Chem, 1993. **268**(9): p. 6477-86.

190. Patel, S., S.K. Joseph, and A.P. Thomas, *Molecular properties of inositol 1,4,5-trisphosphate receptors.* Cell Calcium, 1999. **25**(3): p. 247-64.

191. Wojcikiewicz, R.J. and S.G. Luo, *Phosphorylation of inositol 1,4,5-trisphosphate receptors by cAMP-dependent protein kinase. Type I, II, and III receptors are differentially susceptible to phosphorylation and are phosphorylated in intact cells.* J Biol Chem, 1998. **273**(10): p. 5670-7.

192. Volpe, P. and B.H. Alderson-Lang, *Regulation of inositol 1,4,5-trisphosphate-induced Ca2+ release. II. Effect of cAMP-dependent protein kinase.* Am J Physiol, 1990. **258**(6 Pt 1): p. C1086-91.

193. Cameron, A.M., et al., *Calcineurin associated with the inositol 1,4,5-trisphosphate receptor-FKBP12 complex modulates Ca2+ flux.* Cell, 1995. **83**(3): p. 463-72.

194. Matter, N., et al., *Stimulation of nuclear protein kinase C leads to phosphorylation of nuclear inositol 1,4,5-trisphosphate receptor and accelerated calcium release by inositol 1,4,5-trisphosphate from isolated rat liver nuclei.* J Biol Chem, 1993. **268**(1): p. 732-6.

Biographical Sketch

NAME: Martha Iveth Garcia

PRESENT POSITION AND ADDRESS:

08/2012-Present

Cell Biology Graduate Assistant

Graduate School of Biomedical Science

University of Texas Medical Branch

Galveston, TX

BIOGRAPHICAL:

Birthdate: March 3rd, 1986

Birthplace: Brownsville, TX

Current Address: 1800 El Paseo St. Apt # 713

Houston, TX 77054

Phone Number: (956) 640 - 7983

EDUCATION:

08/2005-05/2010

Bachelor of Science**,** Concentration: Biomedical Research

University of Texas at Brownsville, Brownsville, TX, 2010

Minority Biomedical Research Support-Research Initiative for Scientific Enhancement (MBRS-RISE) Scholar– 2008-2010

Society for Advancement of Chicanos and Native Americans in Science (SACNAS) Travel Scholarship - 2009

STARS Excellence-College of Science, Math & Tech Scholarship-UT Brownsville - 2007-2008

UT-Brownsville Dean's List - 2005-2009

PROFESSIONAL WORK HISTORY AND TEACHING EXPERIENCE:

08/2008-05/2010

Research Assistant, Minority Biomedical Research Support Research Initiative for Scientific Enhancement Program (MBRS RISE) Scholar

University of Texas at Brownsville

Brownsville, Texas

Advisor: Emilio Garrido-Sanabria, Ph.D.

07/2009-09/2009

Research Assistant, Summer Undergraduate Research Program (SURP)

University of Utah

Huntsman Cancer Institute

Salt Lake City, Utah

Advisor: NikolausTrede, M.D.

05/2010-06/2011

Lab Technician, Department of Neuroscience

University of Texas at Brownsville

Brownsville, Texas

Advisor: Luis V. Colom, Ph.D.

06/2011-06/2012

Research Assistant, Post-Baccalaureate Research Education Program (PREP)

University of Texas Medical Branch

Galveston, Texas

Advisor: Darren Boehning, Ph.D.

Project: Role of BRCA1 in apoptotic calcium release.

Teaching:

08/2013-12/2013

Small group facilitator for BBSC-6401 Biochemistry.

University of Texas Medical Branch at Galveston

CURRENT RESEARCH ACTIVITIES:

Area of Research: Understanding the role of inositol 1, 4, 5-trisphosphate receptor (IP_3R) in the progression of ventricular hypertrophy

PI: Darren Boehning

HONORS:

Shirley Patricia Parker Scholarship Endowment, UTMB – 2016

Basic Cardiovascular Sciences Cardiovascular Outreach Award- American Heart Association - 2016

Basic Cardiovascular Sciences Minority Travel Grant- American Heart

Association - 2015

Shirley Patricia Parker Scholarship Endowment, UTMB – 2014

COMMITTEE RESPONSIBILITIES:

2013-2014 Secretary, Student Society of Cell Biology

PEER REVEIWED ARTICLES:

Garcia MI, Boehning D. Cardiac inositol 1,4,5-trisphosphate receptors. Biochim Biophys Acta. 2016 Nov 21. In Press.

Hedgepeth SC, **Garcia MI**, Wagner LE 2nd, Rodriguez AM, Chintapalli SV, Snyder RR, Hankins GD, Henderson BR, Brodie KM, Yule DI, van Rossum DB, Boehning D. The BRCA1 Tumor Suppressor Binds to Inositol 1,4,5-Trisphosphate Receptors to Stimulate Apoptotic Calcium Release. *J. Biol. Chem*. 2015 Mar 13;290(11):7304-13.

Rudner LA, Brown KH, Dobrinski KP, Bradley DF, **Garcia MI**, Smith ACH, Downie JK, Meeker ND, Look AT, Downing JR, Gutierrez A, Mullighan CG, Schiffman JD, Lee C, Trede NS, Frazer JK. (2011). Shared acquired genomic changes in zebrafish and human T-ALL. *Oncogene.* 2011 Oct 13;30(41):4289-96

ABSTRACTS:

Functional role of inositol 1,4,5-trisphosphate receptors in cardiac hypertrophy

M. Iveth Garcia[1,2], Anja Karlstaedt[3], Heinrich Taegtmeyer[3], and Darren Boehning[1]
Poster Presentation
Meeting:European Calcium Society 2016 Meeting

Functional role of inositol 1,4,5-trisphosphate receptors in cardiac hypertrophy

M. Iveth Garcia[1,2], Anja Karlstaedt[3], Heinrich Taegtmeyer[3], and Darren Boehning[1]
Poster Presentation
Meeting:Basic Cardiovascular Sciences (BCVS) Scientific Sessions 2015

Expression and function of inositol 1,4,5-trisphosphate receptors in the heart

M. Iveth Garcia[1,2], Darren Boehning[1]
Poster Presentation
Meeting: Biophysical Society 2015 Annual Meeting, Baltimore, Maryland.

GCAMP6 As A New Tool To Study Long-Term Calcium Dynamics During

Apoptosis

M. Iveth Garcia[1], Darren Boehning[1,2]
Poster Presentation
Meeting: Annual UTHSC-Houston Biochemistry and Molecular Biology Graduate Program Retreat 2014

Amyloid β 1-42 Induces Oxidative Stress in Septal Neurons

Martha I. Garcia[1], Sofia Hernandez[1], Miriam Perez-Cordova[1], Ahmed Touhuami[2], Luis V. Colom[1]
Poster Presentation
Meeting: University of Texas at Brownsville Research Symposium 2011, Brownsville, TX.

Serial Transplantation of hlk Tumor Cells to Allogeneic Host

Martha Iveth Garcia[1], Lynnie Rudner[2], J. Kimbleel Frazer[2], Nikolaus Trede[2]
Poster Presentation
Meeting: Society for Advancement of Chicanos and Native Americans in Science (SACNAS) 2009, Dallas, TX.

Excitatory Synapses in Differentiated Hippocampal Neuron-Derived H19-7 Cells

Martha I. Garcia[1], Bianca Dotson[1], Luis Pacheco[1], Emilio R. Garrido-Sanabria[1].
Poster Presentation
Meeting: Annual Biomedical Research Conference for Minority Students (ABRCMS) 2008, Orlando Florida

This dissertation was typed by Martha Iveth Garcia.